DEPARTMENT OF
MATERIALS SCIENCE AND ENGINEERING

Modeling of Thermoelastic Stresses in Thermal Barrier Coatings

Sean P. Donegan and Anthony D. Rollett (PI)

UCR/HBCU Review Meeting

June 12, 2013

CARNEGIE MELLON UNIVERSITY PITTSBURGH PENNSYLVANIA 1900

DEPARTMENT OF ENERGY UNITED STATES OF AMERICA

NETL NATIONAL ENERGY TECHNOLOGY LABORATORY

High Resolution Modeling of Materials for High Temperature Service

- University Coal Research: Award Number: DE-FE0003840
- Vito Cedro, Program Manager

PROJECT DELIVERABLES:

- Identify algorithm for matching both grain and particle microstructures Implement and deliver software code for synthesis of digital microstructures from experimental images
- Demonstrate that the Fast Fourier Transform (FFT) code can run as parallel (Message Passing Interface) code on a small cluster Demonstrate that the FFT code can run on a large computer cluster (at least 200 nodes)
- Characterize a candidate refractory alloy system, build the synthetic microstructure for that alloy from experimental images, perform computer simulations of mechanical response and compare computer simulations with experimental data.
- Write and submit final report and deliver kinetic database in electronic form suitable for use by other scientists and engineers. Final report will include documentation of the 3D FFT software and the complete code for generating the synthetic microstructures and performing the mechanical response simulations

Outline

Introduction
- Motivation
- Objectives

Background
- Thermoelastic Stress
- Thermal Barrier Coatings
- Materials Selection
- Synthetic Structure Creation

Analytical Techniques
- Thermoelastic FFT
- Extreme Value Analysis

Results
- Resolution Dependence
- Elastic Energy Density of Thermal Barrier Coatings
  - MAX Phase Bond Coats
  - Industry Standard Systems

Conclusions

Future Work
- Microstructure Generation
- Hot Spots in Relation to Microstructural Features

DEPARTMENT OF
MATERIALS SCIENCE AND ENGINEERING

Introduction

- Metallic components in gas-turbine engines are exposed to extreme levels of te[illegible]ure.
- Thermal barrier [illegible] metallic com[illegible] in h[illegible]

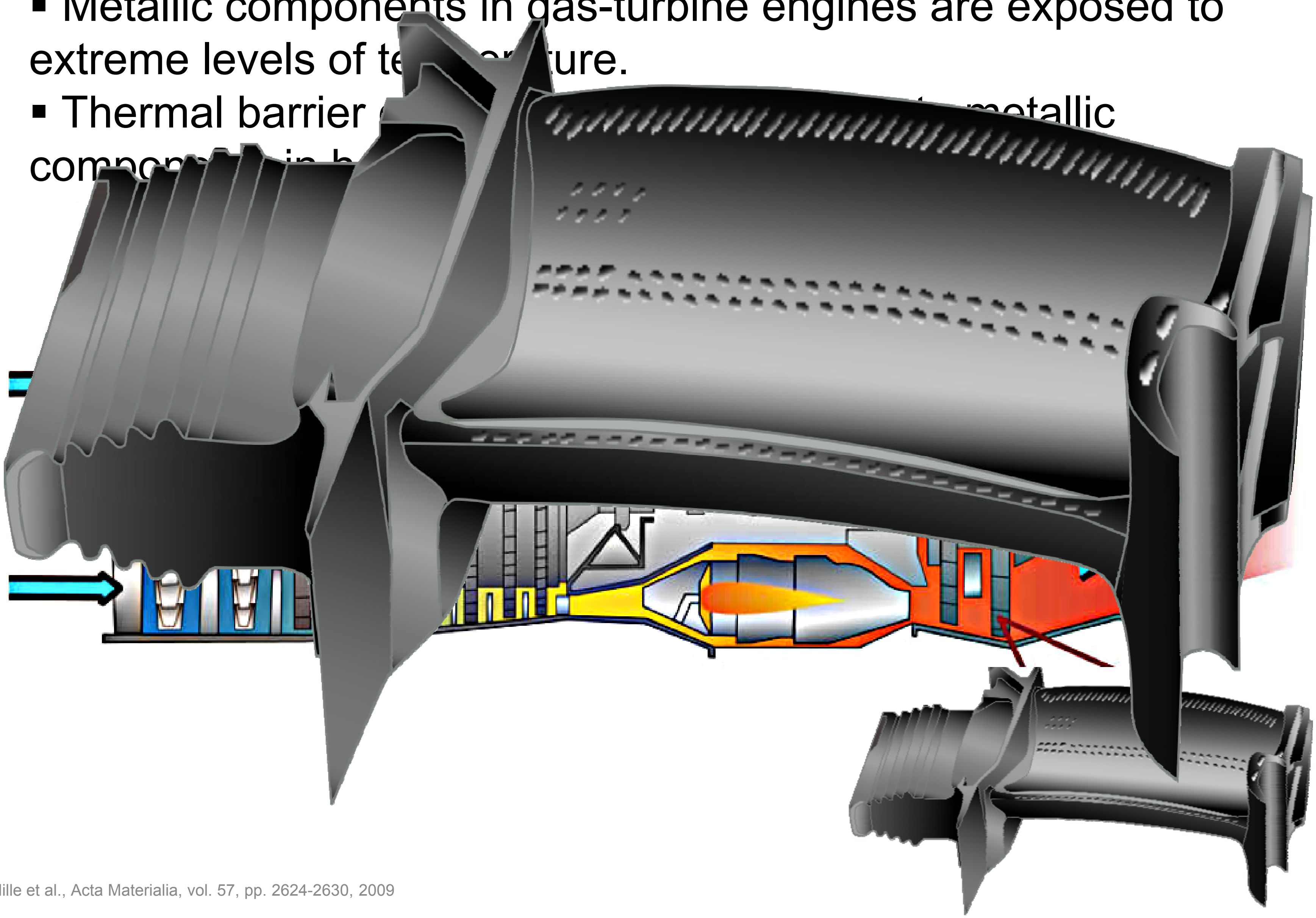

T.S. Hille et al., Acta Materialia, vol. 57, pp. 2624-2630, 2009

Motivation

- Experimental assessment of TBC failure involves cycling the component until failure.
- Scaling prevents FEM simulations from utilizing large structures or limits them to 2D domains.

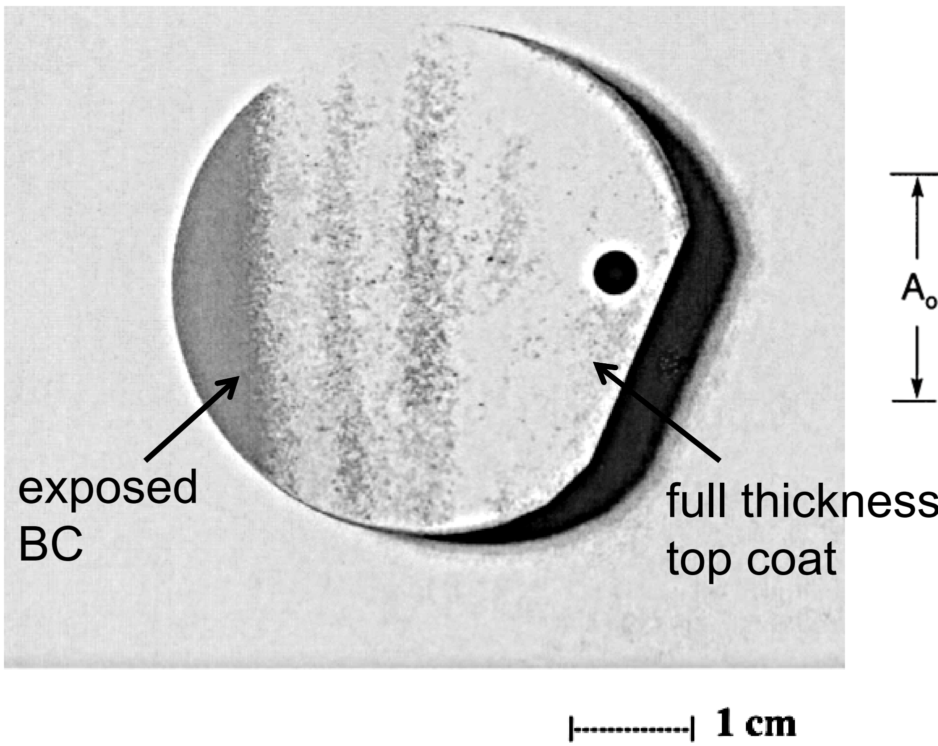

circular TBC test specimen

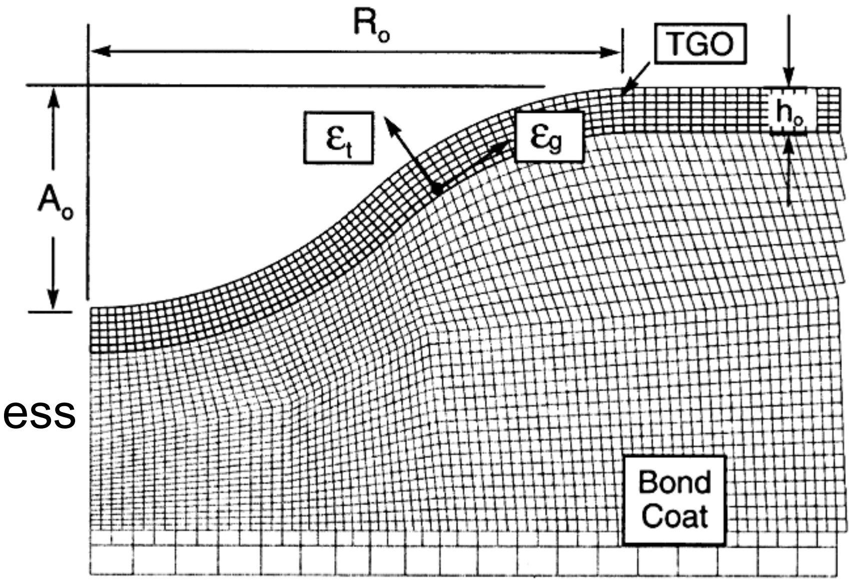

2D FEM mesh

E.A.G. Shillington and D.R. Clarke, Acta Materialia, vol. 47, pp. 1297-1305, 1999
A.M. Karlsson and A.G. Evans, Acta Materialia, vol. 49, pp. 1793-1804, 2001

DEPARTMENT OF MATERIALS SCIENCE AND ENGINEERING

Outline

Introduction
- Motivation
- Objectives

Background
- Thermoelastic Stress
- Thermal Barrier Coatings
- Materials Selection
- Synthetic Structure Creation

Analytical Techniques
- Thermoelastic FFT
- Extreme Value Analysis

Results
- Resolution Dependence
- Elastic Energy Density of Thermal Barrier Coatings
  - MAX Phase Bond Coats
  - Industry Standard Systems

Conclusions

Future Work
- Microstructure Generation
- Hot Spots in Relation to Microstructural Features

Thermoelastic Stress

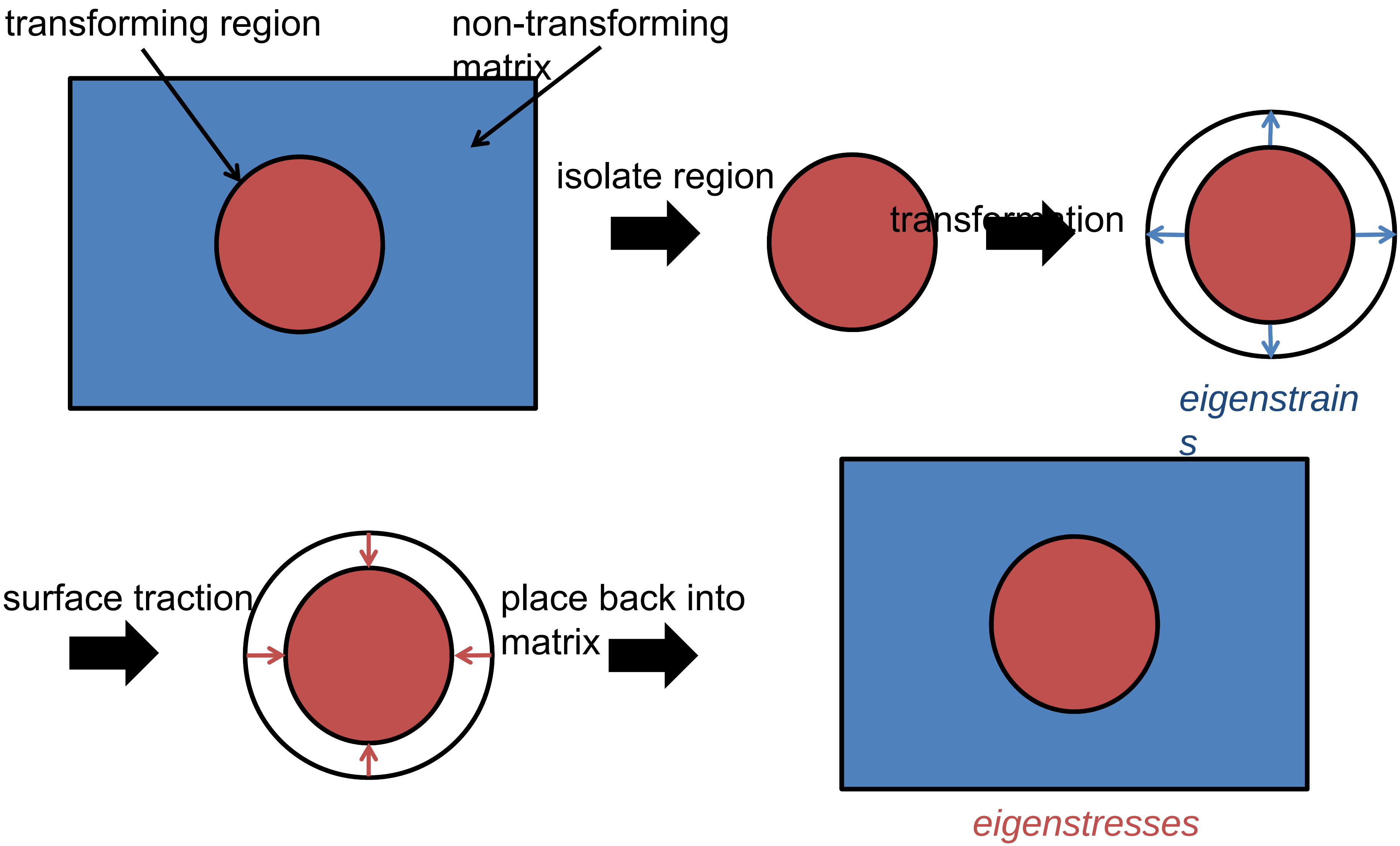

J. D. Eshelby, Proceedings of the Royal Society of London A, vol. 252, pp. 561-569, 1959

Thermoelastic Stress

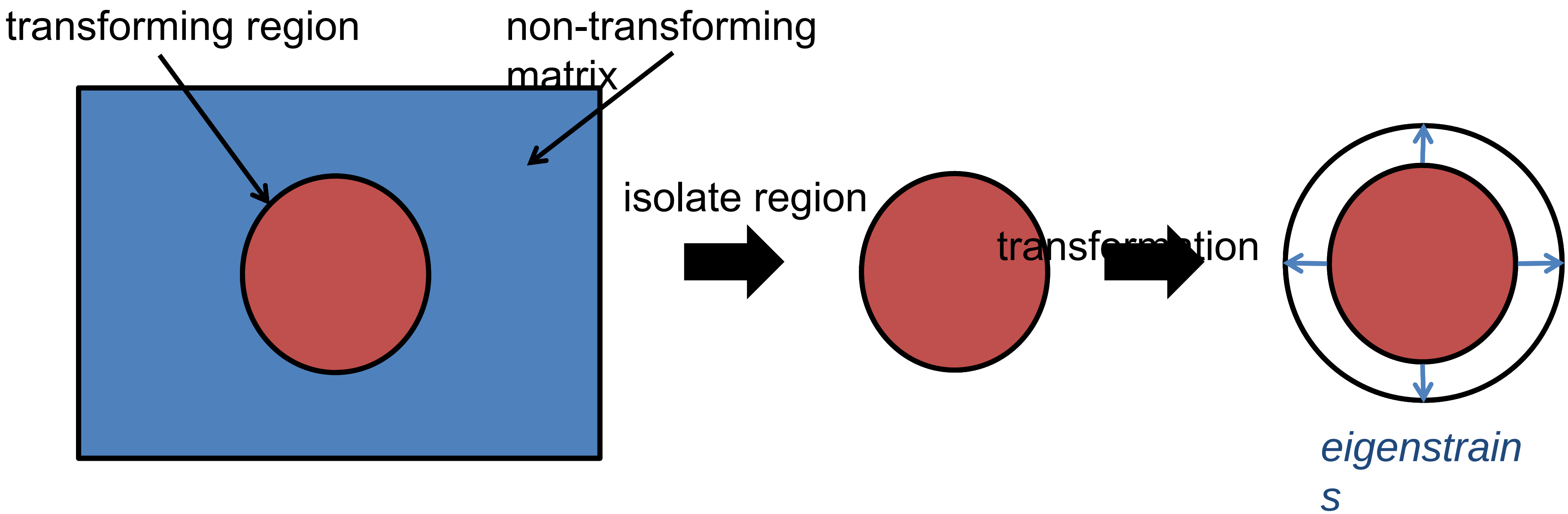

Eigenstrains resulting from thermal expansion:

$$\epsilon^*_{ij} = \alpha_{ij} \Delta T$$

strain tensor

thermal expansion tensor

applied temperature

Thermoelastic Stress

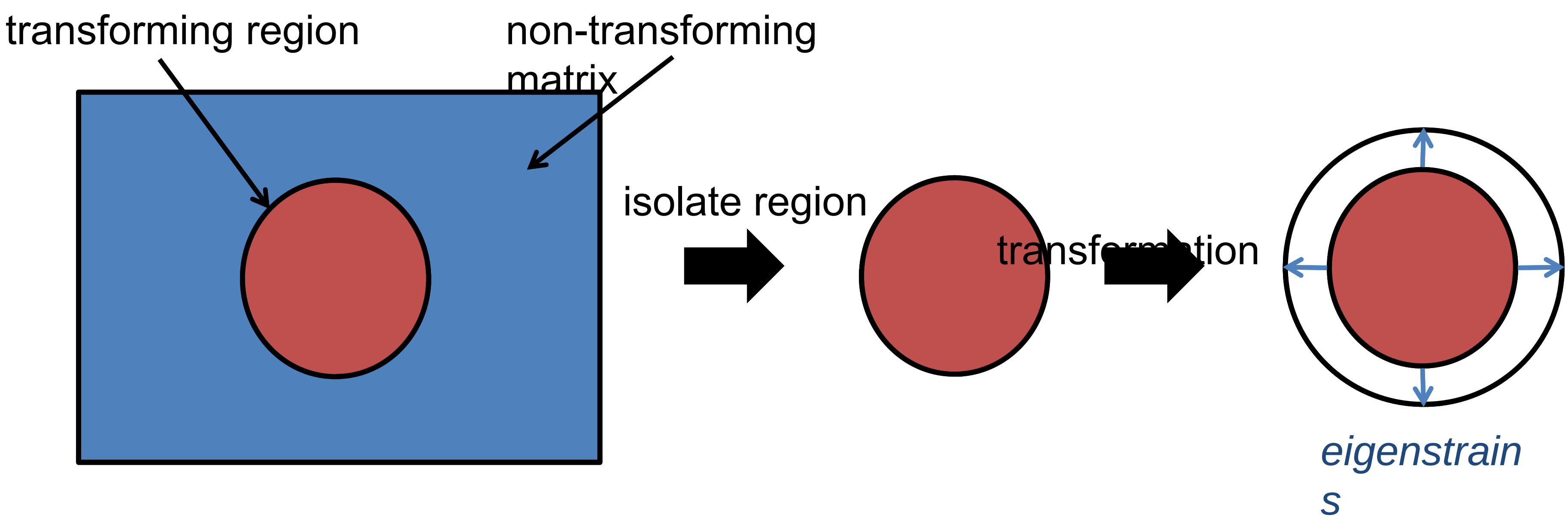

Hooke's Law:

$$\sigma_{ij} = C_{ijkl}\epsilon^{e}_{kl}$$

stress tensor

stiffness tensor

strain tensor

Thermoelastic Stress

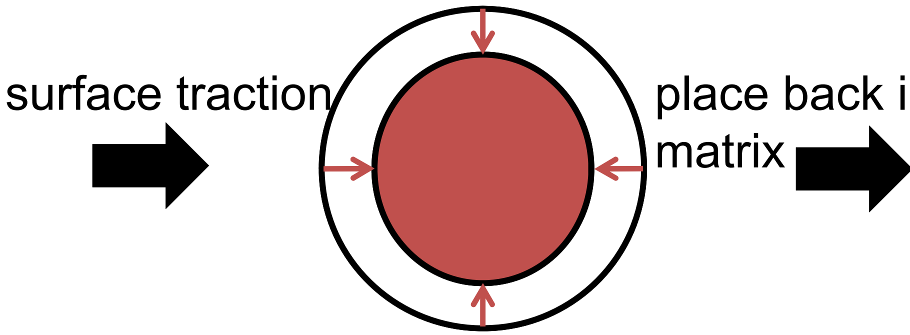

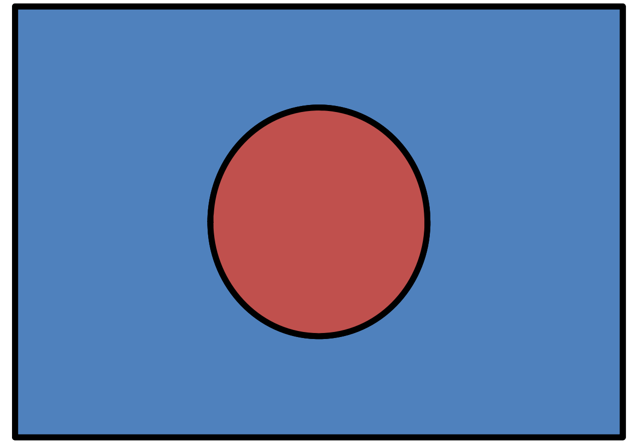

eigenstresses

Total Strain:

$$\epsilon(x) = \epsilon^e(x) + \epsilon^*(x)$$

Modified Hooke's Law:

$$\epsilon(x) = C^{-1}(x) : \sigma(x) + \epsilon^*(x)$$

Thermoelastic Stress

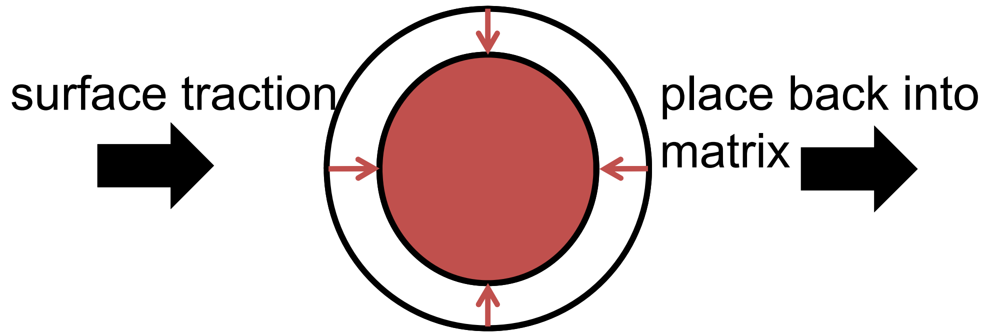

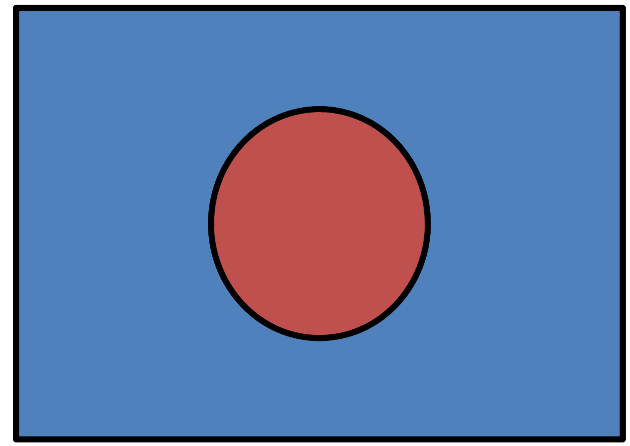

eigenstresses

Eigenstresses resulting from thermal expansion:

$$\sigma(x) = C(x) : (\epsilon(x) - \epsilon^*(x)) =$$

$$C(x) : \epsilon(x) + \underbrace{\Lambda(x)}_{\text{eigenstress}}$$

Thermal Barrier Coatings

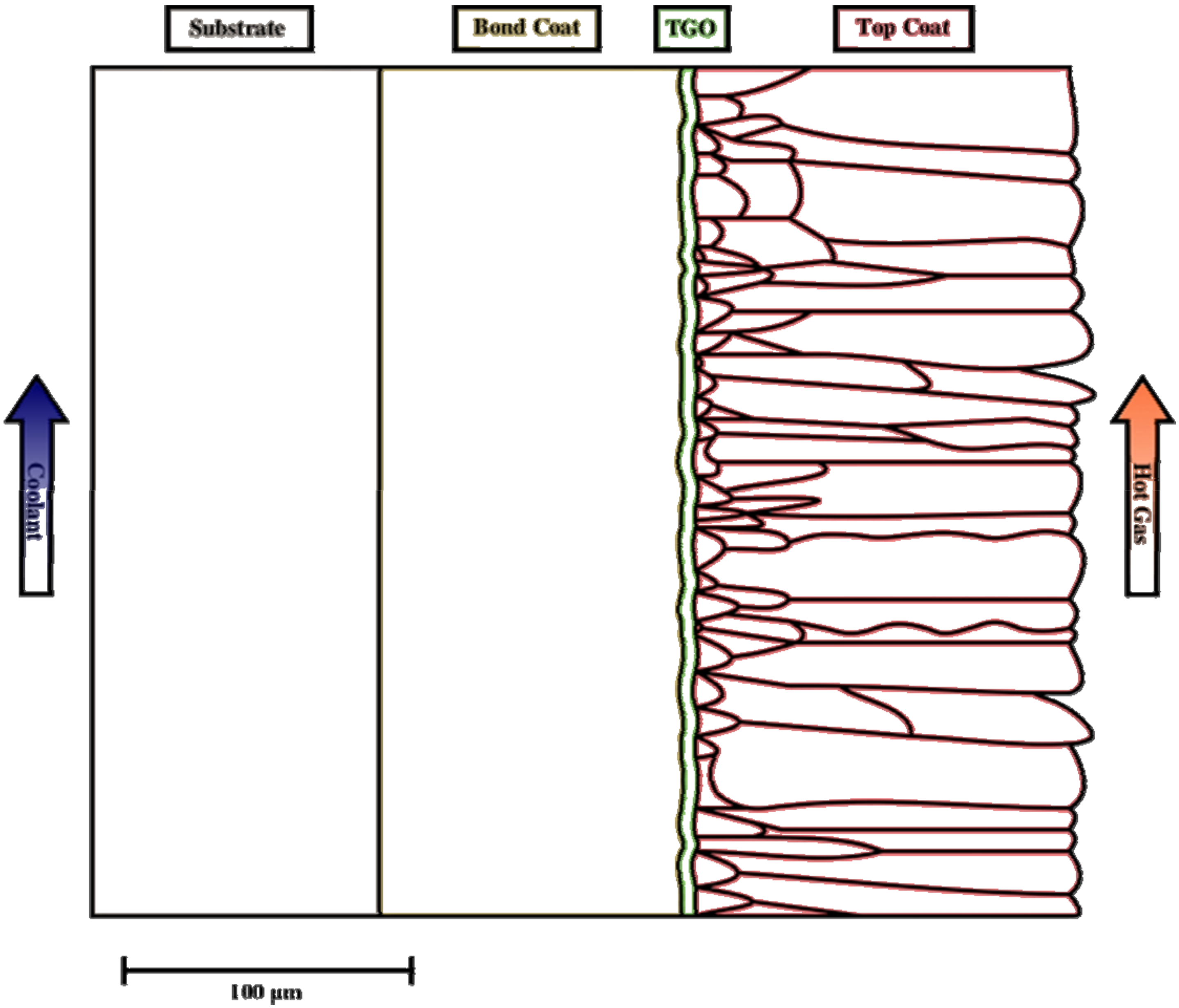

TBC Failure

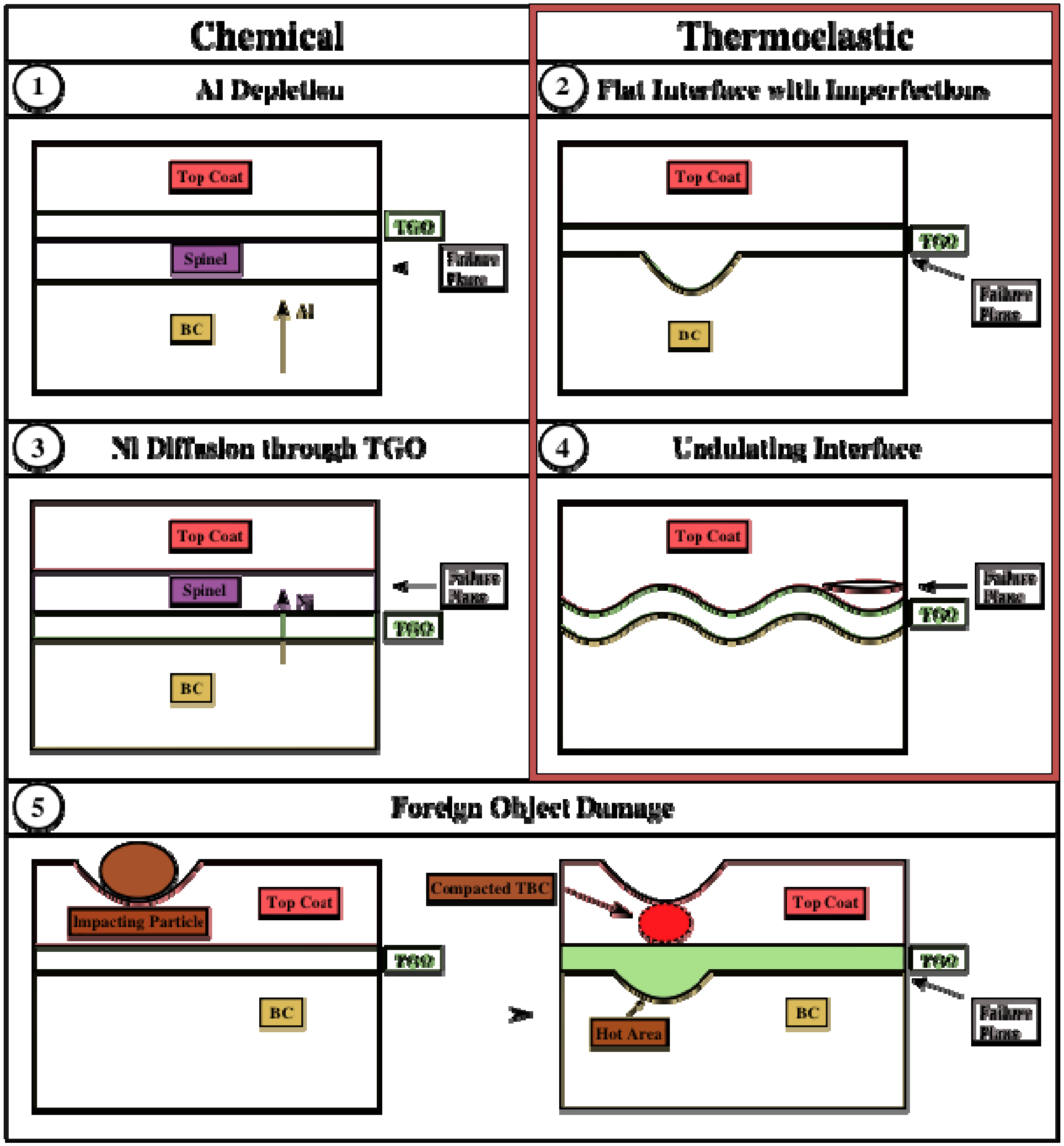
Chemical
Thermoelastic
1 Al Depletion
2 Flat Interface with Imperfections
Top Coat
TGO
Spinel
Failure Plane
BC
Al
3 Ni Diffusion through TGO
4 Undulating Interface
Ni
5 Foreign Object Damage
Impacting Particle
Compacted TBC
Hot Area

DEPARTMENT OF
MATERIALS SCIENCE AND

TBC Co

Top Coat

Bond Co

TGO

Substrate

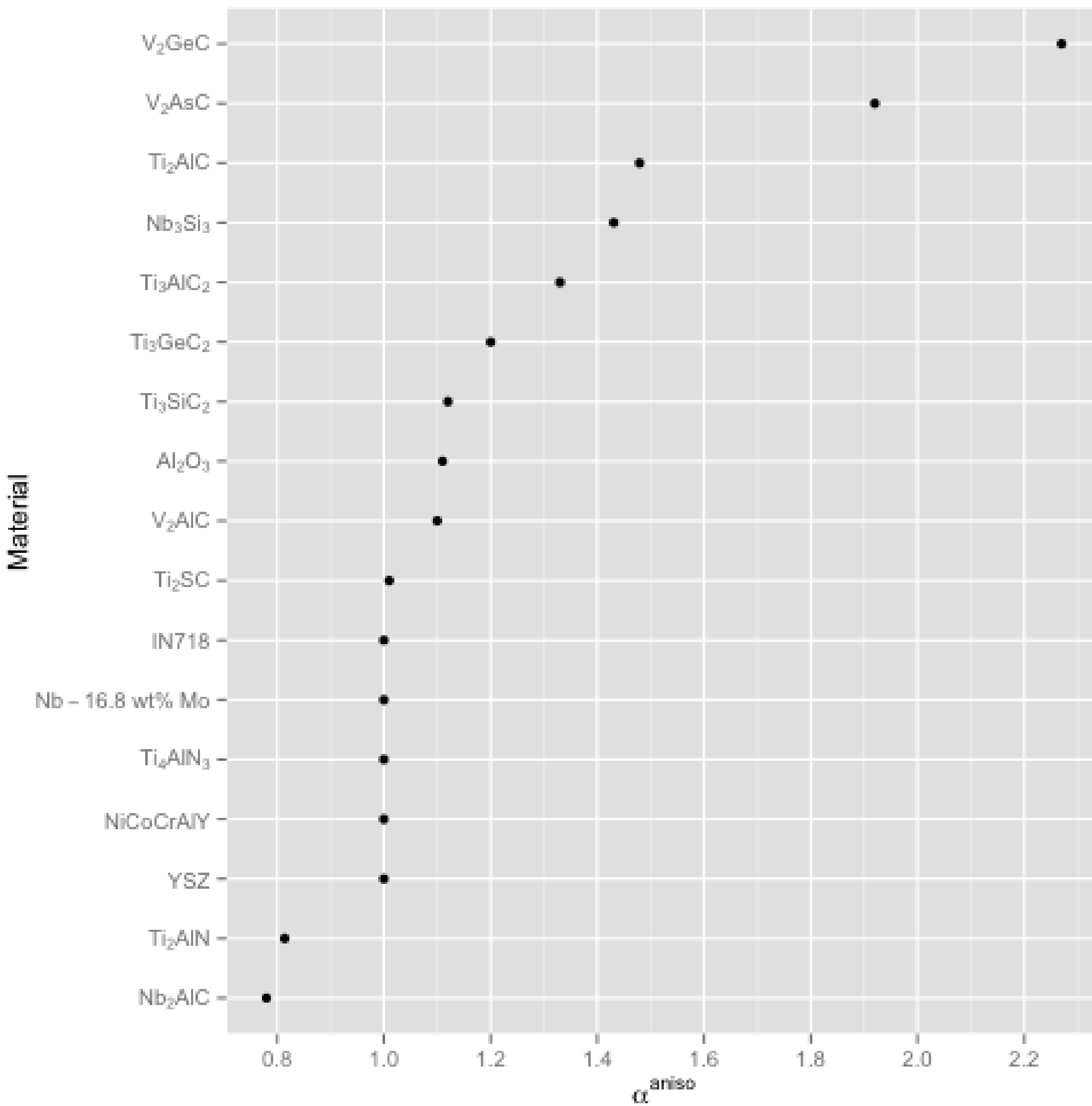

$$iso = \frac{\alpha^c}{\alpha^a}$$

Synthetic Structure Creation

Microstructure, especially at the top BC/top coat interface, plays a crucial role in TBC failure. To better appreciate the role of microstructure, *DREAM.3D* is used to generate test microstructures.

DREAM.3D is a tool used to generate and analyze material microstructure. DREAM.3D can create a 3D microstructure from a set of statistical data.

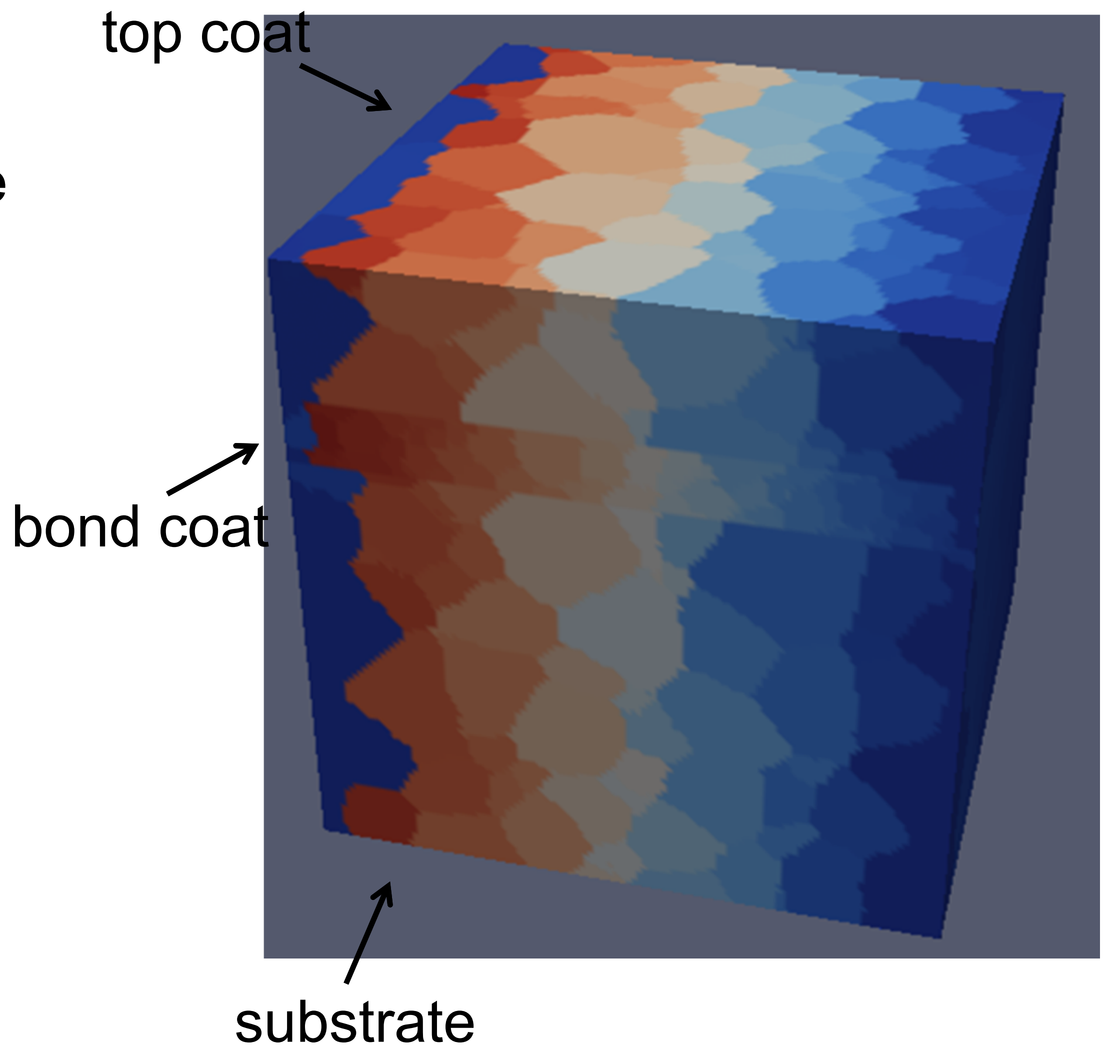

dream3d.bluequartz.net

DEPARTMENT OF
MATERIALS SCIENCE AND ENGINEERING

Outline

Introduction
- Motivation
- Objectives

Background
- Thermoelastic Stress
- Thermal Barrier Coatings
- Materials Selection
- Synthetic Structure Creation

Analytical Techniques
- Thermoelastic FFT
- Extreme Value Analysis

Results
- Resolution Dependence
- Elastic Energy Density of Thermal Barrier Coatings
  - MAX Phase Bond Coats
  - Industry Standard Systems

Conclusions

Future Work
- Microstructure Generation
- Hot Spots in Relation to Microstructural Features

Fast Fourier Transforms

- The FFT algorithm provides a computationally efficient way to determine discrete direct and indirect Fourier transforms.
- By re-casting PDEs in frequency space, convolution integrals (Green's function method) become local (tensor) products.
- Since all calculations are local save for the FFT, the method has the potential for NlogN scaling to large domain sizes.
- Full field solutions exists for both the thermoelastic (teFFT) and viscoplastic (vpFFT) cases; both versions

Thermoelastic FFT

We discretize microstructure as a 3D image, or equivalently as a 3D regular grid overlayed on a representative volume element (RVE).

Each point/*node* contains information about the present phase and crystallographic orientation.

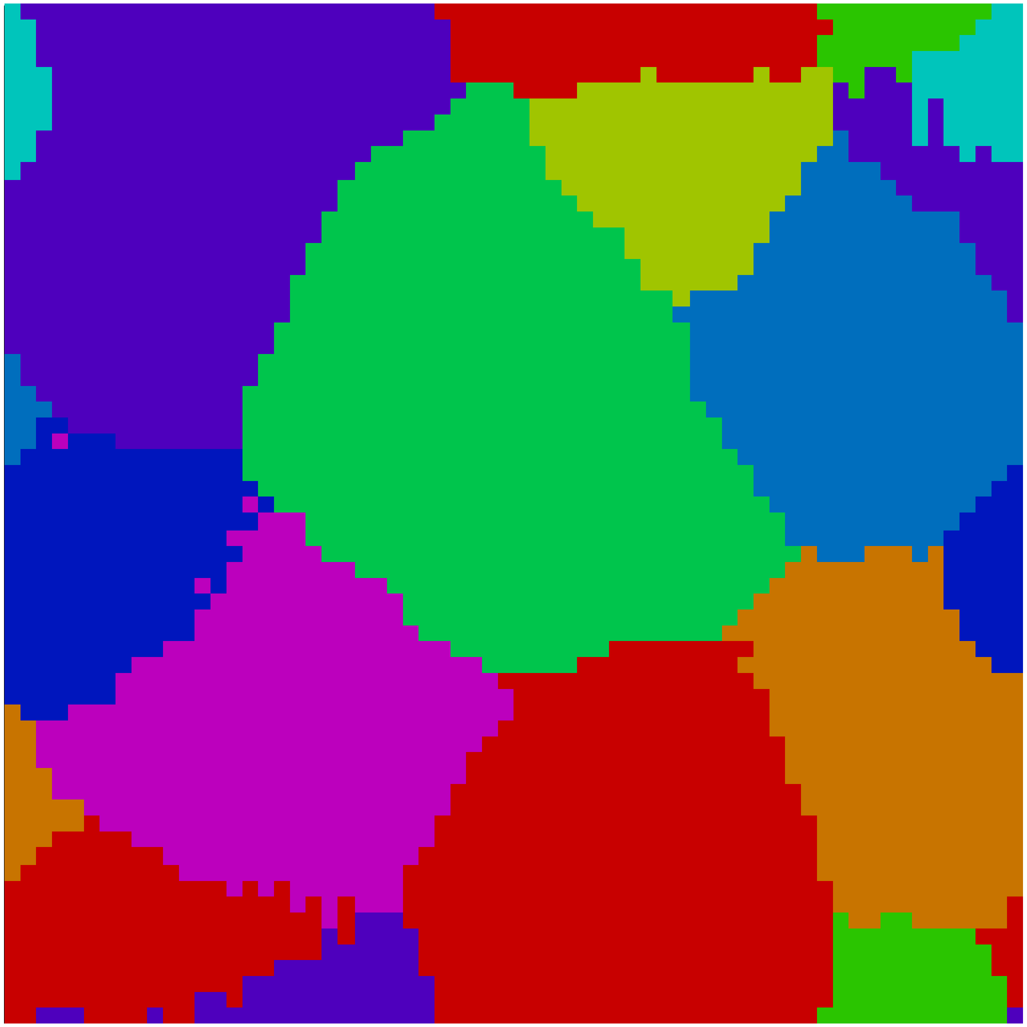

The teFFT algorithm computes stress and strain at each node in the grid; no additional mesh is needed.

Due to the FFT, periodic boundary conditions are required, though buffer layers can be used at RVE boundaries

DEPARTMENT OF MATERIALS SCIENCE AND ENGINEERING

Thermoelastic FFT

$$(1)\ \varepsilon(x) = C^{-1}(x):\sigma(x) + \varepsilon^{*}(x)$$

stiffness tensor of homogeneous solid

$$(2)\ \sigma(x) = \sigma(x) + C^{o}:\varepsilon(x) - C^{o}:\varepsilon(x)$$

$$\sigma(x) = C^{o}:\varepsilon(x) + \left(\sigma(x) - C^{o}:\varepsilon(x)\right)$$

$$\sigma(x) = C^{o}:\varepsilon(x) + \tau(x)$$

perturbation in stress field

$$(3)\ \sigma_{ij,j} = 0$$

$$C^{o}_{ijkl}u_{k,lj}(x) + \tau_{ij,j}(x) = 0$$

periodic boundary conditions in RVE

$$(4)\ C^{o}_{ijkl}G_{km,lj}(x - x') + \delta_{im}\delta(x - x') = 0$$

$$(5)\ \tilde{\varepsilon}_{ij}(x) = \mathrm{sym}\left(\int_{R^3} G_{ik,jl}(x - x')\tau_{kl}(x')dx'\right) \Rightarrow \tilde{\varepsilon}_{ij} = \Gamma^{o}_{ijkl} * \tau_{kl}$$

$$\Rightarrow \mathrm{fft}\left(\varepsilon_{ij} = \Gamma^{o}_{ijkl} * \tau_{kl}\right) \Rightarrow \hat{\tilde{\varepsilon}}_{ij} = \hat{\Gamma}^{o}_{ijkl} : \hat{\tau}_{kl}$$

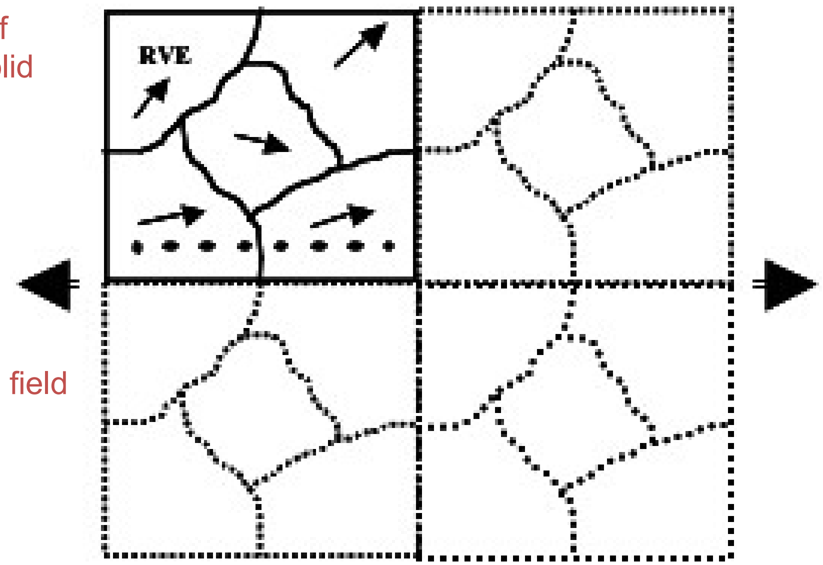

Notation
Strain: ε
Stress: σ
Stiffness: C
Perturbation Stress: τ
Displacement: u
Green's function: G
Xformed Green's: Γ

R.A. Lebensohn, Acta Materialia, vol. 49, pp. 2723-2737, 2001
B.S. Anglin, PhD Thesis, 2012

DEPARTMENT OF MATERIALS SCIENCE AND ENGIN

Extreme Value Analysis

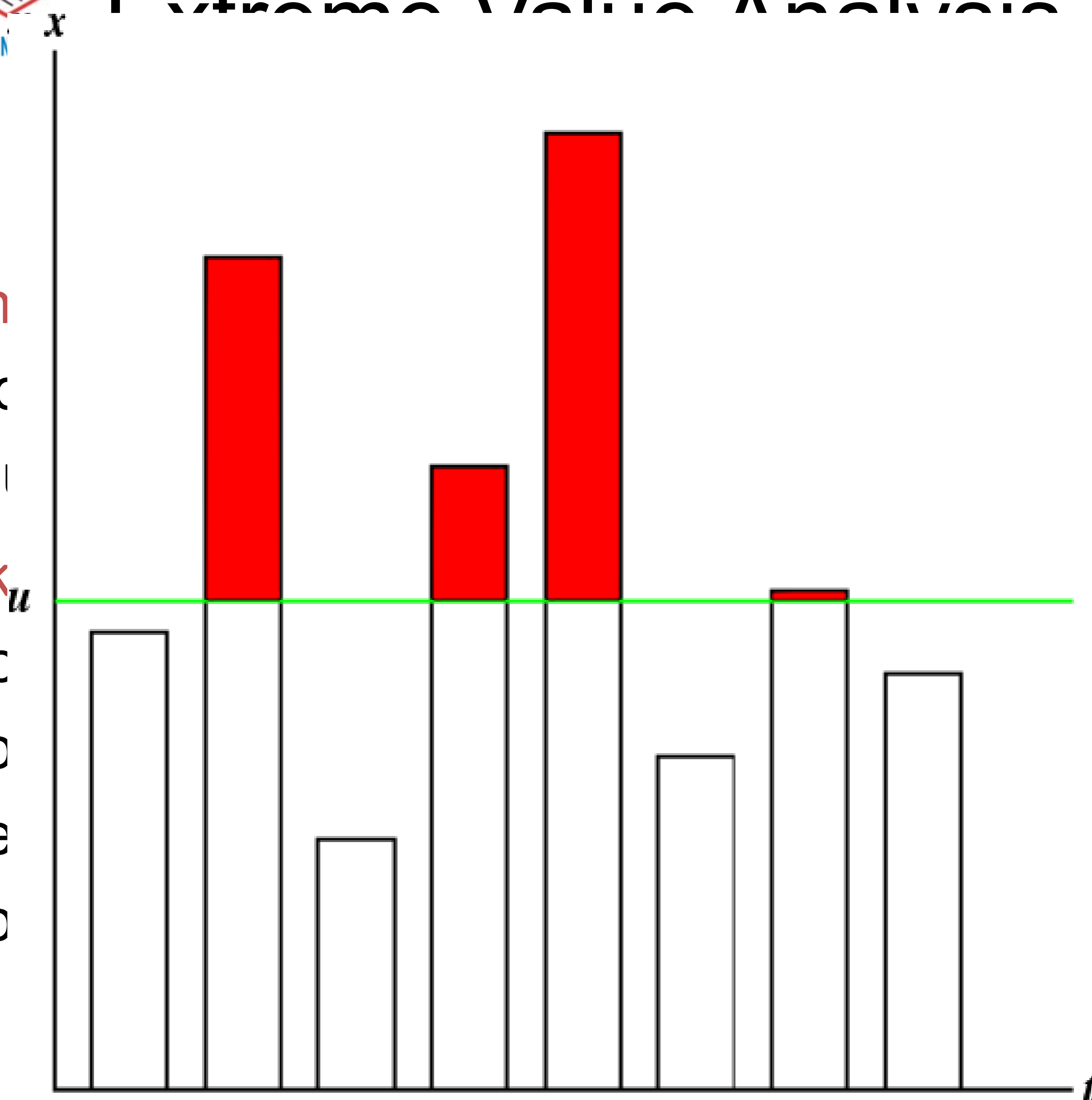

- Fish ... mum of a ranc ... either the G...
- Pick ... me unknc ... distrib ... , conve ... reto distrib

R.A. Fisher and L.H.C. Tippett, Mathematical Proceedings of the Cambridge Philosophical Society, vol. 24, pp. 180-190, 1927
J. Pickands, Annals of Statistics, vol. 3, pp. 119-131, 1975

Extreme Value Analysis

$$G_{\xi,\mu,\sigma}(x) = \begin{cases} 1 - \left(1 + \frac{\xi(x-\mu)}{\sigma}\right)^{-\frac{1}{\xi}} & \text{if } \xi \neq 0 \\ 1 - \exp\left(-\frac{x-\mu}{\sigma}\right) & \text{if } \xi = 0 \end{cases}$$

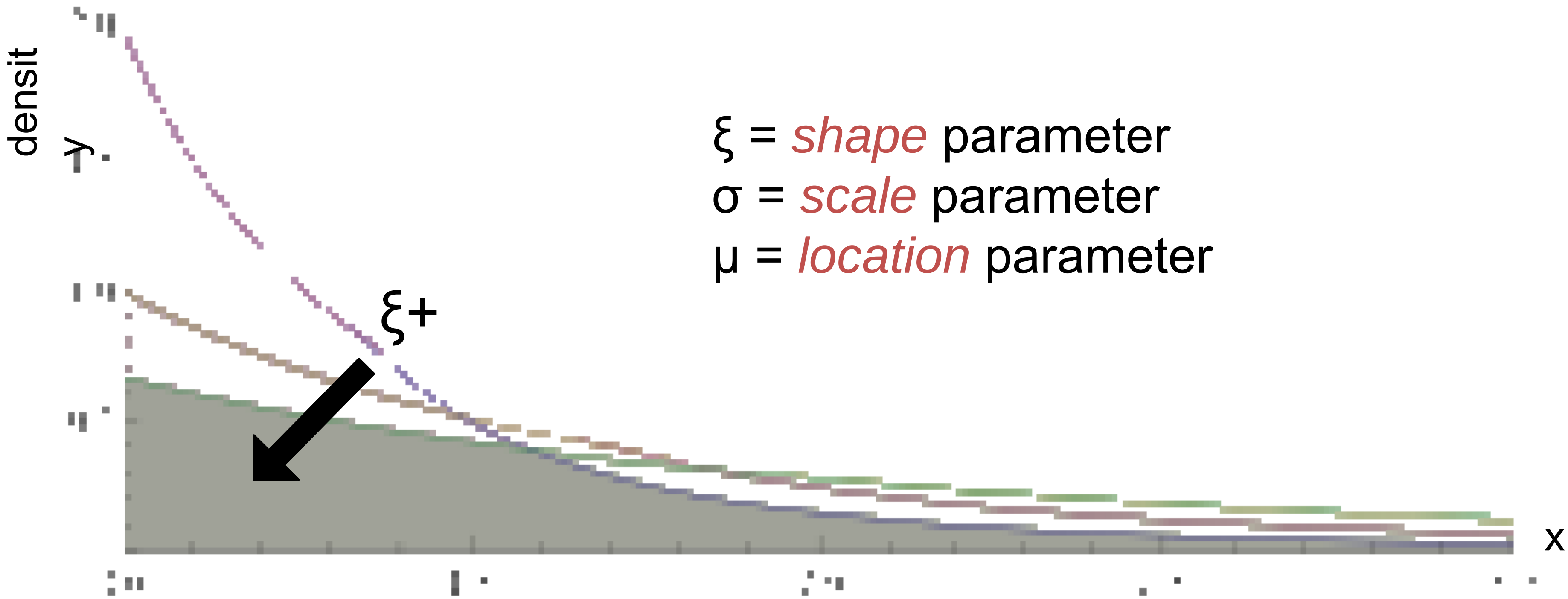

ξ = *shape* parameter
σ = *scale* parameter
μ = *location* parameter

DEPARTMENT OF
MATERIALS SCIENCE AND ENGINEERING

Outline

Introduction
- Motivation
- Objectives

Background
- Thermoelastic Stress
- Thermal Barrier Coatings
- Materials Selection
- Synthetic Structure Creation

Analytical Techniques
- Thermoelastic FFT
- Extreme Value Analysis

Results
- Resolution Dependence
- Elastic Energy Density of Thermal Barrier Coatings
  - MAX Phase BCs
  - Industry Standard Systems

Conclusions

Future Work
- Microstructure Generation
- Hot Spots in Relation to Microstructural Features

DEPARTMENT OF MATERIALS SCIENCE AND

32^3 structu

128^3 struct

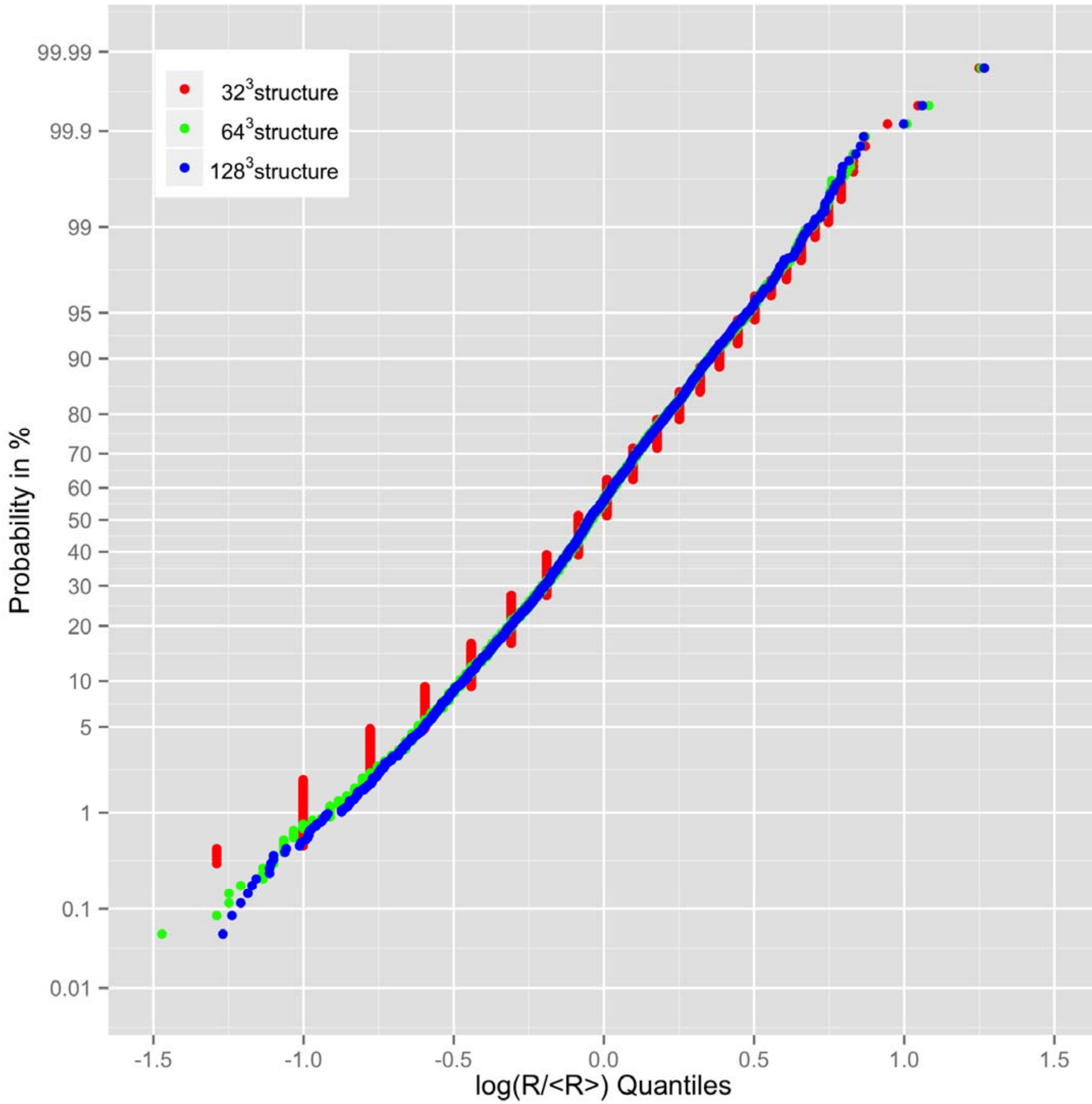

DEPARTMENT OF MATERIALS SCIENCE AND

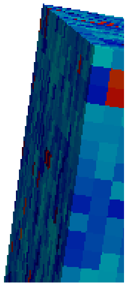

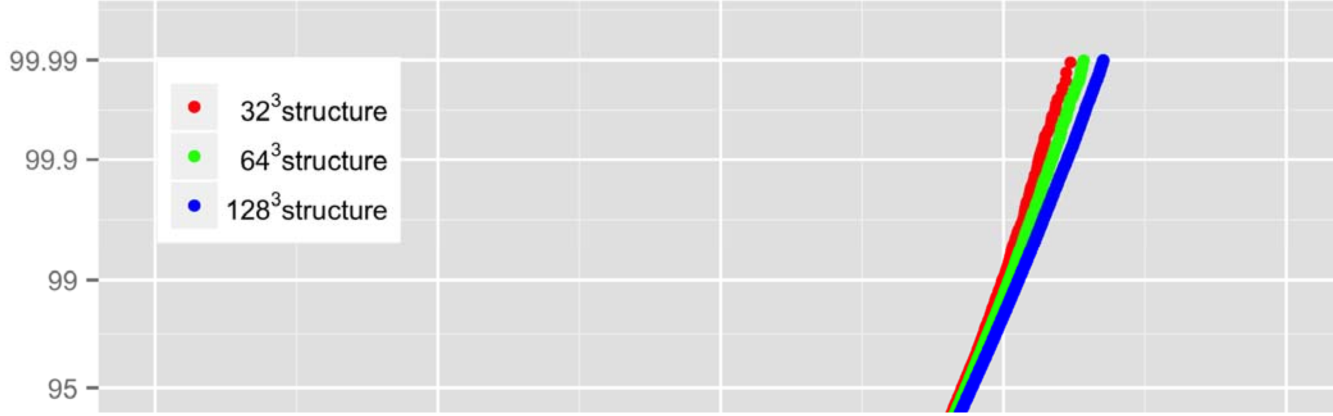

	128^3 **Microstructure**	64^3 **Microstructure**	32^3 **Microstructure**
Threshold Call, u	-14.45	-14.45	-14.45
e^u	$5.3*10^{-5}$ GPa	$5.3*10^{-5}$ GPa	$5.3*10^{-5}$ GPa
Points	2097152	262144	32768
Points Above Threshold	238390	26860	3254
Fraction Above Threshold	0.1137	0.1025	0.0993
Scale, σ (SE)	0.2796 ($1.9*10^{-6}$)	0.2664 (0.001771)	0.2481 (0.005201)
Shape, ξ (SE)	-0.167 ($1.9*10^{-6}$)	-0.1942 (0.002906)	-0.2159 (0.012096)

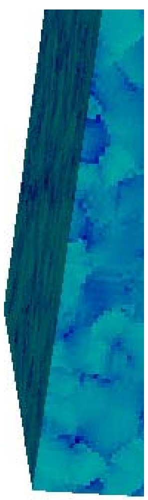

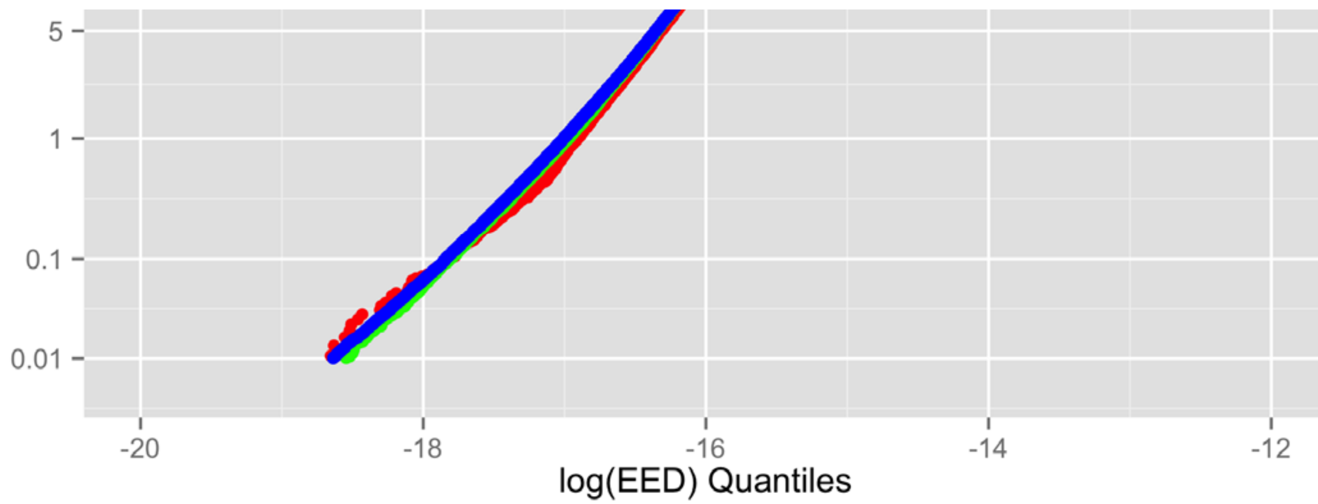

ϵ_{ij}

MAX Phase BCs

$M_{n+1}AX_n$ (MAX) phases are ternary hexagonal compounds composed of an early transition metal (M), an A group element (A), and either carbon or nitrogen (X).

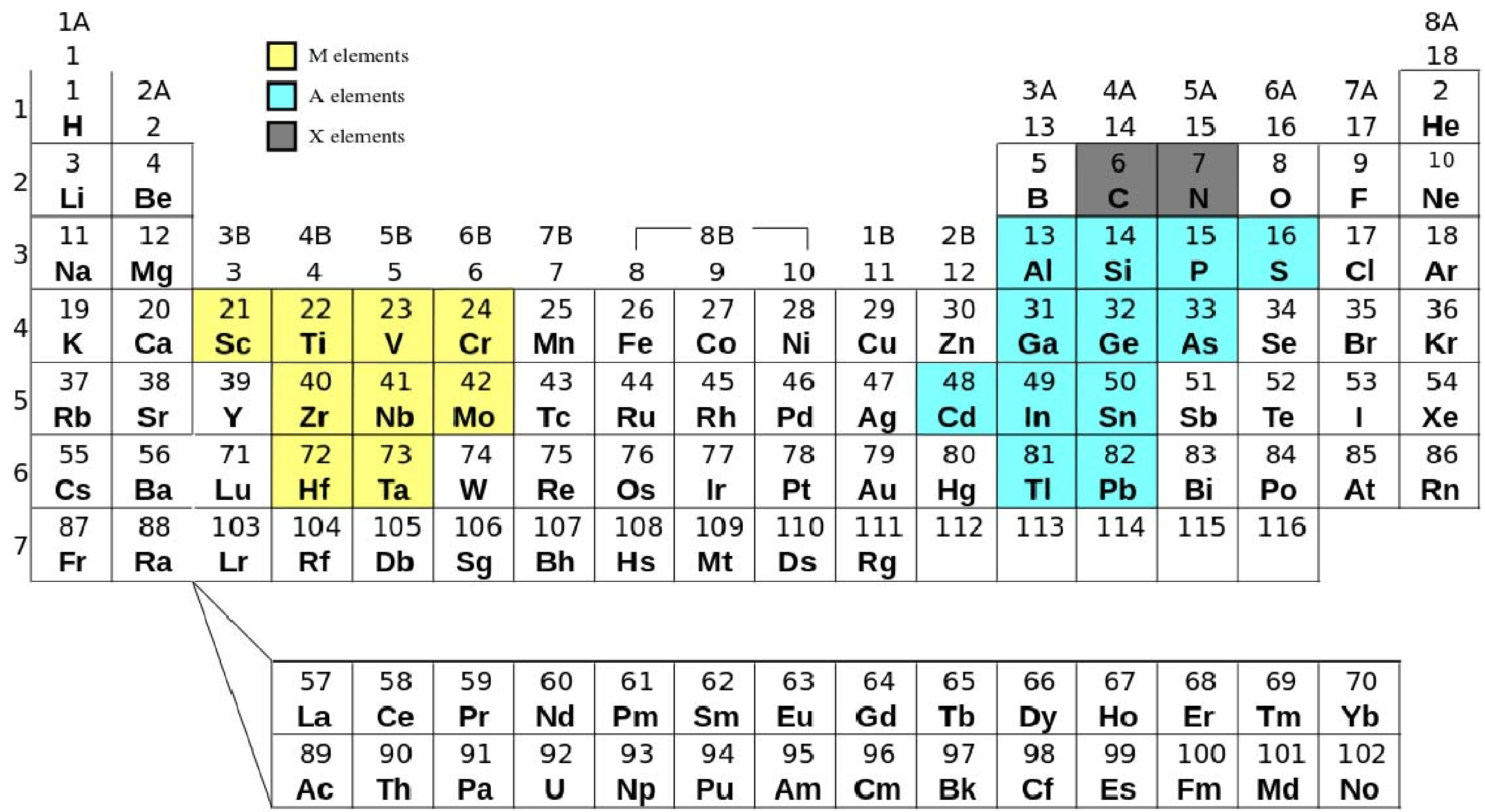

MAX Phase BCs

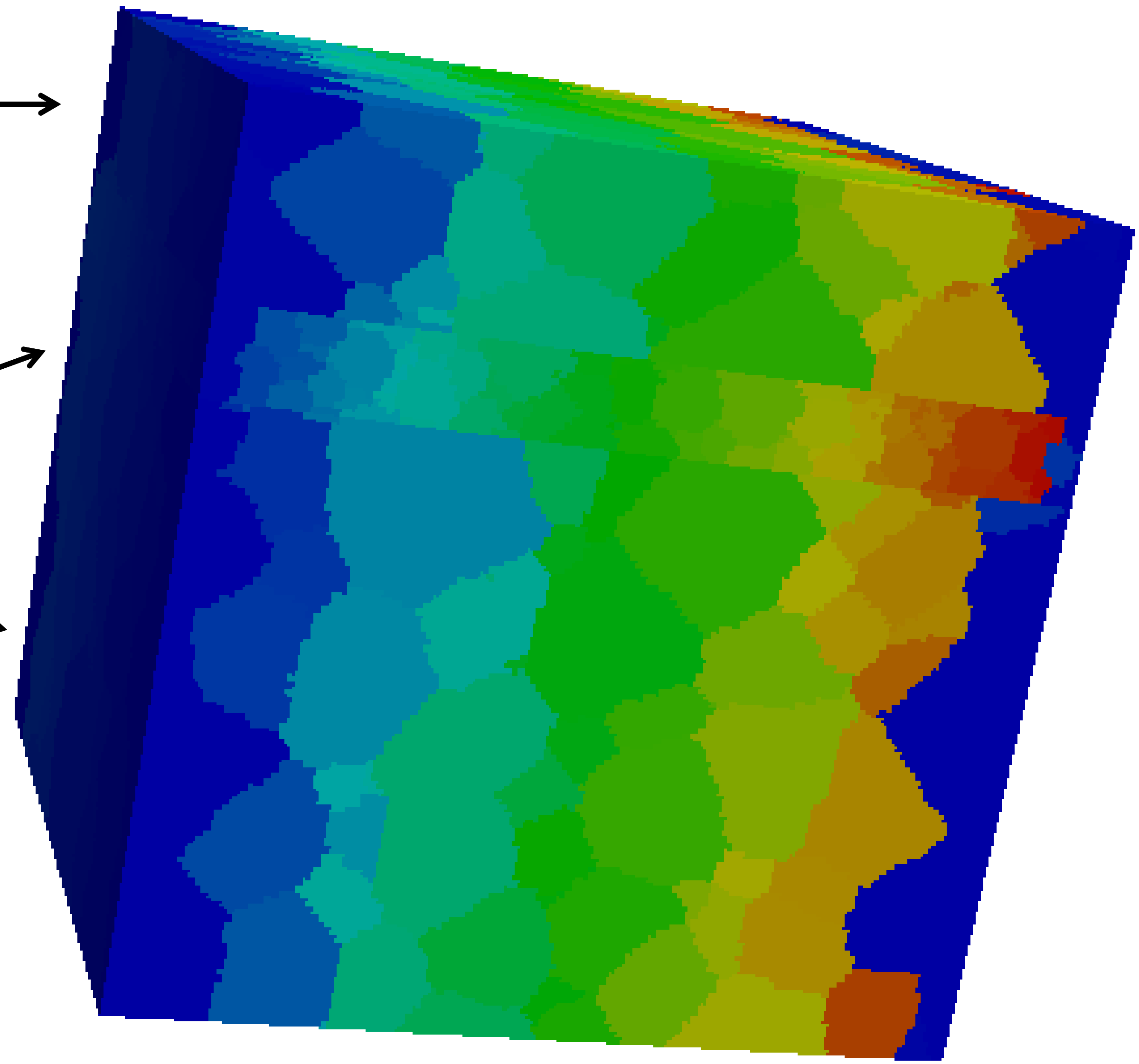

$\Delta T = 1000$ K

DEPARTMENT OF
MATERIALS SCIENCE AN

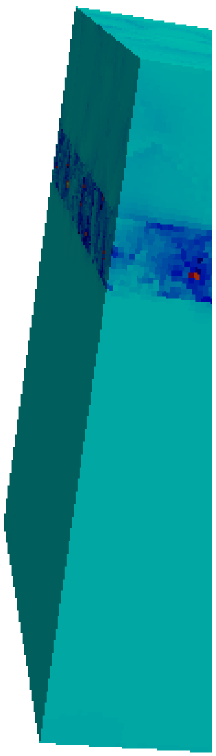

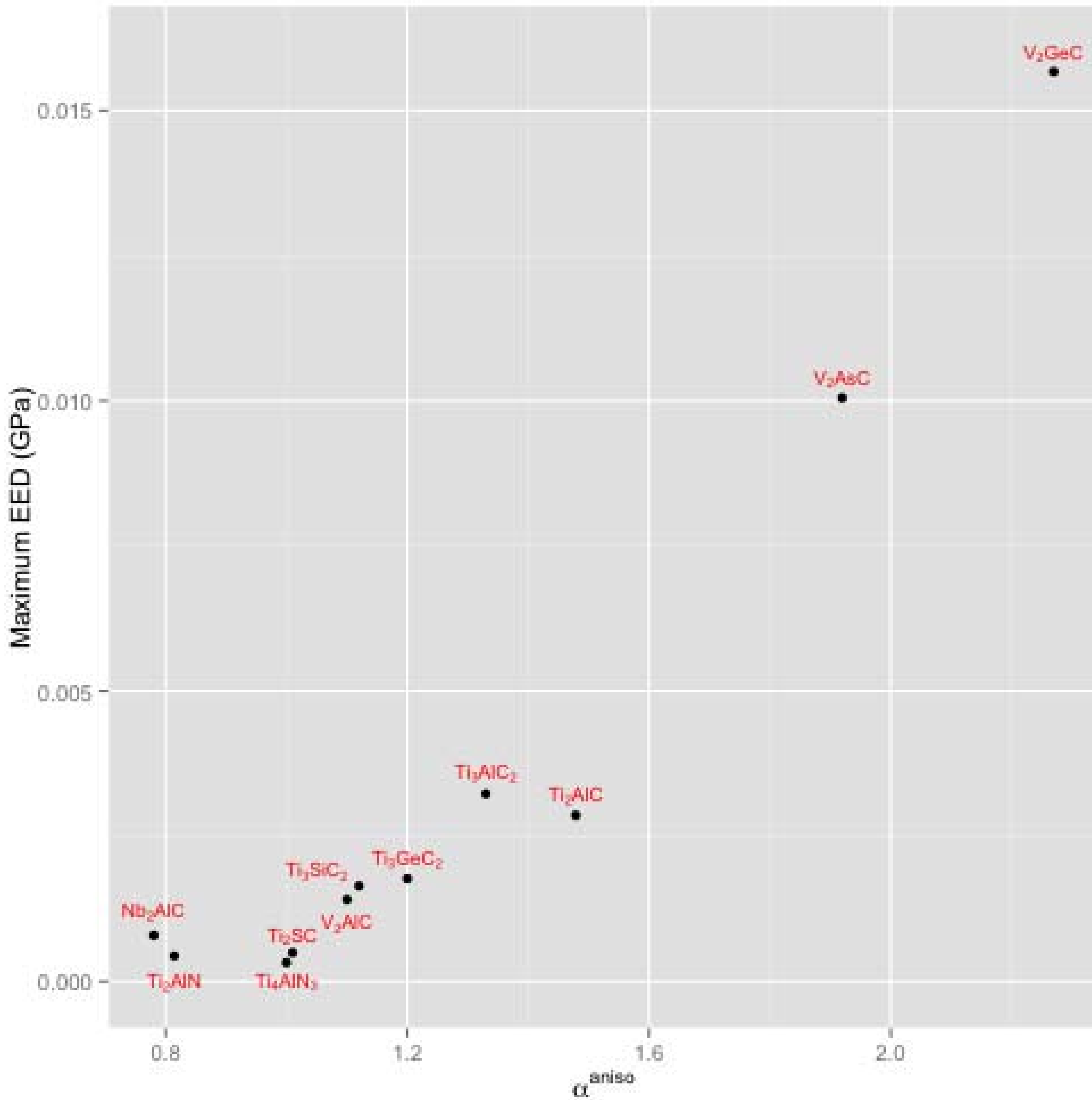

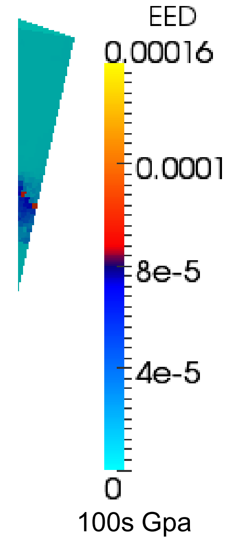

DEPARTMENT OF MATERIALS SCIENCE AND ENGINEERING

Industry Standard Systems

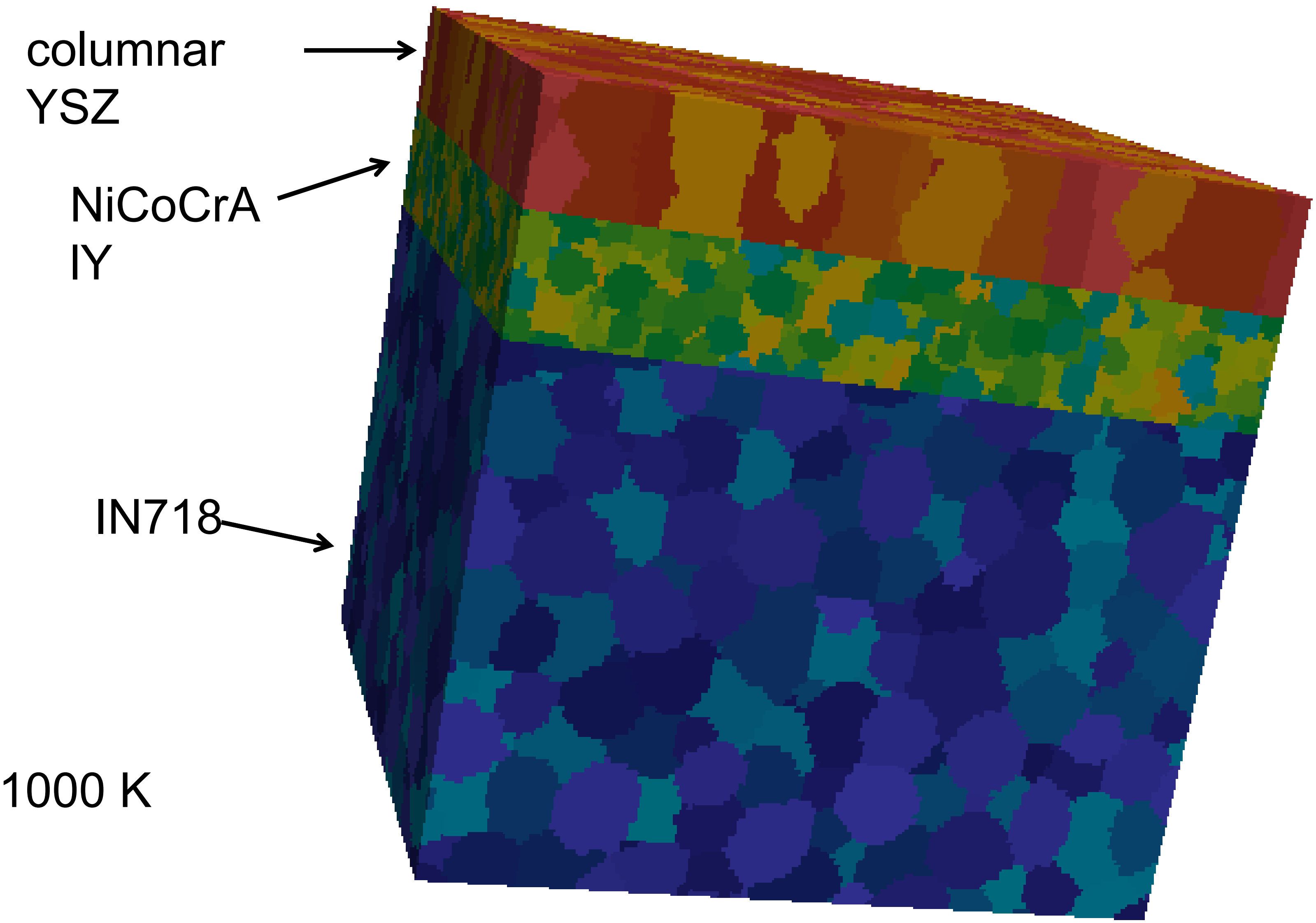

ΔT = 1000 K

Industry Standard Systems

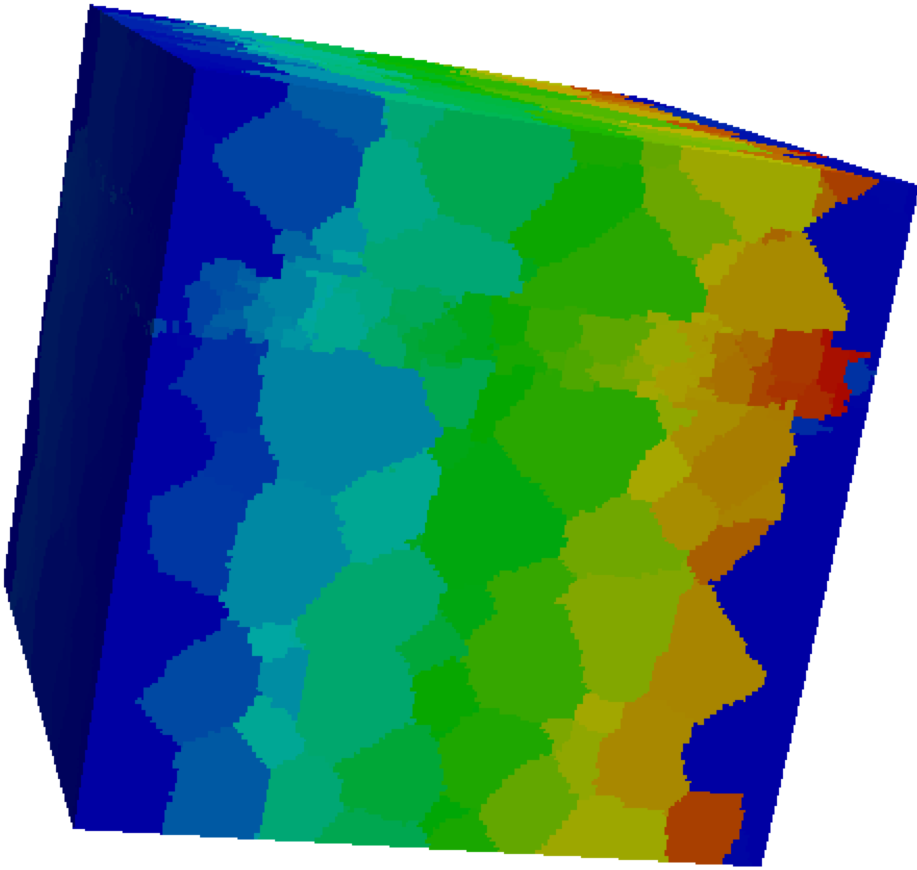

periodic structure

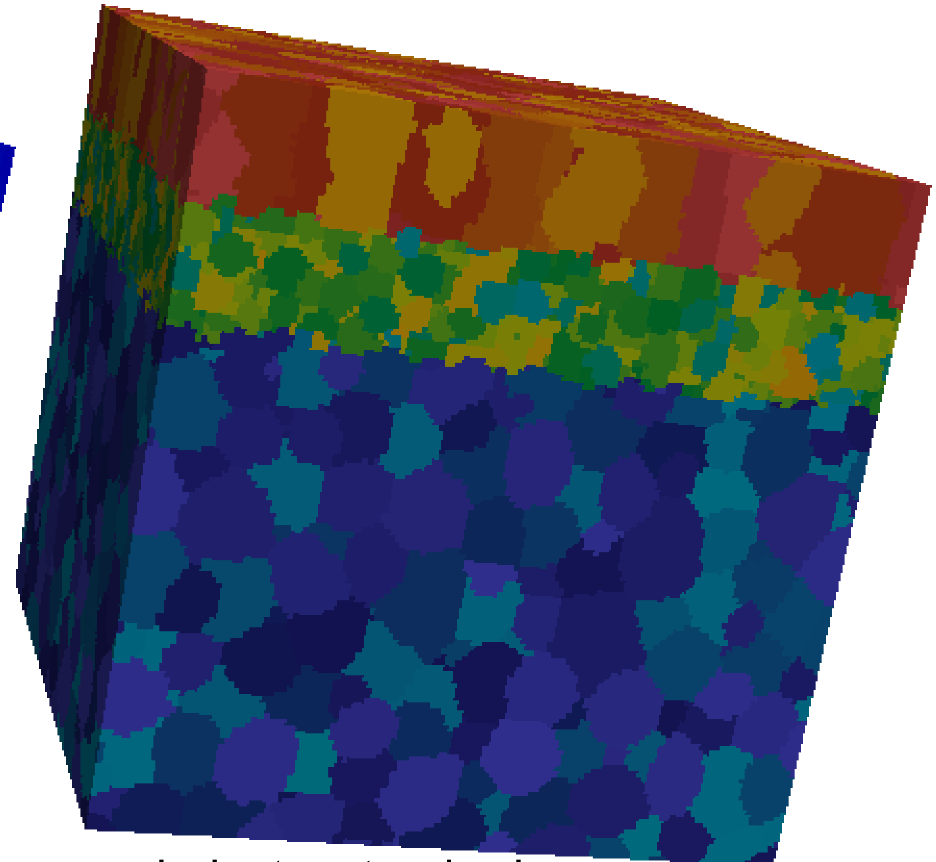

industry standard structure

TBCs used in industry display roughened interfaces either due to deposition technique or cyclic BC creep. A Potts model grain growth approach was used to locally roughen grains near the interfaces.

Industry Standard Systems

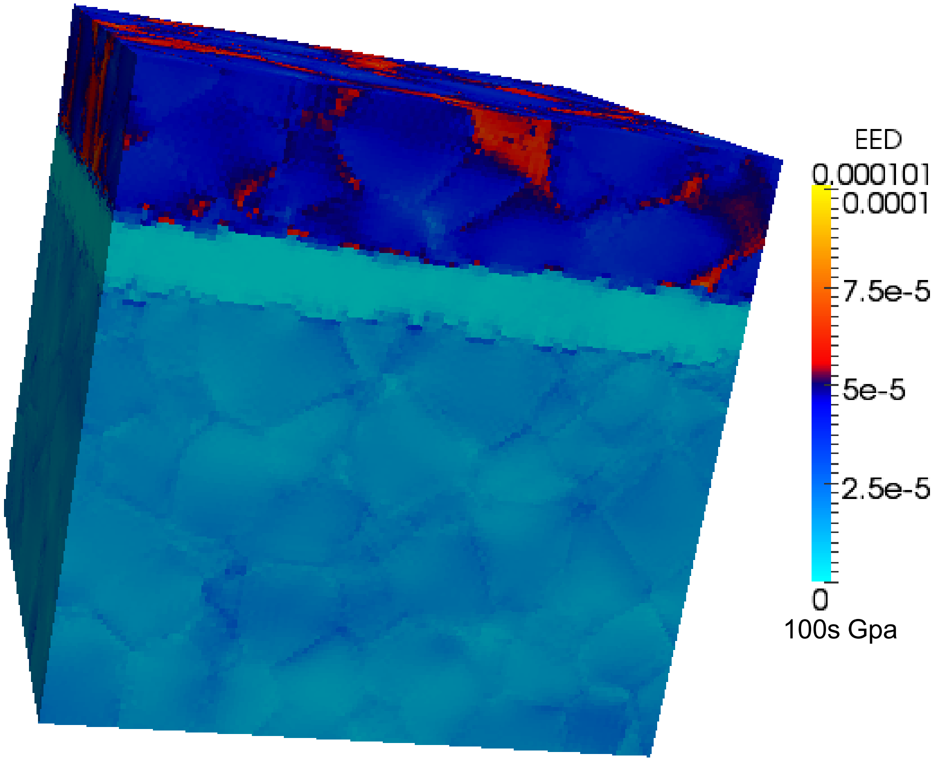

periodic structure

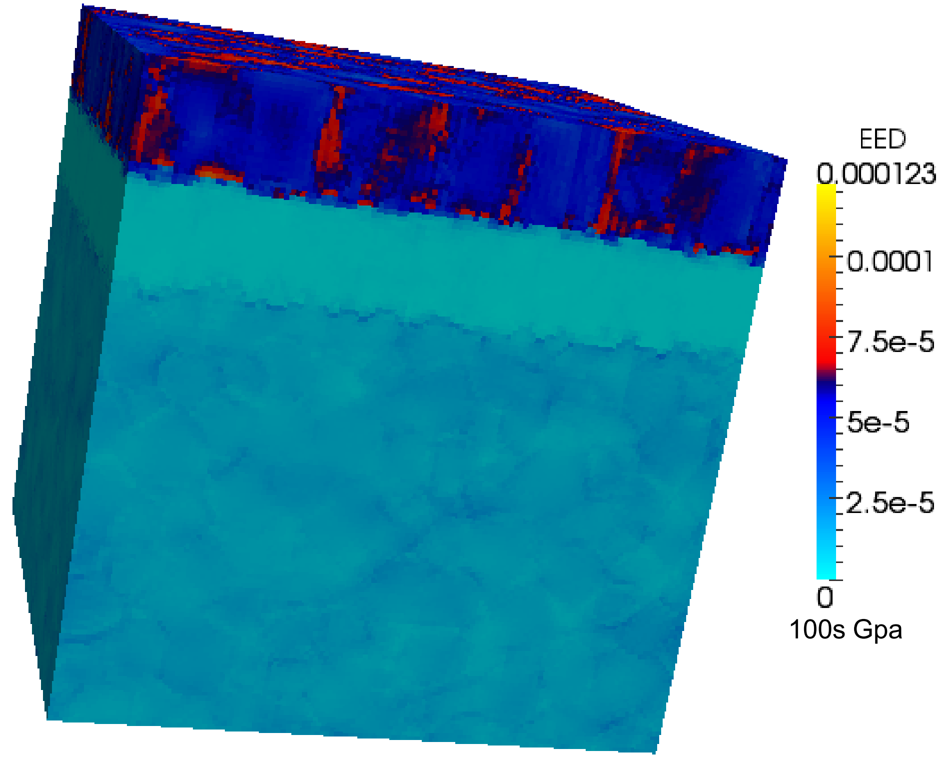

industry standard structure

Microstructure	Maximum Principle Stress (GPa)	Maximum EED (GPa)
Periodic, flat interfaces	2.091	0.00949
Periodic, rough interfaces	2.399	0.01011
Industry Standard, flat interfaces	2.148	0.01106
Industry Standard, rough interfaces	2.226	0.01226

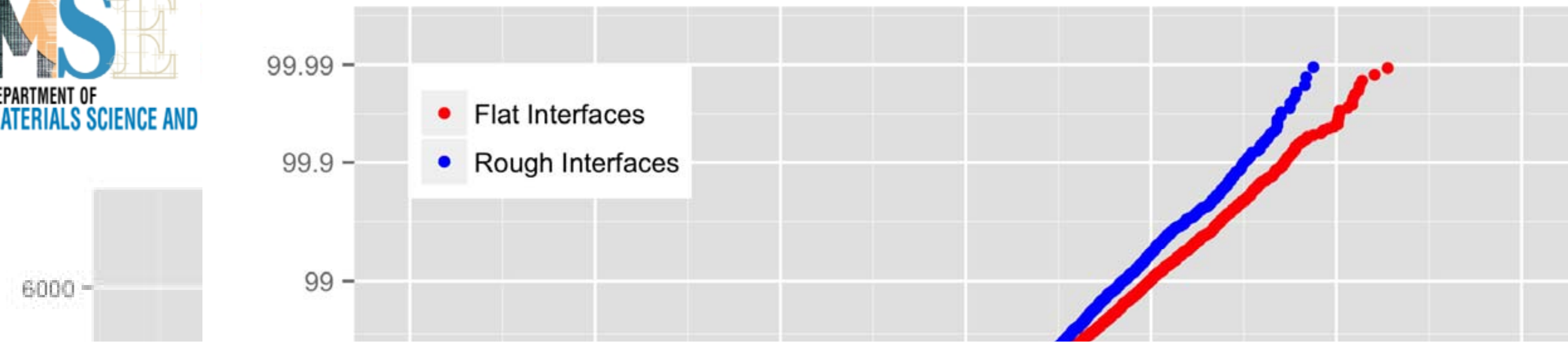

	Flat Interface	Rough Interface
Threshold Call, u	-9.4	-9.4
e^u	$8.27*10^{-5}$ GPa	$8.27*10^{-5}$ GPa
Points	32688	50245
Points Above Threshold	199	493
Fraction Above Threshold	0.0061	0.0098
Scale, σ (SE)	0.0678 (0.005992)	0.0726 (0.004223)
Shape, ξ (SE)	-0.2161 (0.054949)	-0.1042 (0.037174)

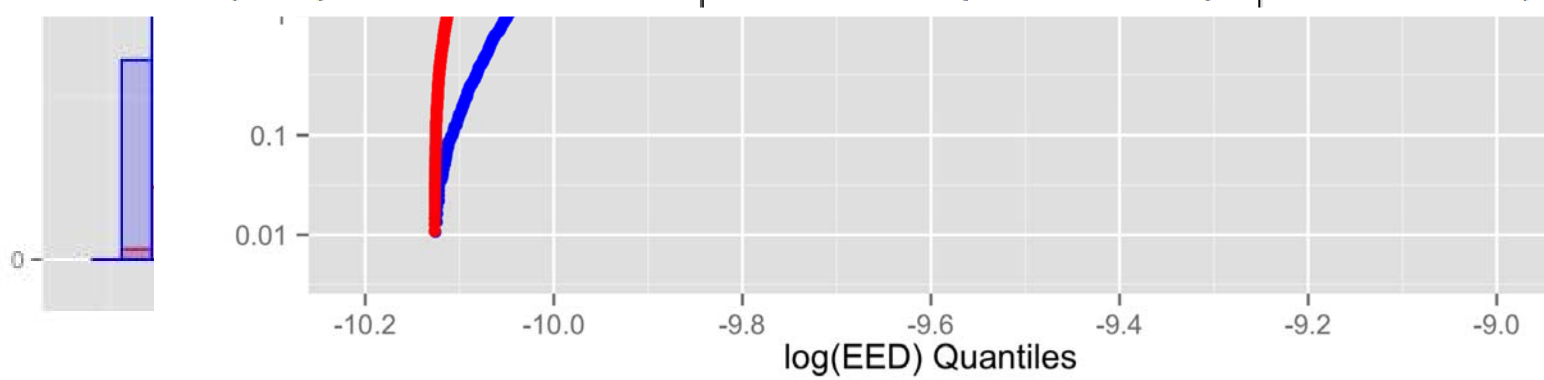

og-
r.

DEPARTMENT OF MATERIALS SCIENCE AND ENGINEERING

Outline

Introduction
- Motivation
- Objectives

Background
- Thermoelastic Stress
- Thermal Barrier Coatings
- Materials Selection
- Synthetic Structure Creation

Analytical Techniques
- Thermoelastic FFT
- Extreme Value Analysis

Results
- Resolution Dependence
- Elastic Energy Density of Thermal Barrier Coatings
  - MAX Phase BCs
  - Industry Standard Systems

Conclusions

Future Work
- Microstructure Generation
- Hot Spots in Relation to Microstructural Features

Future Work

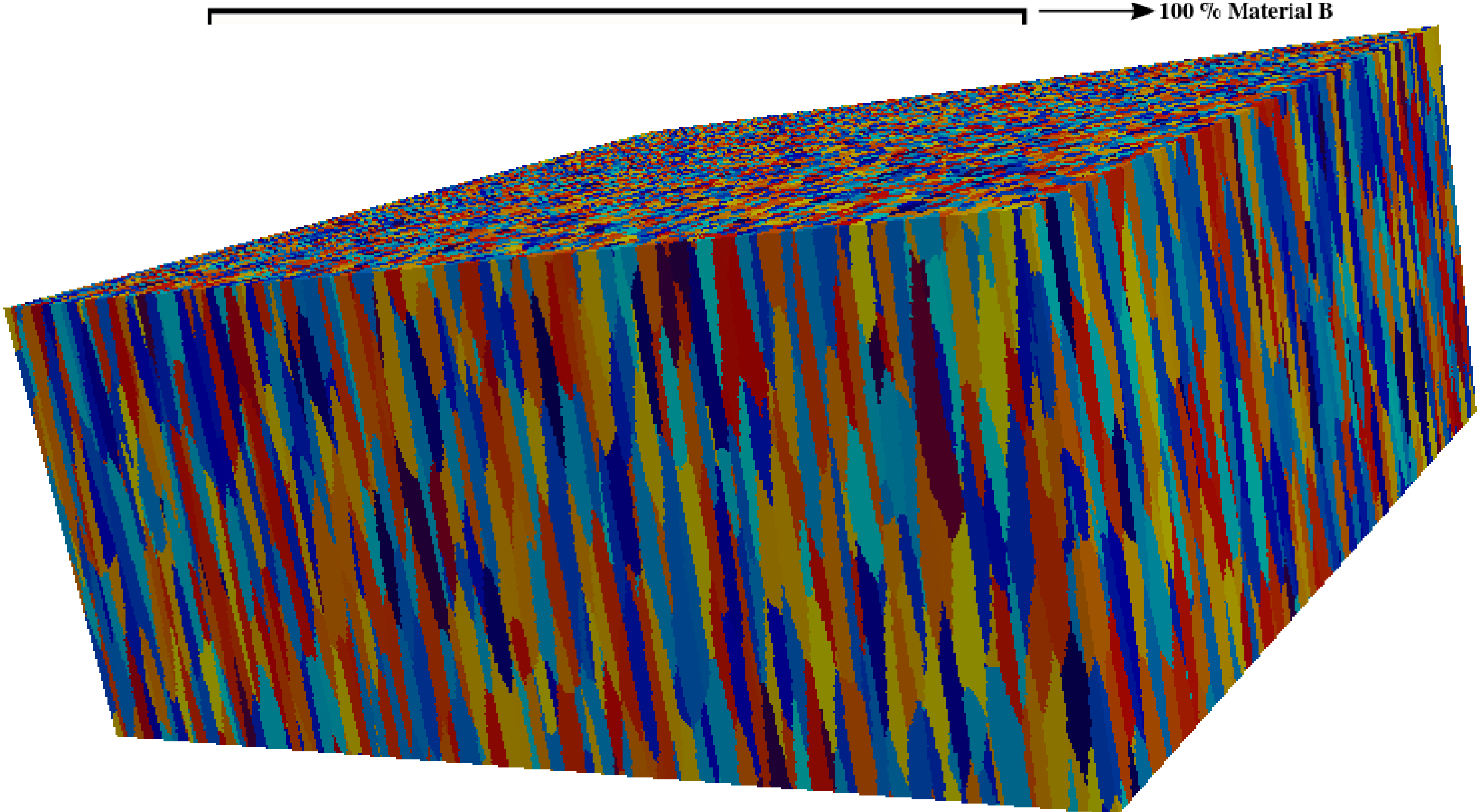

of APS top coats; porosity and cracking in all top coat morphologies.

THANK YOU!

Supplemental Slides

Thermoelastic Stress

Thermal Expansion Tensors

Transformation of thermal expansion tensor:

$$\alpha'_{ij} = O\alpha_{ij}O^T$$

Thermal expansion tensors of various crystal symmetries:

$$\text{cubic} = \begin{pmatrix} \alpha & 0 & 0 \\ 0 & \alpha & 0 \\ 0 & 0 & \alpha \end{pmatrix} \qquad \text{hexagonal} \sim \text{trigonal} = \begin{pmatrix} \alpha_{11} & 0 & 0 \\ 0 & \alpha_{11} & 0 \\ 0 & 0 & \alpha_{33} \end{pmatrix}$$

Stiffness Tensors

Symmetry of the stiffness tensor:

$$C_{ijkl} = C_{jikl} = C_{ijlk} = C_{jilk}$$

Stiffness tensor using Voigt notation:

$$\begin{pmatrix} \sigma_1 \\ \sigma_2 \\ \sigma_3 \\ \sigma_4 \\ \sigma_5 \\ \sigma_6 \end{pmatrix} = \begin{pmatrix} C_{11} & C_{12} & C_{13} & C_{14} & C_{15} & C_{16} \\ C_{21} & C_{22} & C_{23} & C_{24} & C_{25} & C_{26} \\ C_{31} & C_{32} & C_{33} & C_{34} & C_{35} & C_{36} \\ C_{41} & C_{42} & C_{43} & C_{44} & C_{45} & C_{46} \\ C_{51} & C_{52} & C_{53} & C_{54} & C_{55} & C_{56} \\ C_{61} & C_{62} & C_{63} & C_{64} & C_{65} & C_{66} \end{pmatrix} \begin{pmatrix} \epsilon_1 \\ \epsilon_2 \\ \epsilon_3 \\ \epsilon_4 \\ \epsilon_5 \\ \epsilon_6 \end{pmatrix}$$

Stiffness Tensors

$$\text{cubic} = \begin{pmatrix} C_{11} & C_{12} & C_{12} & 0 & 0 & 0 \\ C_{12} & C_{11} & C_{12} & 0 & 0 & 0 \\ C_{12} & C_{12} & C_{11} & 0 & 0 & 0 \\ 0 & 0 & 0 & C_{44} & 0 & 0 \\ 0 & 0 & 0 & 0 & C_{44} & 0 \\ 0 & 0 & 0 & 0 & 0 & C_{44} \end{pmatrix}$$

$$\text{hexagonal} = \begin{pmatrix} C_{11} & C_{12} & C_{13} & 0 & 0 & 0 \\ C_{12} & C_{11} & C_{13} & 0 & 0 & 0 \\ C_{13} & C_{13} & C_{33} & 0 & 0 & 0 \\ 0 & 0 & 0 & C_{44} & 0 & 0 \\ 0 & 0 & 0 & 0 & C_{44} & 0 \\ 0 & 0 & 0 & 0 & 0 & \frac{1}{2}(C_{11} - C_{12}) \end{pmatrix}$$

$$\text{trigonal} = \begin{pmatrix} C_{11} & C_{12} & C_{13} & C_{14} & 0 & 0 \\ C_{12} & C_{11} & C_{13} & -C_{14} & 0 & 0 \\ C_{13} & C_{13} & C_{33} & 0 & 0 & 0 \\ C_{14} & -C_{14} & 0 & C_{44} & 0 & 0 \\ 0 & 0 & 0 & 0 & C_{44} & 0 \\ 0 & 0 & 0 & 0 & C_{14} & \frac{1}{2}(C_{11} - C_{12}) \end{pmatrix}$$

Principal Stresses

The principal stresses are those stresses normal to planes whose normals are parallel to stress vectors with zero shear component. They are then the eigenvalues of the stress tensor, and the stress tensor can be rewritten:

$$\sigma_{ij} = \begin{pmatrix} \sigma_1 & 0 & 0 \\ 0 & \sigma_2 & 0 \\ 0 & 0 & \sigma_3 \end{pmatrix}$$

Thermal Barrier Coatings

YSZ Phase Diagrams

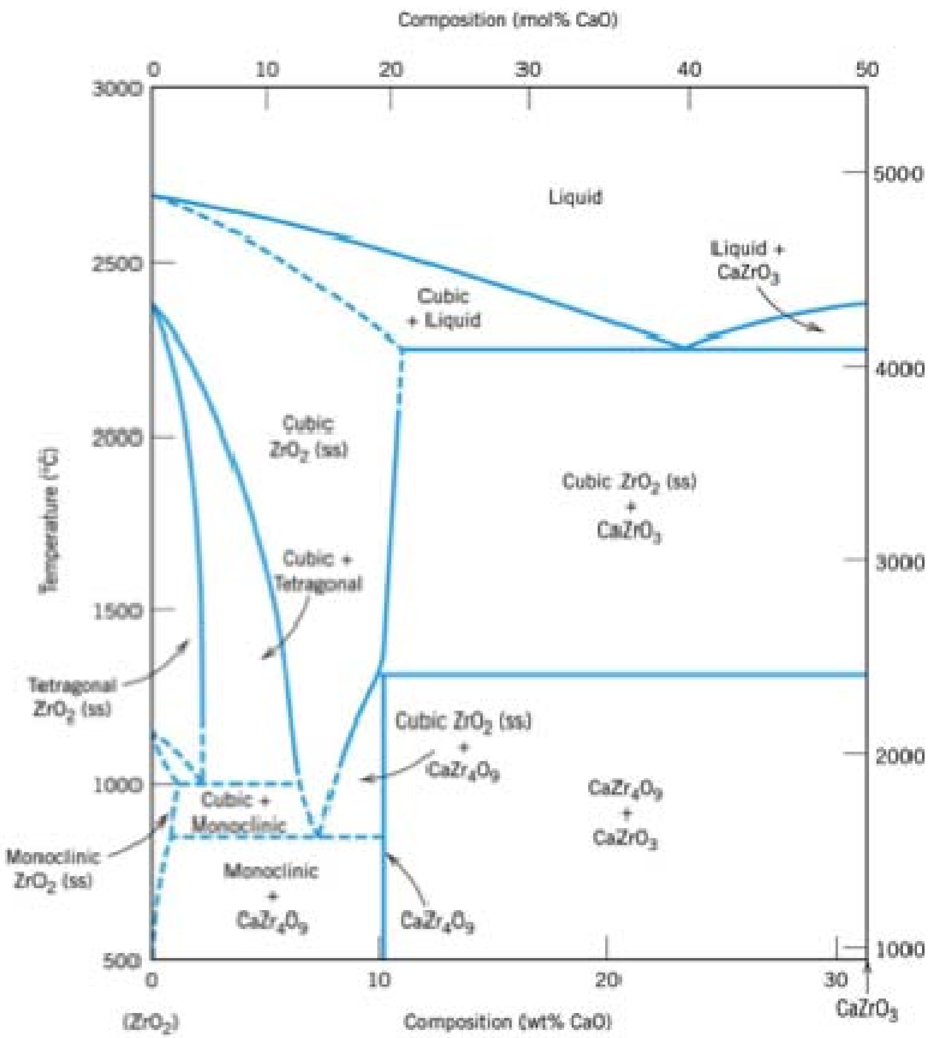

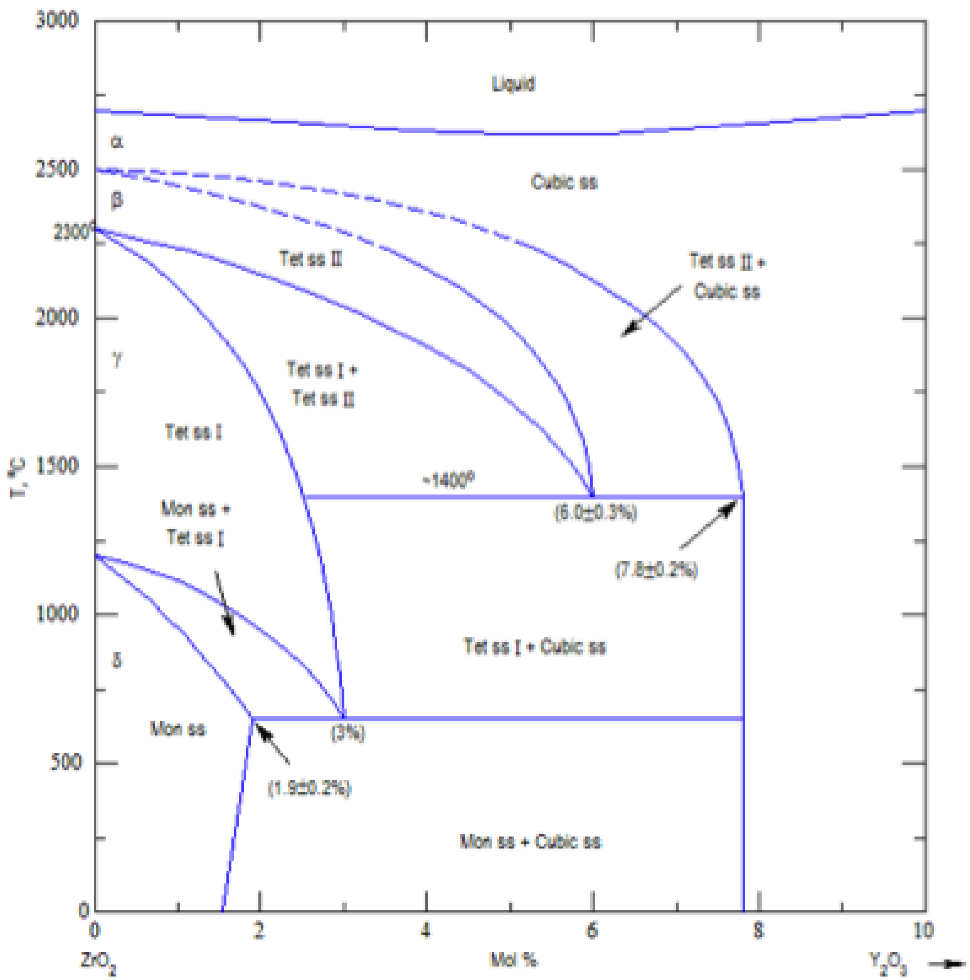

MAX Phase Unit Cell

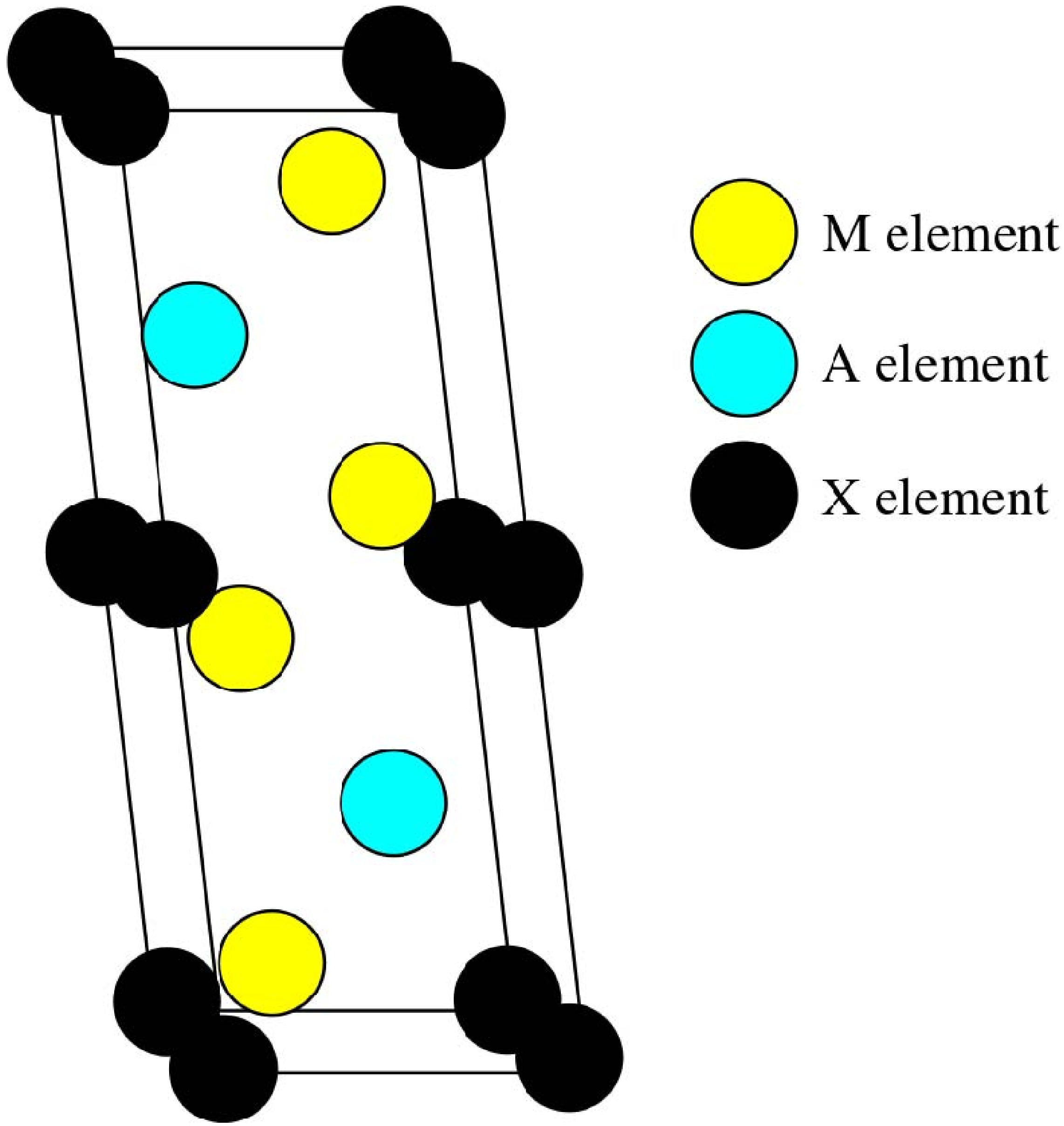

MAX Phase Space Group

$P6_3/mmc$ $P\ 6_3/m\ 2/m\ 2/c$ $6/mmm$ No. 194

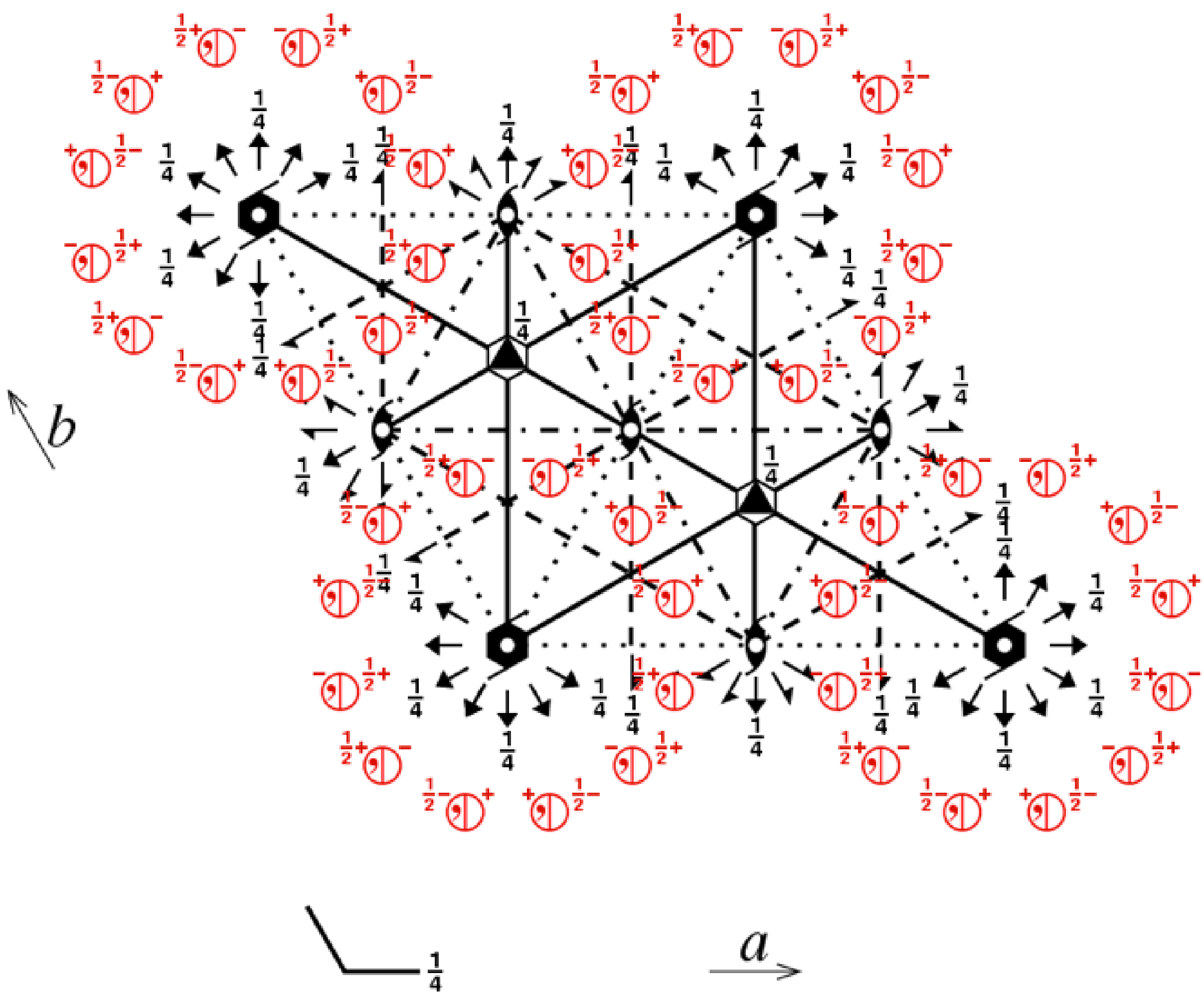

1 x, y, z
2 $\bar{y}, x-y, z$
3 $\bar{x}+y, \bar{x}, z$
4 $\bar{x}, \bar{y}, \frac{1}{2}+z$
5 $x-y, x, \frac{1}{2}+z$
6 $y, \bar{x}+y, \frac{1}{2}+z$
7 $\bar{y}, \bar{x}, z$
8 $\bar{x}+y, y, z$
9 $x, x-y, z$
10 $y, x, \frac{1}{2}+z$
11 $x-y, \bar{y}, \frac{1}{2}+z$
12 $\bar{x}, \bar{x}+y, \frac{1}{2}+z$
13 $\bar{x}, \bar{y}, \bar{z}$
14 $y, \bar{x}+y, \bar{z}$
15 $x-y, x, \bar{z}$
16 $x, y, \frac{1}{2}-z$
17 $\bar{x}+y, \bar{x}, \frac{1}{2}-z$
18 $\bar{y}, x-y, \frac{1}{2}-z$
19 $y, x, \bar{z}$
20 $x-y, \bar{y}, \bar{z}$
21 $\bar{x}, \bar{x}+y, \bar{z}$
22 $\bar{y}, \bar{x}, \frac{1}{2}-z$
23 $\bar{x}+y, y, \frac{1}{2}-z$
24 $x, x-y, \frac{1}{2}-z$

Extreme Value Analysis

Log-Normal Distribution

The log-normal distribution describes a random variable whose natural logarithm follows the normal distribution. The cumulative distribution function (cdf) of a log-normal distribution is:

$$F_{\mu,\sigma}(x) = \frac{1}{2}\operatorname{erfc}\left[-\frac{\ln(x)-\mu}{\sigma\sqrt{2}}\right] = \Phi\left[\frac{\ln(x)-\mu}{\sigma}\right]$$

Fisher-Tippett-Gnedenko Theorem

Consider a set of random variables $X_1, X_2, X_3, \ldots, X_n$. Let $M_n = \max(X_1, X_2, \ldots, X_n)$. Now suppose two normalizing constants $a_n > 0$ and b_n exist such that:

$$\lim_{n\to\infty} P\left(\frac{M_n - b_n}{a_n} \leq x\right) = F(x)$$

According to the first theorem in extreme value theory, referred to as the Fisher-Tippett-Gnedenko theorem, F(x) must be a particular case of the generalized extreme value (GEV) distribution, defined as:

$$GEV(x) = \exp\left\{-\left(1 + \xi\frac{x-\mu}{\sigma}\right)^{\frac{1}{\xi}}\right\}$$

Pickands-Balkema-de Haan Theorem

The interest is in approximating F_u, the distribution function of X above the threshold u. F_u is defined as follows:

$$F_u(x) = P(X - u \leq x \mid X > u) = \frac{F(u+x) - F(u)}{1 - F(u)}$$

Given an unknown underlying distribution function F, the conditional excess distribution, F_u, converges to the GPD as the threshold approaches the right endpoint of F. Alternatively:

$$F_u(x) \to G_{\xi,\sigma}(x) \text{ as } u \to \infty$$

Threshold Choice Plots

The threshold choice plot shows how an increasing threshold affects the value of the scale (σ) and the shape (ξ) parameter. Consider a random variable X that is distributed as $G_{\xi 0, \mu 0, \sigma 0}$. The location parameter, μ_0, is the same as the threshold call. Now allow another threshold, $\mu_1 > \mu_0$. The new random variable X | X > μ_1 is also described by the GPD. The updated parameters are $\sigma_1 = \sigma_0 + \xi_0(\mu_1 - \mu_0)$ and $\xi_1 = \xi_0$. Let $\sigma_* = \sigma_1 - \xi_1\mu_1$.

In this new parameterization, σ_* is independent of μ_0. Therefore, σ_* and ξ_1 are constant above μ_0 if μ_0 is a reasonable threshold choice. The threshold choice plot displays graphically σ_* and ξ_1 against a range of thresholds. Reasonable threshold choices occur where σ_* and ξ_1 remain constant. Confidence intervals are calculated using the profile likelihood method

Profile Likelihood Confidence Intervals

Likelihood ratio statistic:

$$2\ln\left[\frac{L(\hat{\theta})}{L(\theta_0)}\right] \sim \chi^2$$

The 95% confidence interval for θ is then all values of θ_0 for which the following inequality holds:

$$2\ln\left[\frac{L(\hat{\theta})}{L(\theta_0)}\right] < \chi^2(0.95)$$

Mean Residual Life Plots

The mean residual life plot consists of the points:

$$\left\{ \left(\mu, \frac{1}{n_\mu} \sum_{i=1}^{n_\mu} x_i - \mu \right) : \mu \leq x_{\max} \right\}$$

Since the empirical mean is assumed normally distributed by the central limit theorem, confidence intervals can also be plot- ted. The data are a good fit to the GPD where the mean residual life plot follows a straight line.

DEPARTMENT OF MATERIALS SCIENCE AND ENGINEERING

Return Periods

Return period related to the probability of non-exceedance:

$$T = \frac{1}{npy(1-p)}$$

Quantile function of the GPD:

$$G^{-1}_{\xi,\mu,\sigma}(p) - \mu + \frac{\sigma((1-p)^{-\xi} - 1)}{\xi}$$

Thermoelastic FFT

Stress Equilibrium

$$\begin{cases} \frac{\delta \sigma_{xx}}{\delta x} + \frac{\delta \sigma_{xy}}{\delta y} + \frac{\delta \sigma_{xz}}{\delta z} = 0 \\ \frac{\delta \sigma_{yx}}{\delta x} + \frac{\delta \sigma_{yy}}{\delta y} + \frac{\delta \sigma_{yz}}{\delta z} = 0 \\ \frac{\delta \sigma_{zx}}{\delta x} + \frac{\delta \sigma_{zy}}{\delta y} + \frac{\delta \sigma_{zz}}{\delta z} = 0 \end{cases}$$

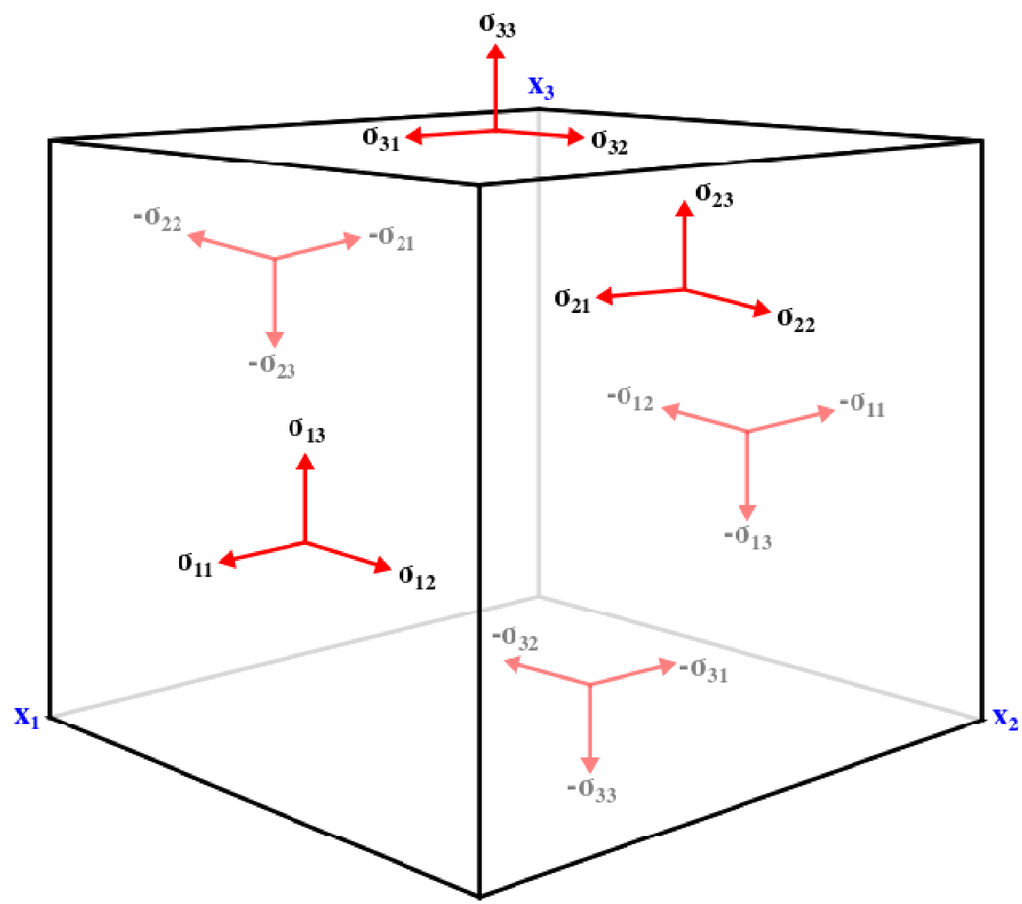

Compatibility

For infinitesimal strains, compatibility is satisfied if the following equation holds:

$$\epsilon_{ij} = \frac{1}{2}(u_{i,j} + u_{j,i})$$

Compatibility ensures a unique strain field is obtainable from a particular displacement field. Conceptually, if a continuous body is thought to be divided into infinitesimal volumes, compatibility describes the necessary conditions under which the body deforms without developing gaps or overlaps between said volumes.

Thermoelastic FFT

Modified Hooke’s Law with incorporated eigentrains in reference to a homogeneous medium:

$$\sigma_{ij}(x) = C^{o}_{ijkl} : (\epsilon_{kl}(x) - \epsilon^{*}_{kl}(x)) + \tau_{ij}(x)$$

Application of stress equilibrium:

$$C^{o}_{ijkl} u_{k,lj}(x) + \tau_{ij,j}(x) = 0$$

Thermoelastic FFT

Application of Green's function:

$$C^{o}_{ijkl}G_{km,lj}(x-x')+\delta_{im}\delta(x-x')=0$$

Application of periodic Green's function to perturbation in stress field:

$$\tilde{u}_k=\int_V G_{ki}(x-x')\tau_{ij,j}(x')\mathrm{d}x'$$

Thermoelastic FFT

Application of compatibility:

$$\epsilon_{ij}(x) - E_{ij} + sym\left(\int_V G_{ik,jl}(x - x')\tau_{kl}(x')\mathrm{d}x'\right)$$

Application of FFT:

$$C^o_{ijkl}\xi_l\xi_j\hat{G}_{km} = \delta_{im}$$

Periodic Green's function in frequency space:

$$\hat{\Gamma}^o_{ijkl} = -(\xi_p\xi_q C^o_{ipkq})^{-1}\xi_j\xi_l$$

Augmented Lagrangian

Non-linear response equation at each iteration:

$$\frac{\delta w}{\delta e}(x, e^i) + C^o : e^i(x) = C^o : \epsilon^i(x) + \lambda^{i-1}(x)$$

Non-linear strain field at each iteration:

$$\lambda^i(x) = \lambda^{i-1}(x) + C^o : (\epsilon^i(x) - e^i(x))$$

Initializations for teFFT

$$
\begin{aligned}
E^0 &= \langle \epsilon^*(x) \rangle - {C^o}^{-1} : \Sigma \\
\lambda^0(x) &= C^o : (E^0 - \epsilon^*(x)) \\
e^0(x) &= E^0
\end{aligned}
$$

teFFT Algorithm

$$\tau^i(x) = \lambda^{i-1}(x) - C^o : e^{i-1}(x) + C(x) : \epsilon^*(x) \quad 1.$$

$$\hat{\tau}^i(\xi) = fft(\tau^i(x)) \quad 2.$$

$$\epsilon^i(x) = E^{i-1} + sym\left(fft^{-1}\left(\hat{\Gamma}^o : \hat{\tau}^i(\xi)\right)\right) \quad 3.$$

$$\begin{aligned} \sigma^i(x) + C^o : (C^{-1}(x) : \sigma^i(x) + \epsilon^*(x)) &= \lambda^{i-1}(x) + C^o : \epsilon^i(x) \\ \sigma^i(x) &= (I + C^o : C^{-1}(x))[\lambda^{i-1}(x) + C^o : (\epsilon^i(x) - \epsilon^*(x))] \end{aligned} \quad 4.$$

$$e^i(x) = C^{-1}(x)\sigma^i(x) + \epsilon^*(x) \quad 5.$$

$$\lambda^i(x) = \lambda^{i-1}(x) + C^o : (\epsilon^i(x) - e^i(x)) \quad 6.$$

$$E^i = \langle \epsilon^i(x) \rangle + {C^o}^{-1} : (\Sigma - \langle \sigma^i(x) \rangle) \quad 7.$$

teFFT Errors

Stress field errors:

$$\mathrm{err}[\lambda^i(x)] = \frac{\langle ||C^o : (\epsilon^i(x) - e^i(x))||\rangle}{||\langle \sigma^i(x)\rangle||}$$

Strain field errors:

$$\mathrm{err}[e^i(x)] = \frac{\langle ||\epsilon^i(x) - e^i(x)||\rangle}{E}$$

Analysis

DEPARTMENT OF MATERIALS SCIENCE AND ENGINEERING

Stiffness Coefficients

TBC Component	Material	C_{11}	C_{12}	C_{13}	C_{14}	C_{33}	C_{44}
Top Coat	YSZ	204	87	–	–	–	158
Bond Coat	NiCoCrAlY	49	-14.7	–	–	–	127.5
	Ti_2AlC	308	55	60	–	270	111
	Ti_2AlN	312	69	86	–	283	127
	Ti_4AlN_3	405	94	102	–	361	160
	V_2GeC	311	122	140	–	291	158
	Nb_2AlC	341	94	117	–	310	150
	Ti_3AlC_2	361	75	70	–	299	124
	Ti_2SC	339	90	100	–	354	162
	Ti_3SiC_2	365	125	120	–	375	122
	Ti_3GeC_2	355	143	80	–	404	172
	V_2AlC	346	71	106	–	314	151
	V_2AsC	334	109	157	–	321	170
	Nb_3Si_3	497	163	116	22	501	147
TGO	α-Al_2O_3	497	163	116	22	501	147
Substrate	Nb-16.8 wt% Mo	271	133.4	–	–	–	29.47
	IN718	339.5	173.3	–	–	–	21.4

DREAM3D Statistics

Sample grain size distribution:

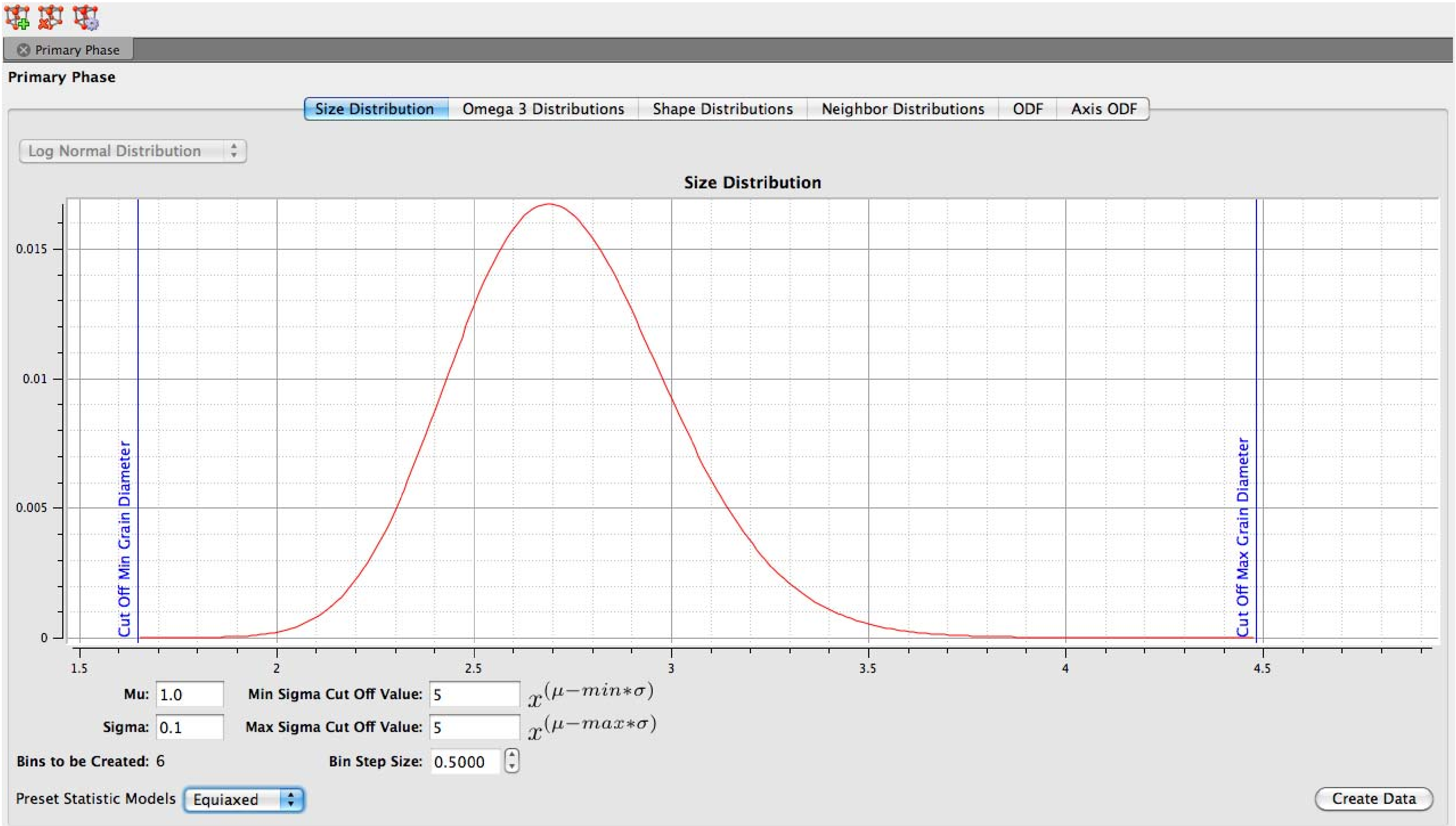

DREAM3D Statistics

Sample axis ODF pole figures:

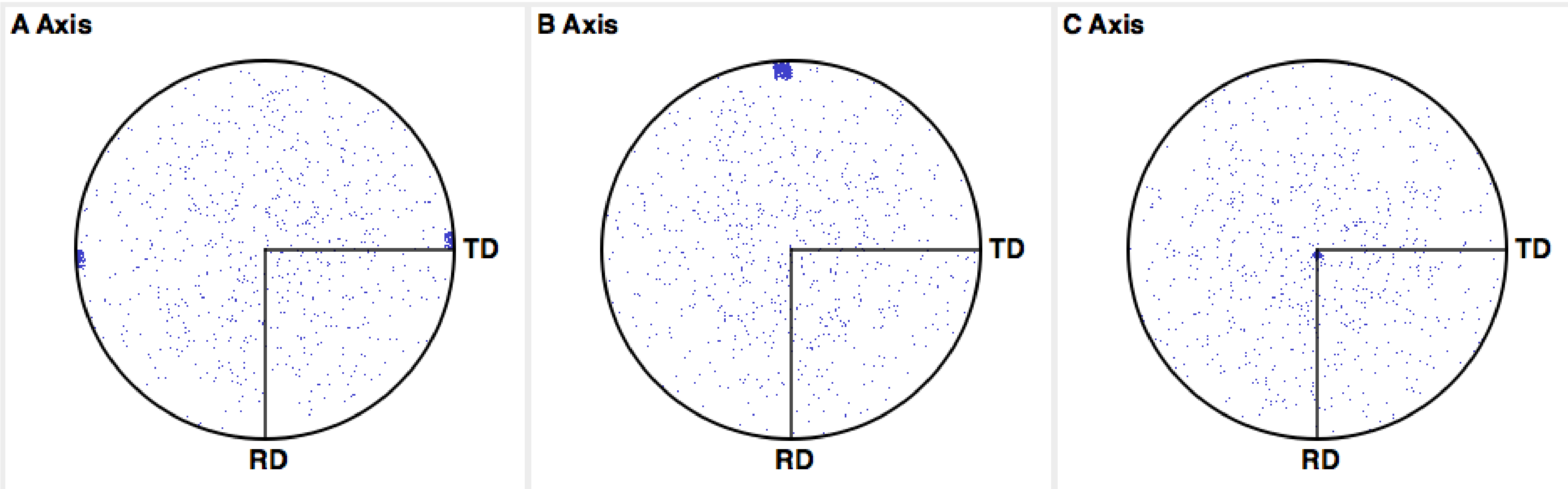

Stitching Procedure

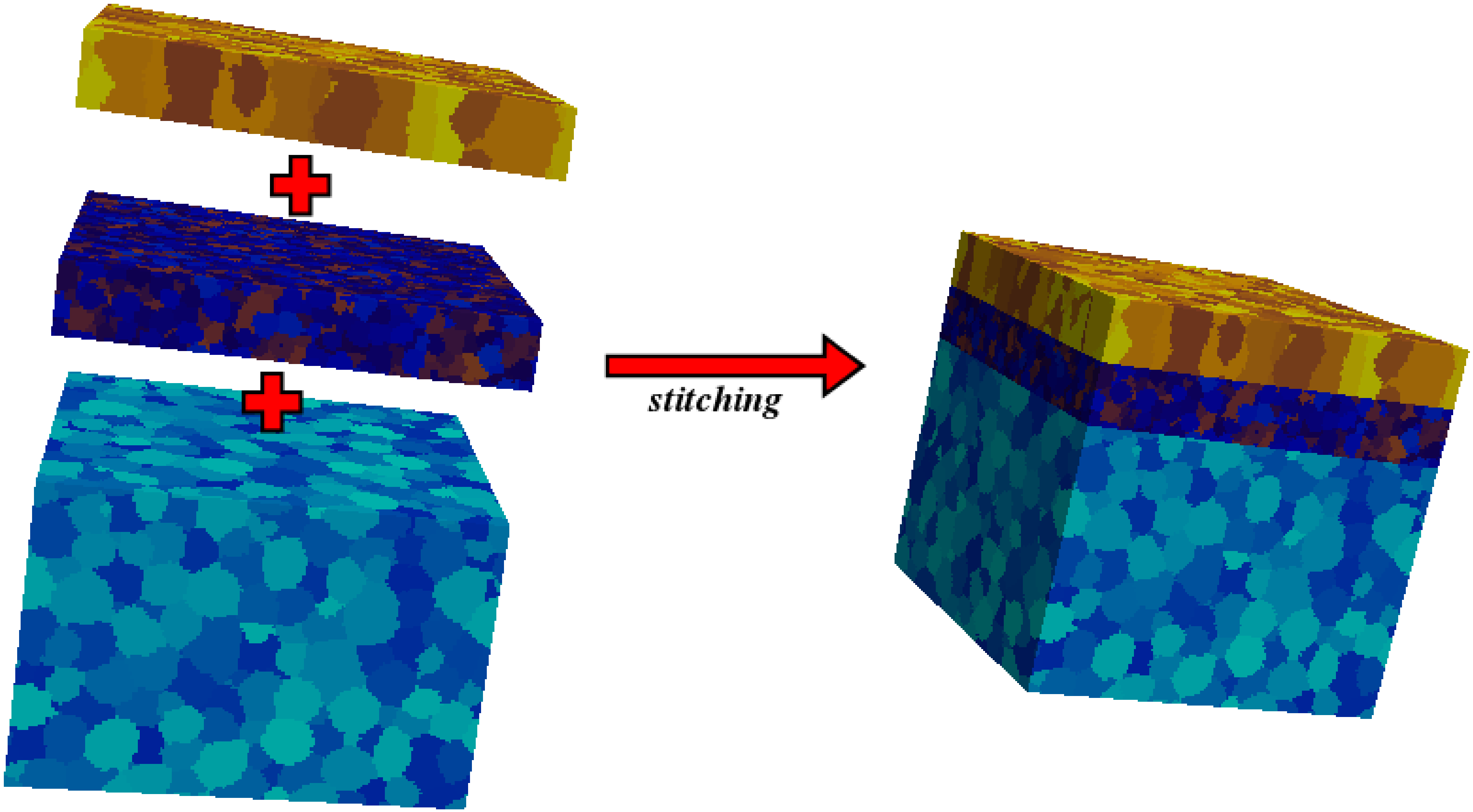

DEPARTMENT OF MATERIALS SCIENCE AND ENGINEERING

Resolution Dependence: Grain Shape

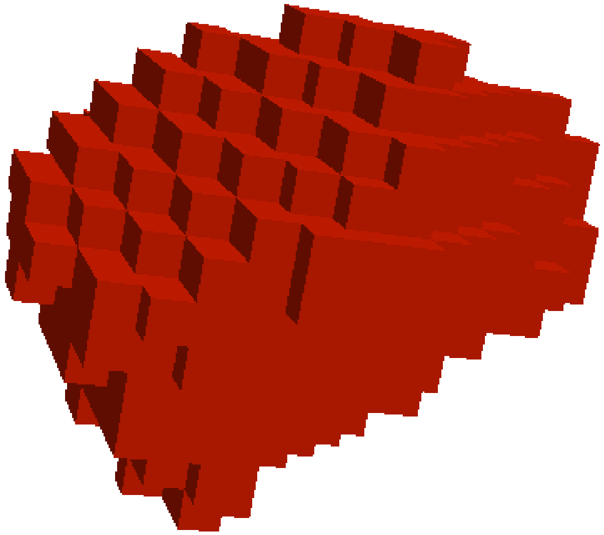

128^3 structure

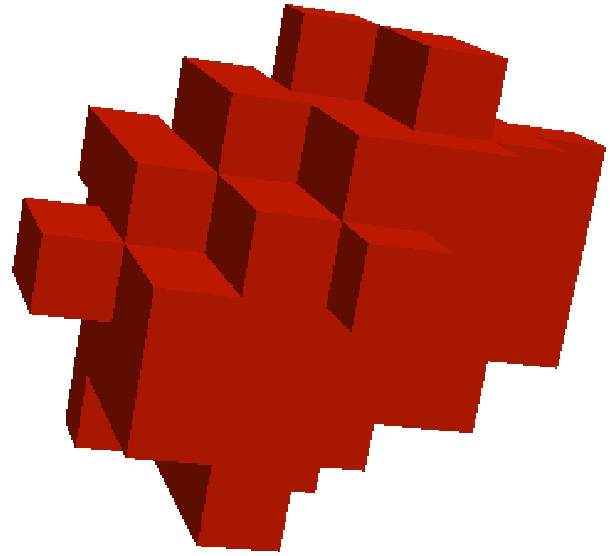

64^3 structure

32^3 structure

Resolution Dependence: POT Analysis

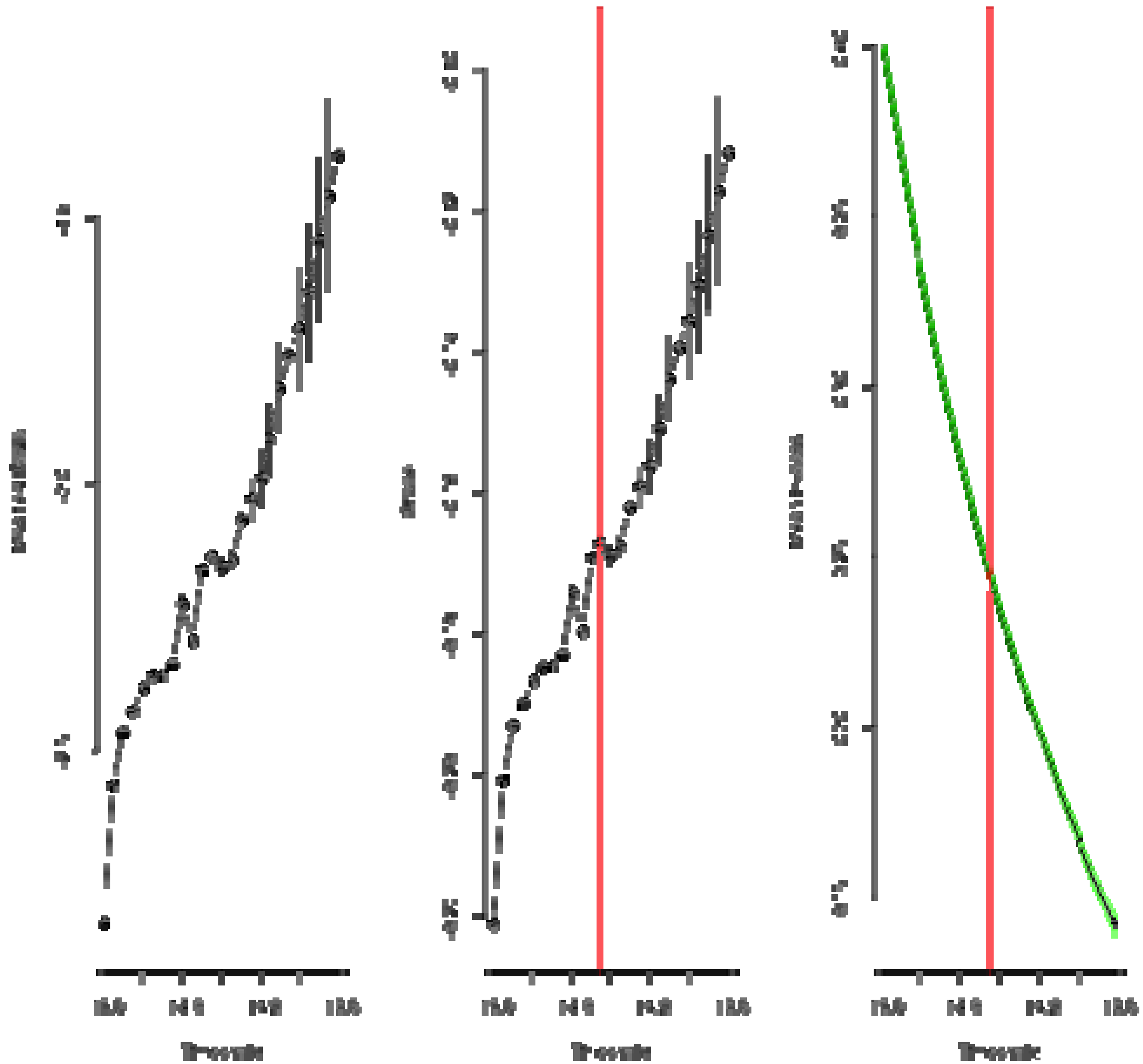

128^3 structure

Resolution Dependence: POT Analysis

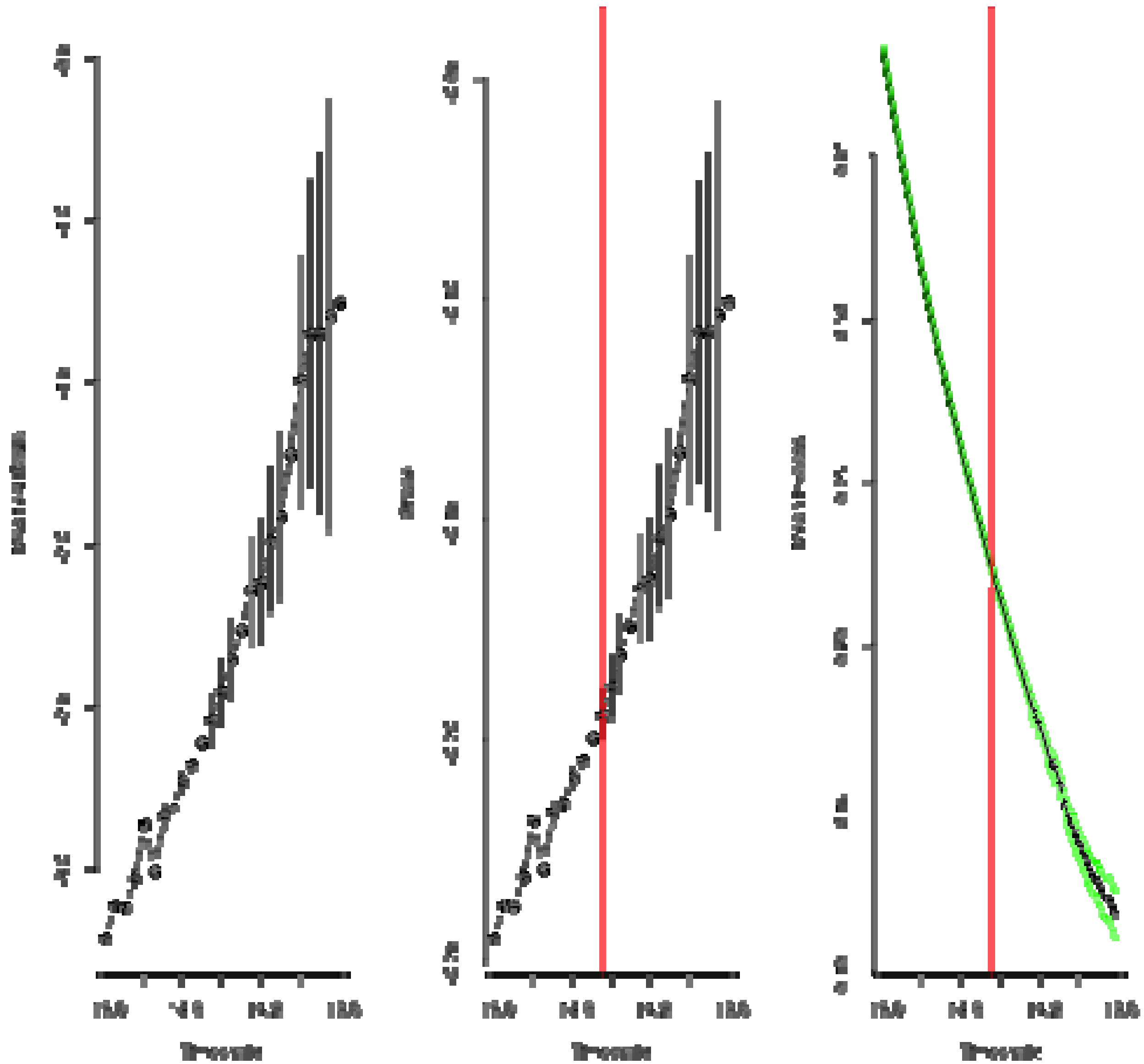

64^3 structure

Resolution Dependence: POT Analysis

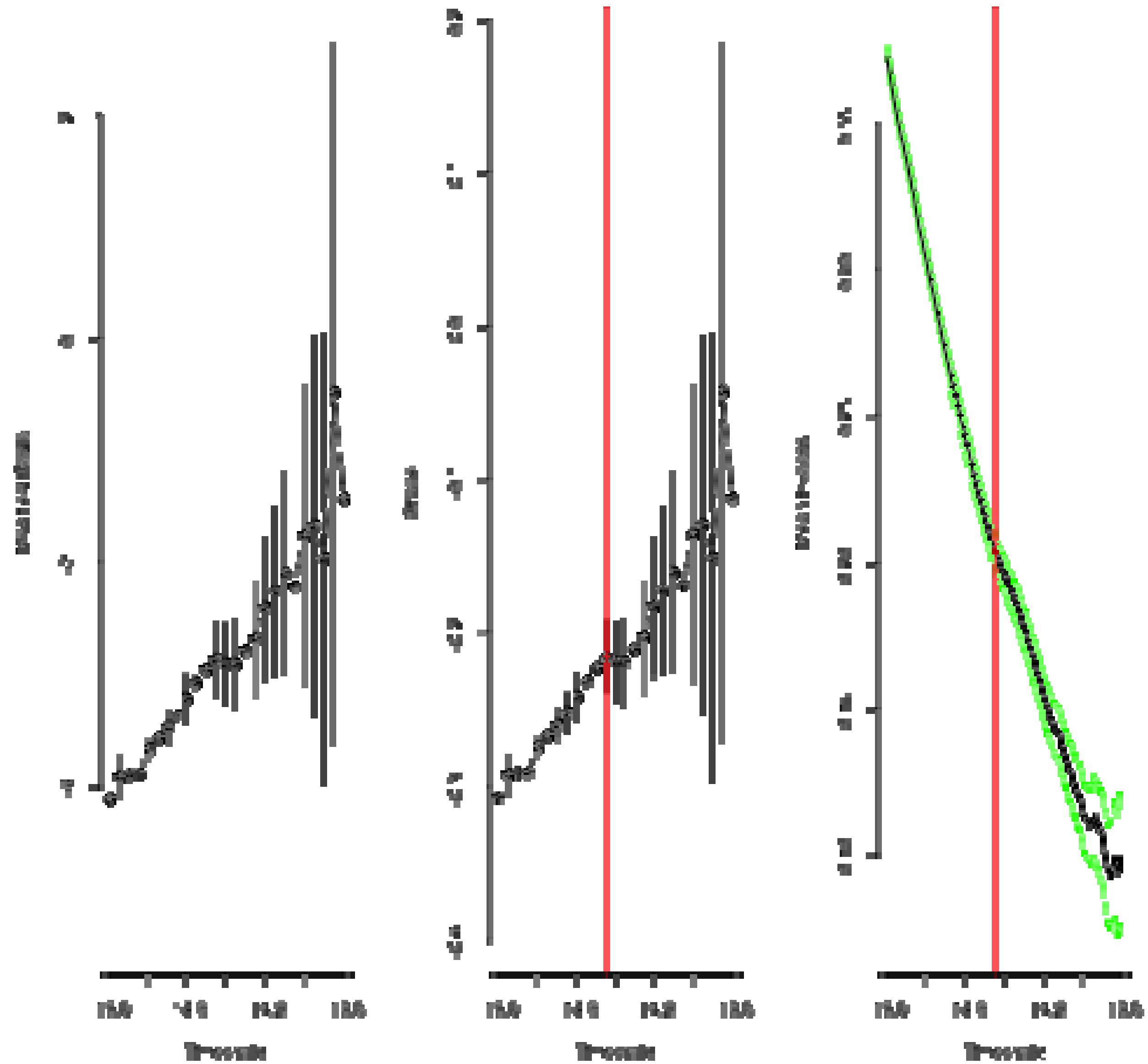

32^3 structure

Resolution Dependence: POT Analysis

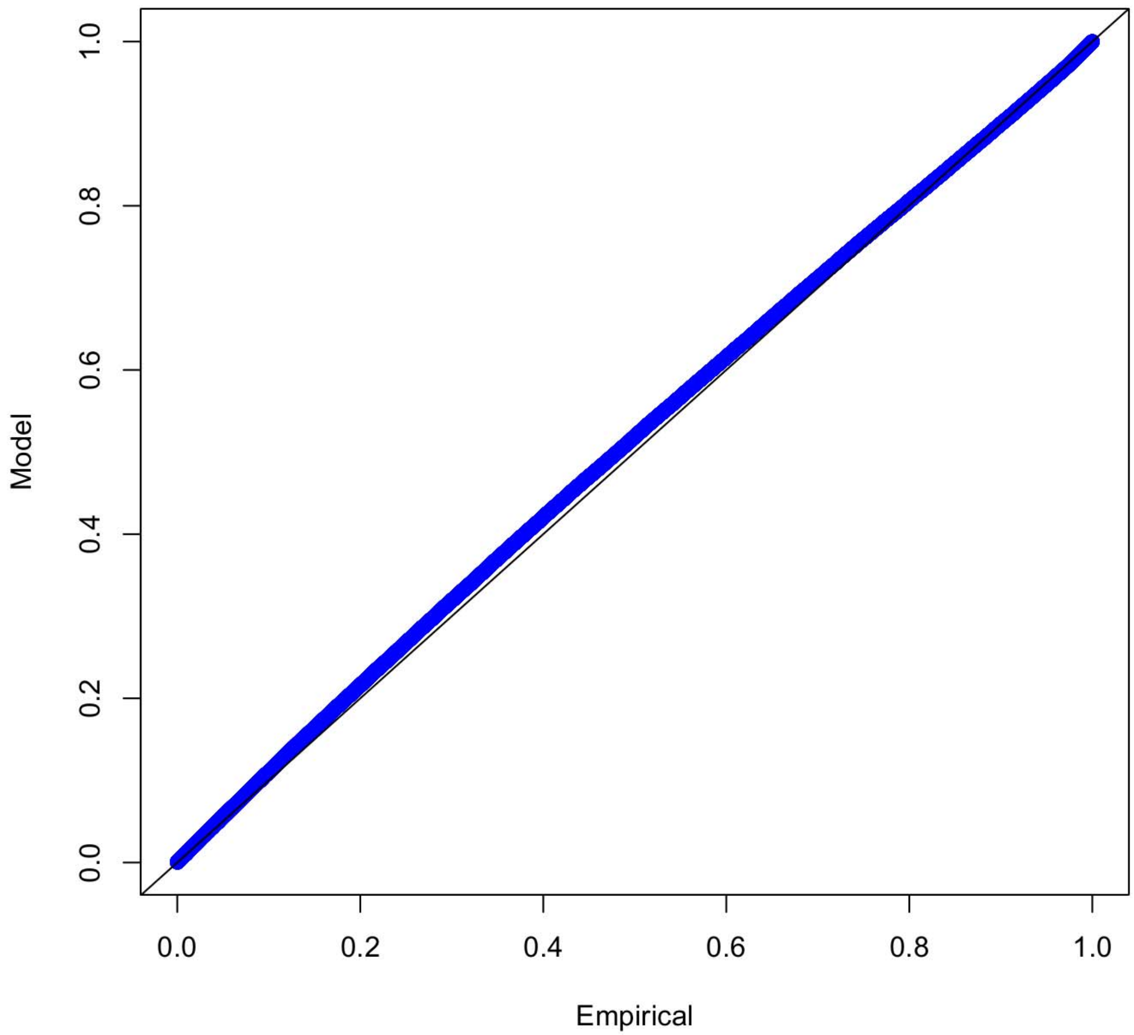

128^3 structure

Resolution Dependence: POT Analysis

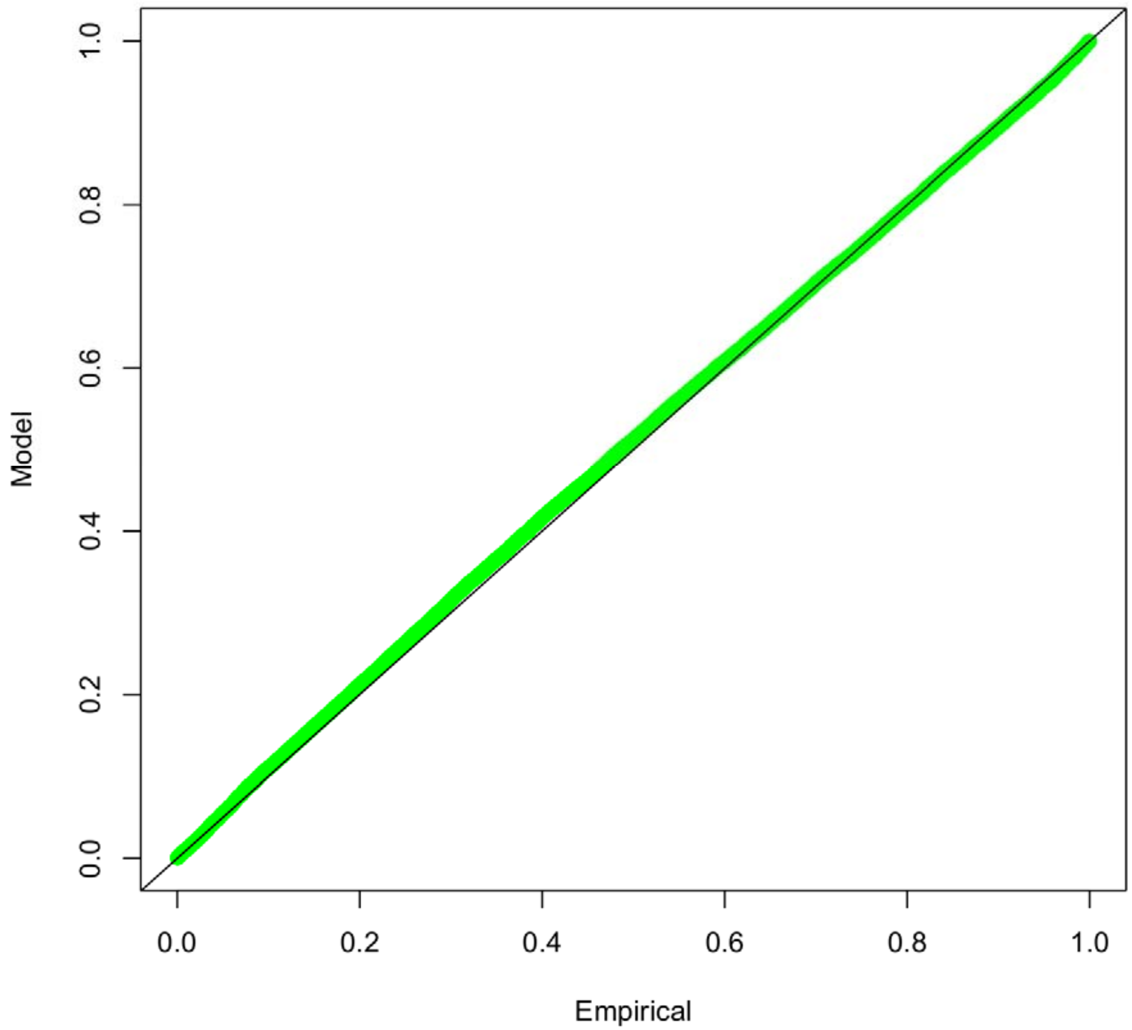

64^3 structure

Resolution Dependence: POT Analysis

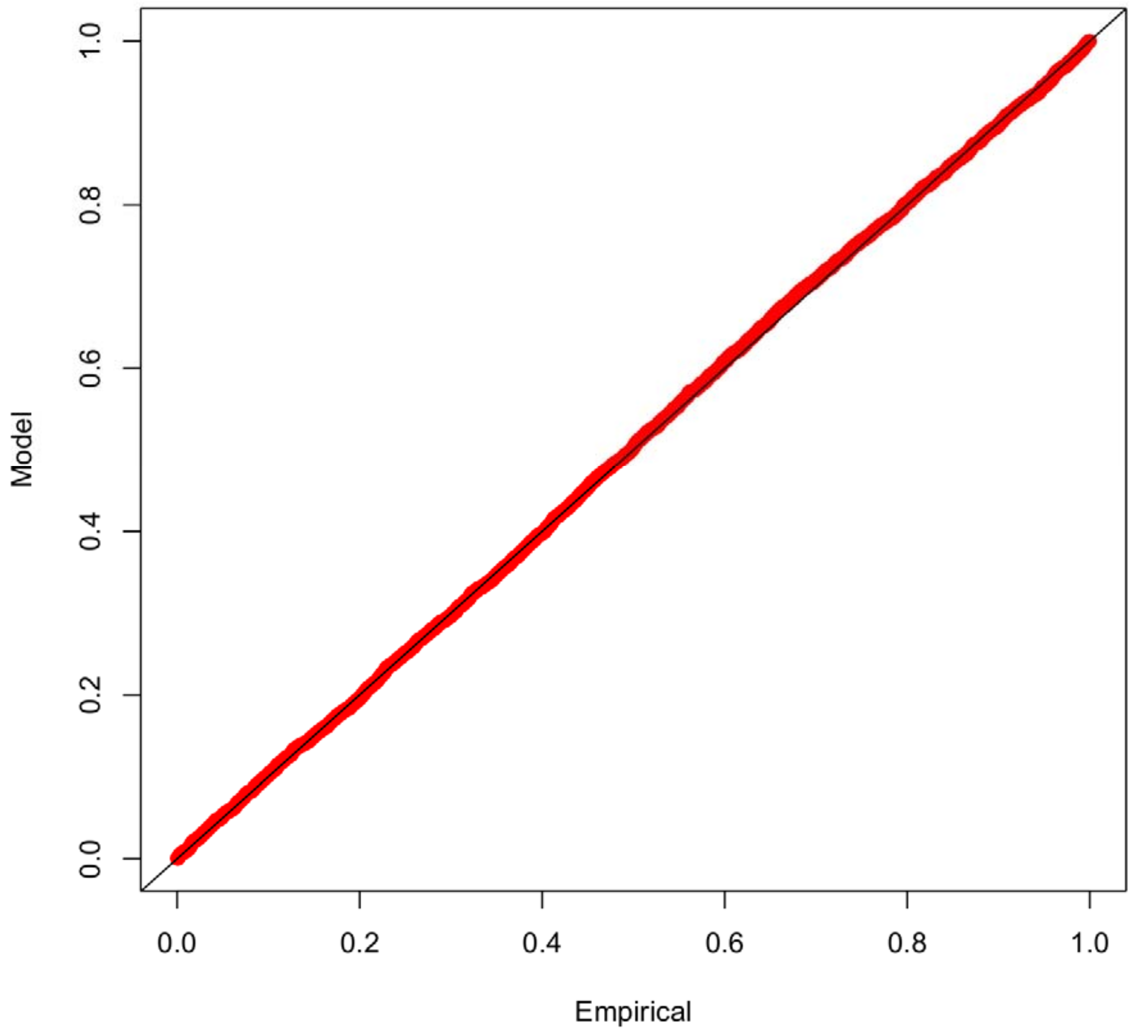

32^3 structure

MAX Phase BCs: Stress

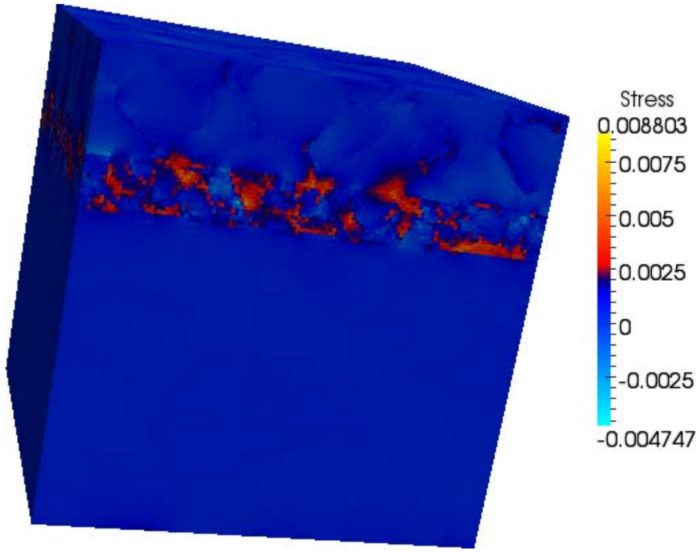

Ti_2AlC BC

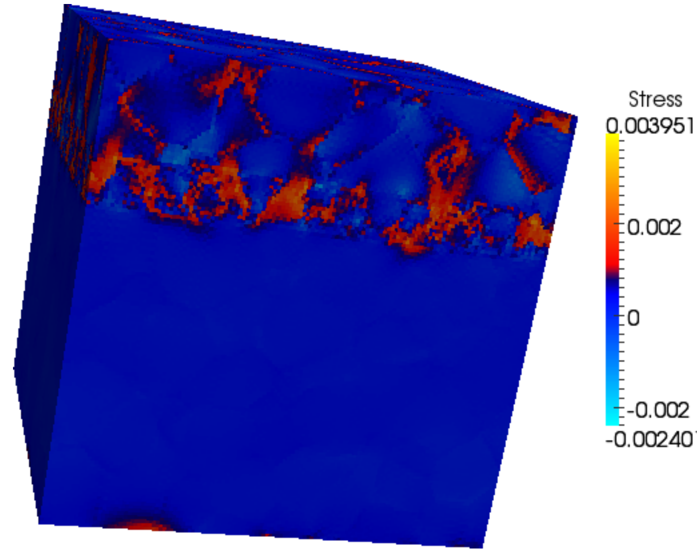

Ti_2AlN BC

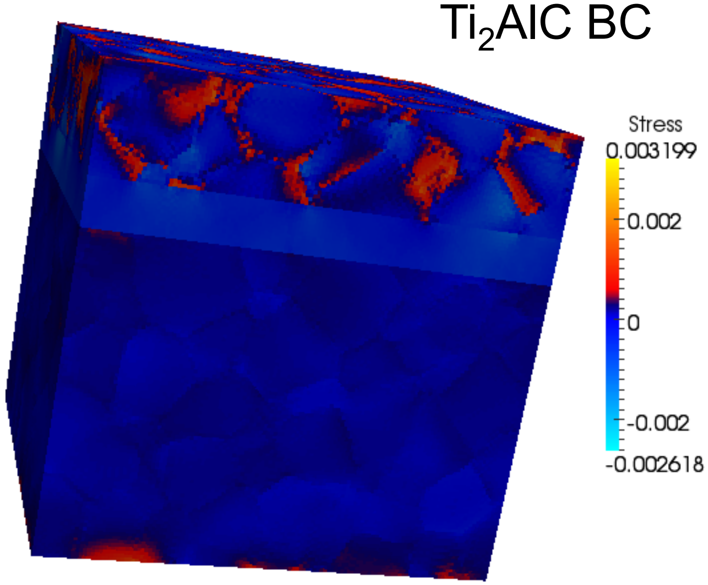

Ti_4AlN_3 BC

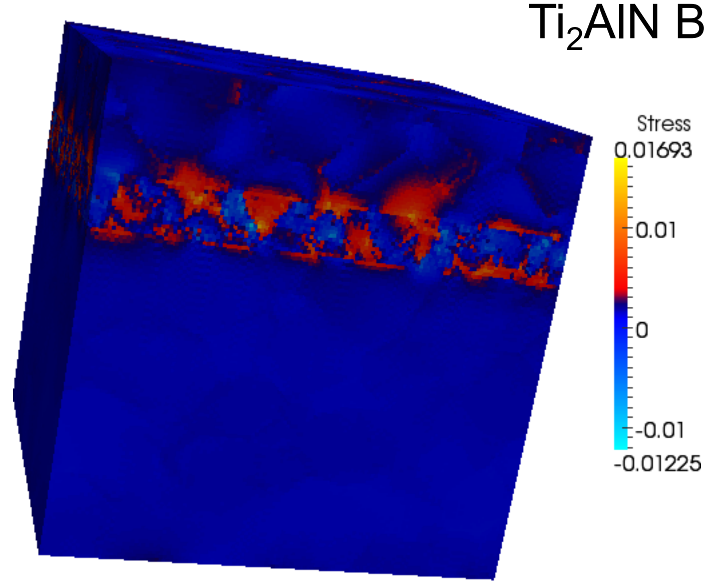

V_2GeC BC

DEPARTMENT OF MATERIALS SCIENCE AND ENGINEERING

MAX Phase BCs: Stress

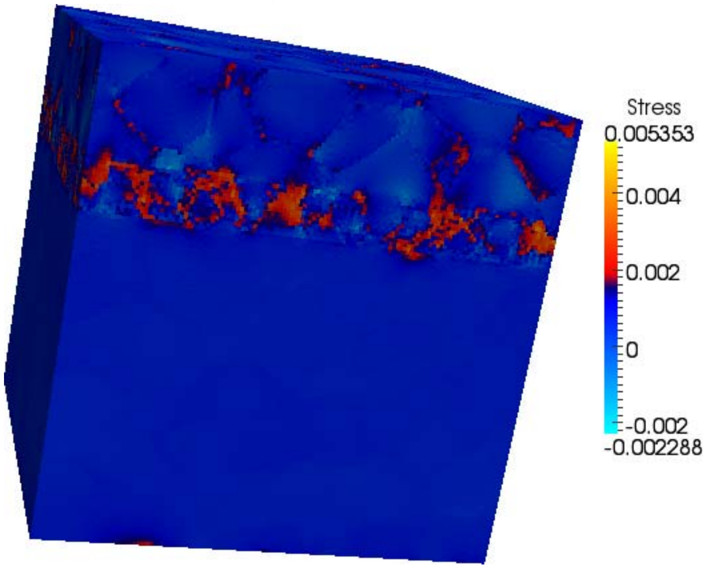

Nb_2AlC BC

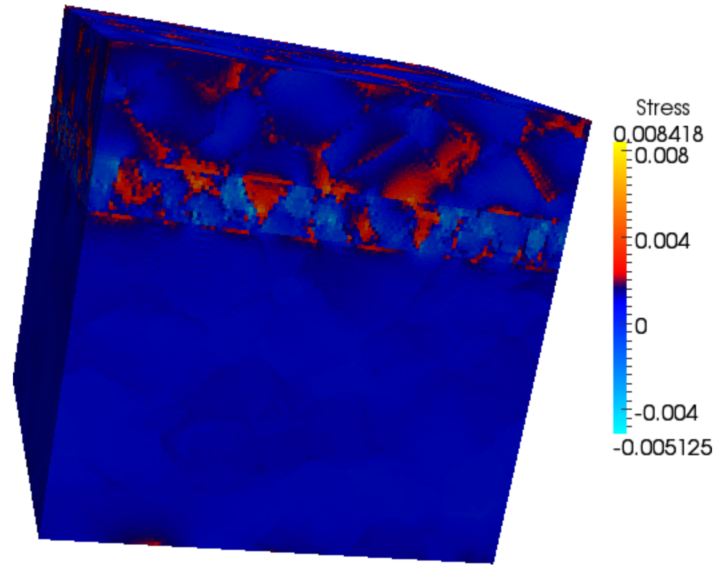

Ti_3AlC_2 BC

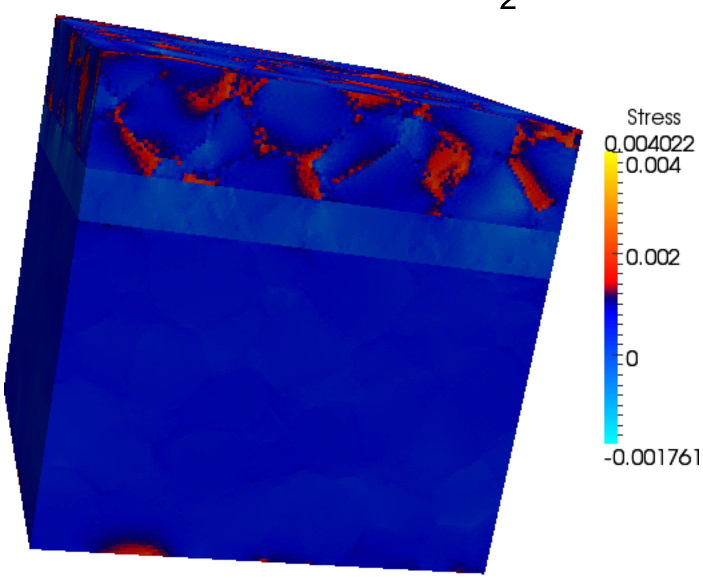

Ti_2SC BC

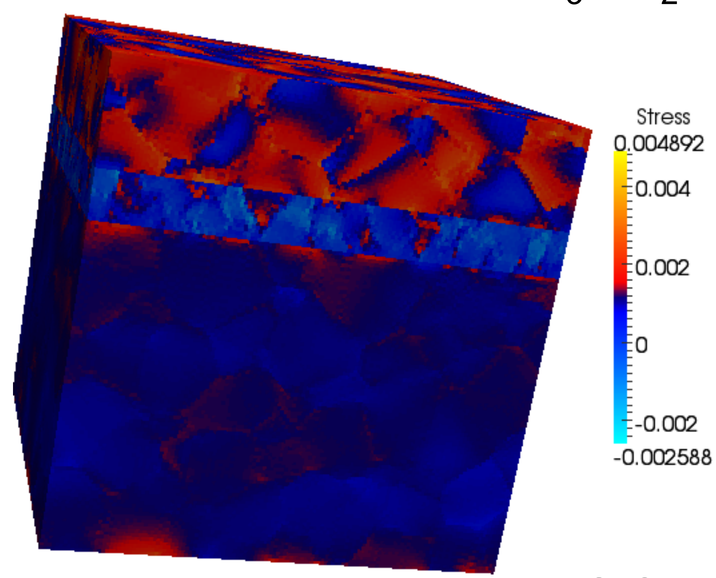

Ti_3SiC_2 BC

MAX Phase BCs: Stress

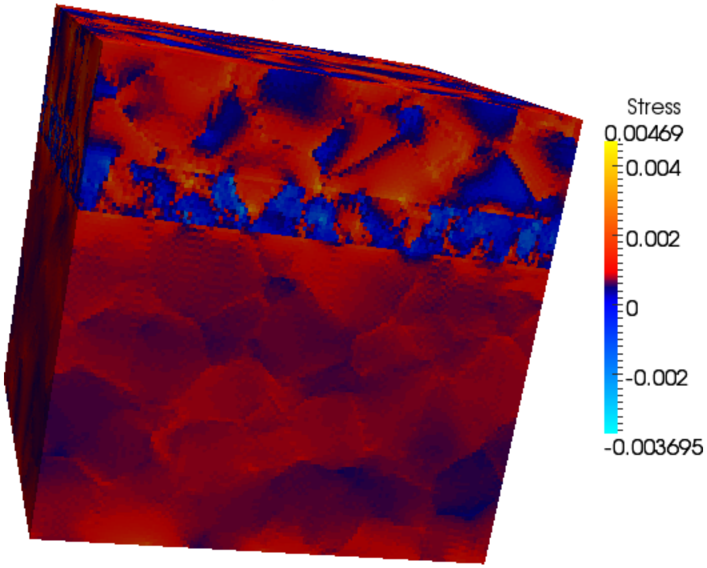

Ti_3GeC_2 BC

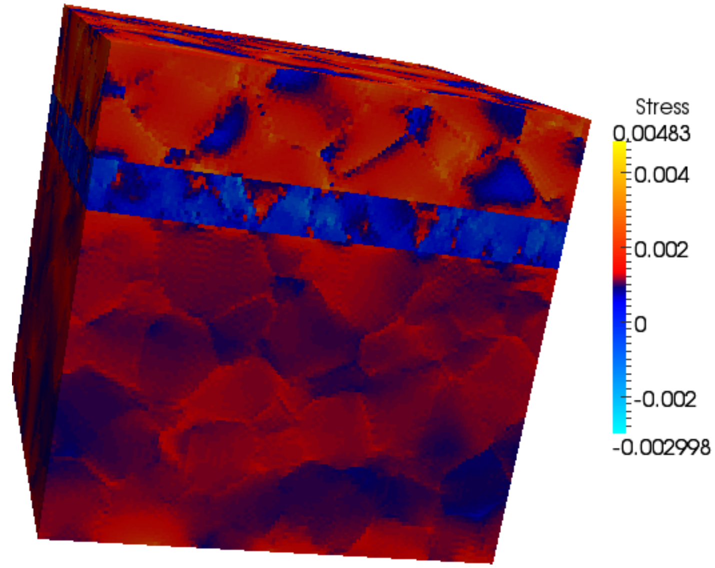

V_2AlC BC

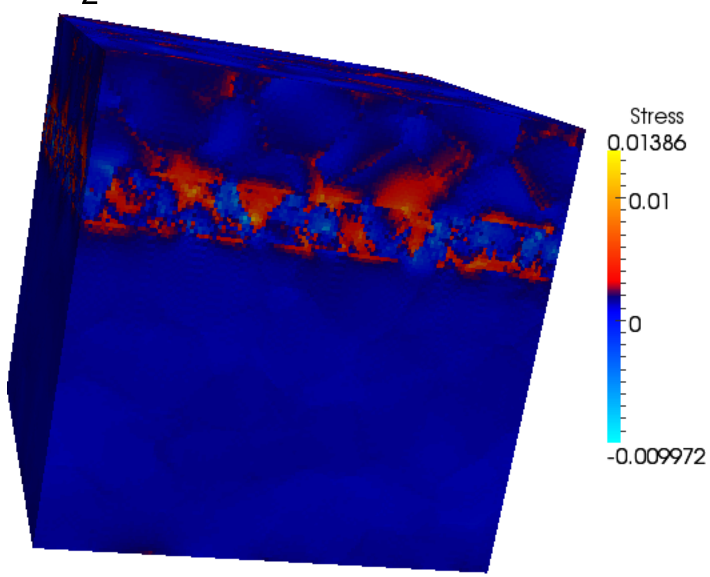

V_2AsC BC

DEPARTMENT OF MATERIALS SCIENCE AND ENGINEERING

MAX Phase BCs: EED

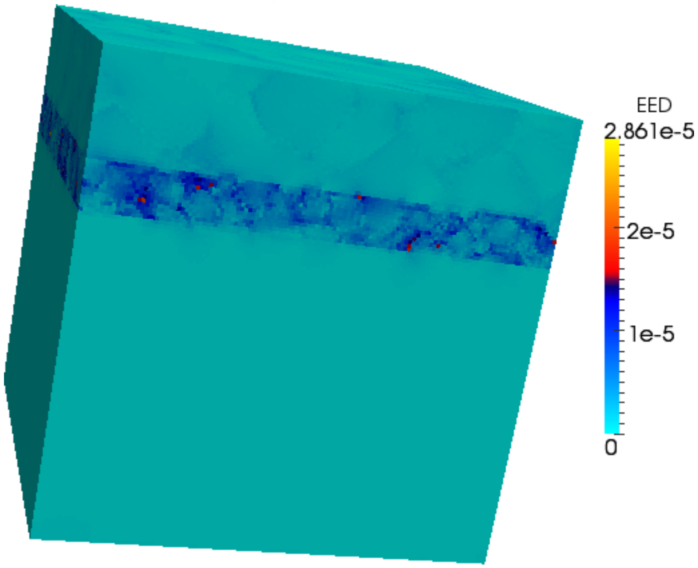

Ti_2AlC BC

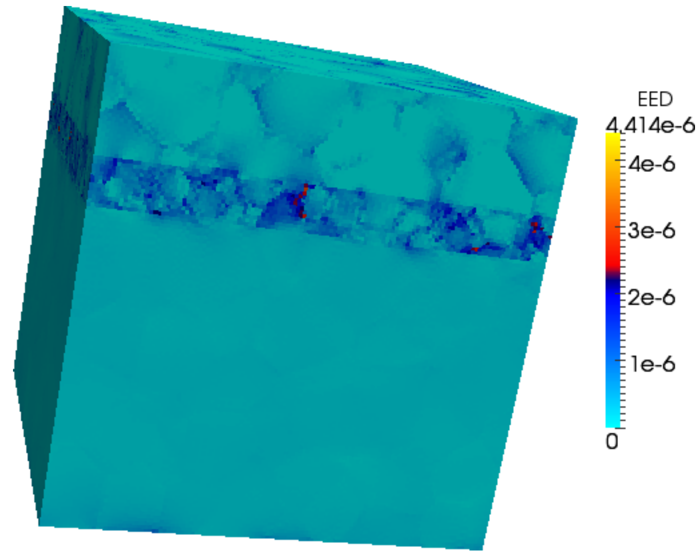

Ti_2AlN BC

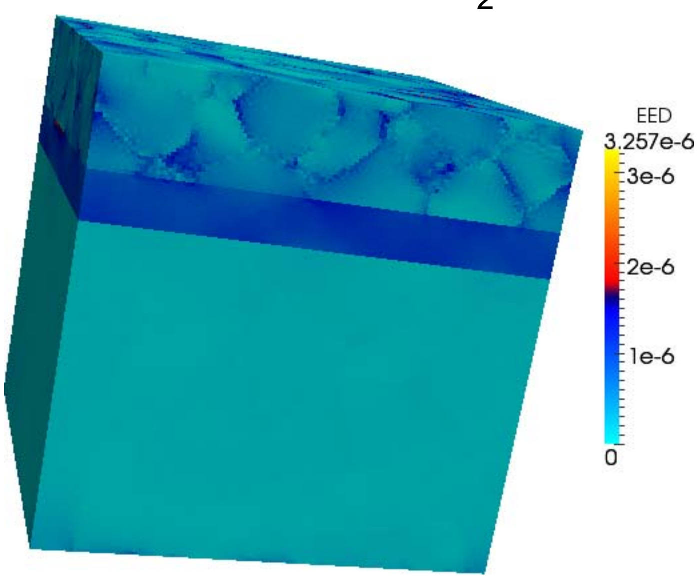

Ti_4AlN_3 BC

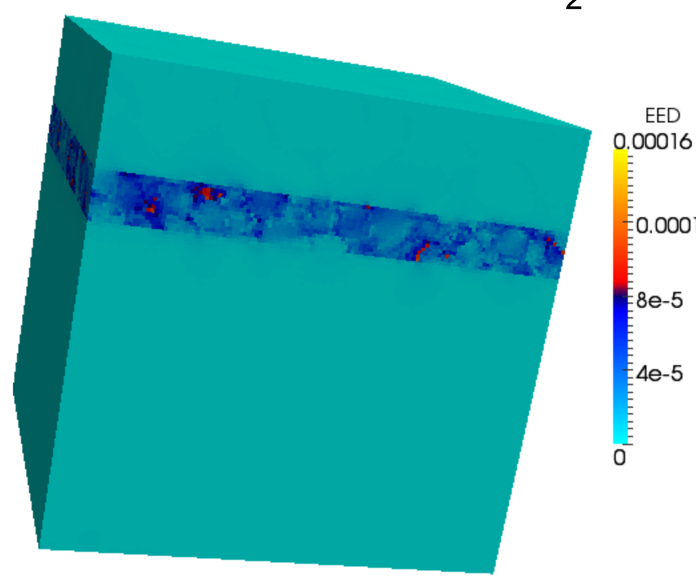

V_2GeC BC

MAX Phase BCs: EED

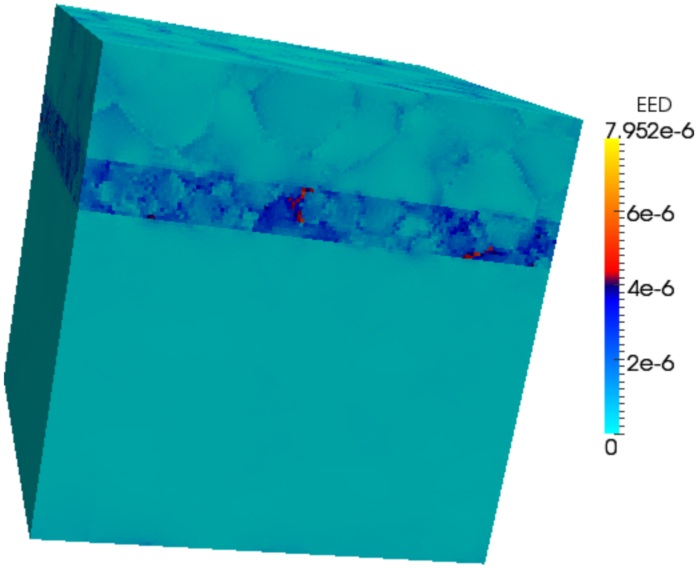

Nb_2AlC BC

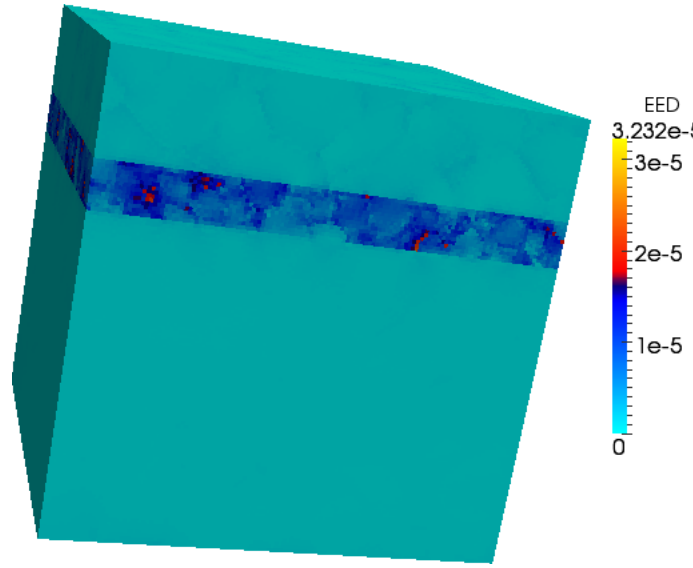

Ti_3AlC_2 BC

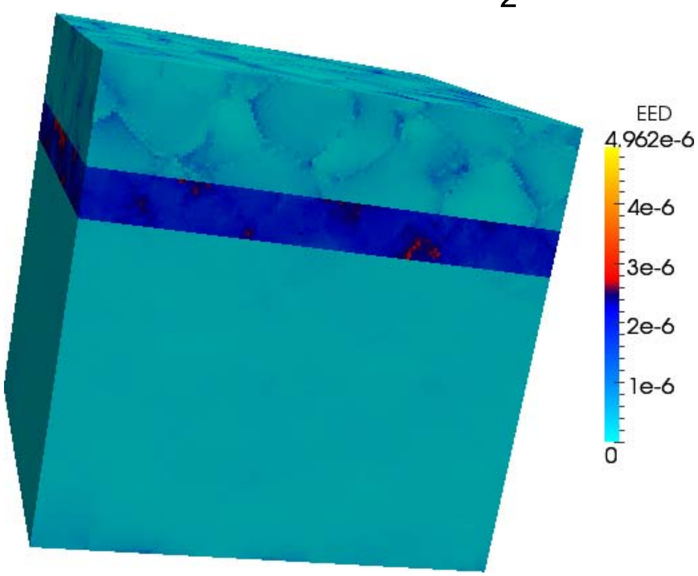

Ti_2SC BC

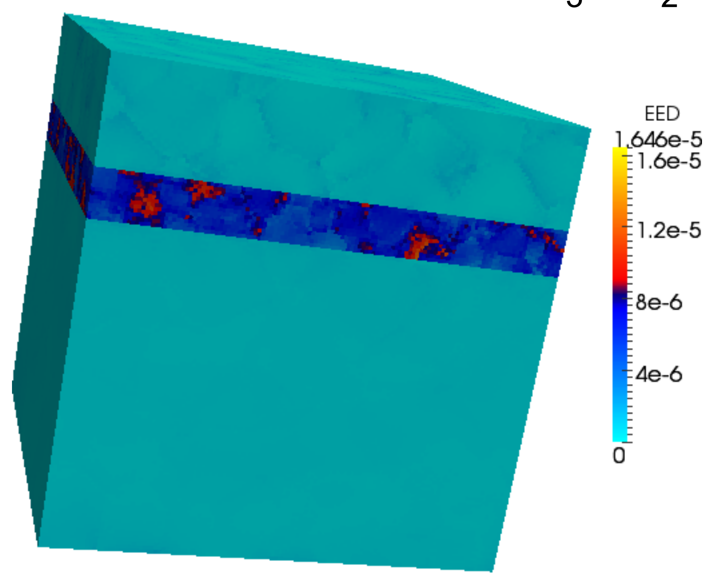

Ti_3SiC_2 BC

MAX Phase BCs: EED

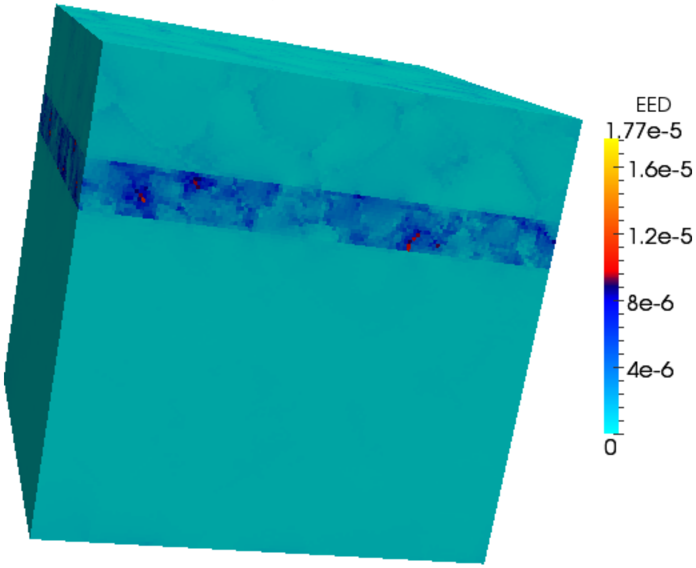

Ti_3GeC_2 BC

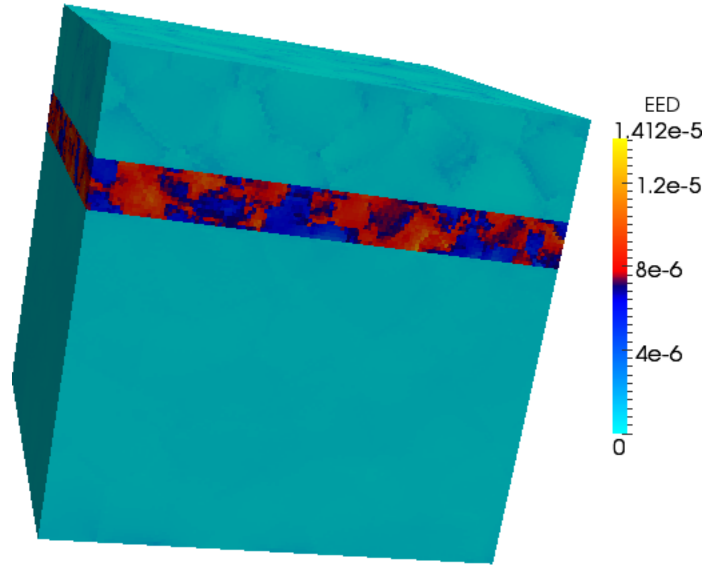

V_2AlC BC

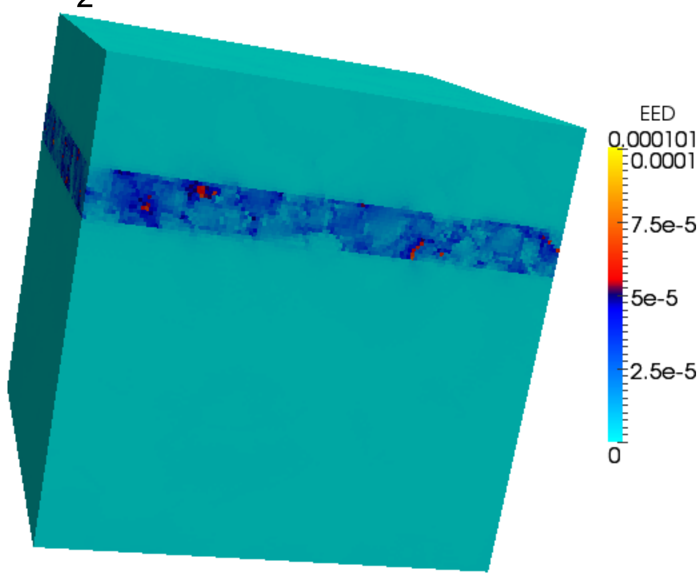

V_2AsC BC

MAX Phase BCs: Summary

BC Material	Maximum Principal Stress (GPa)	Maximum EED (GPa)
Ti_2AlC	0.8803	0.002861
Ti_2AlN	0.3951	0.0004414
Ti_4AlN_3	0.3199	0.0003257
V_2GeC	1.693	0.01597
Nb_2AlC	0.5353	0.0007952
Ti_3AlC_2	0.8418	0.003232
Ti_2SC	0.4022	0.0004962
Ti_3SiC_2	0.4892	0.001646
Ti_3GeC_2	0.469	0.00177
V_2AlC	0.483	0.001412
V_2AsC	1.386	0.01005

MAX Phase BCs: Summary

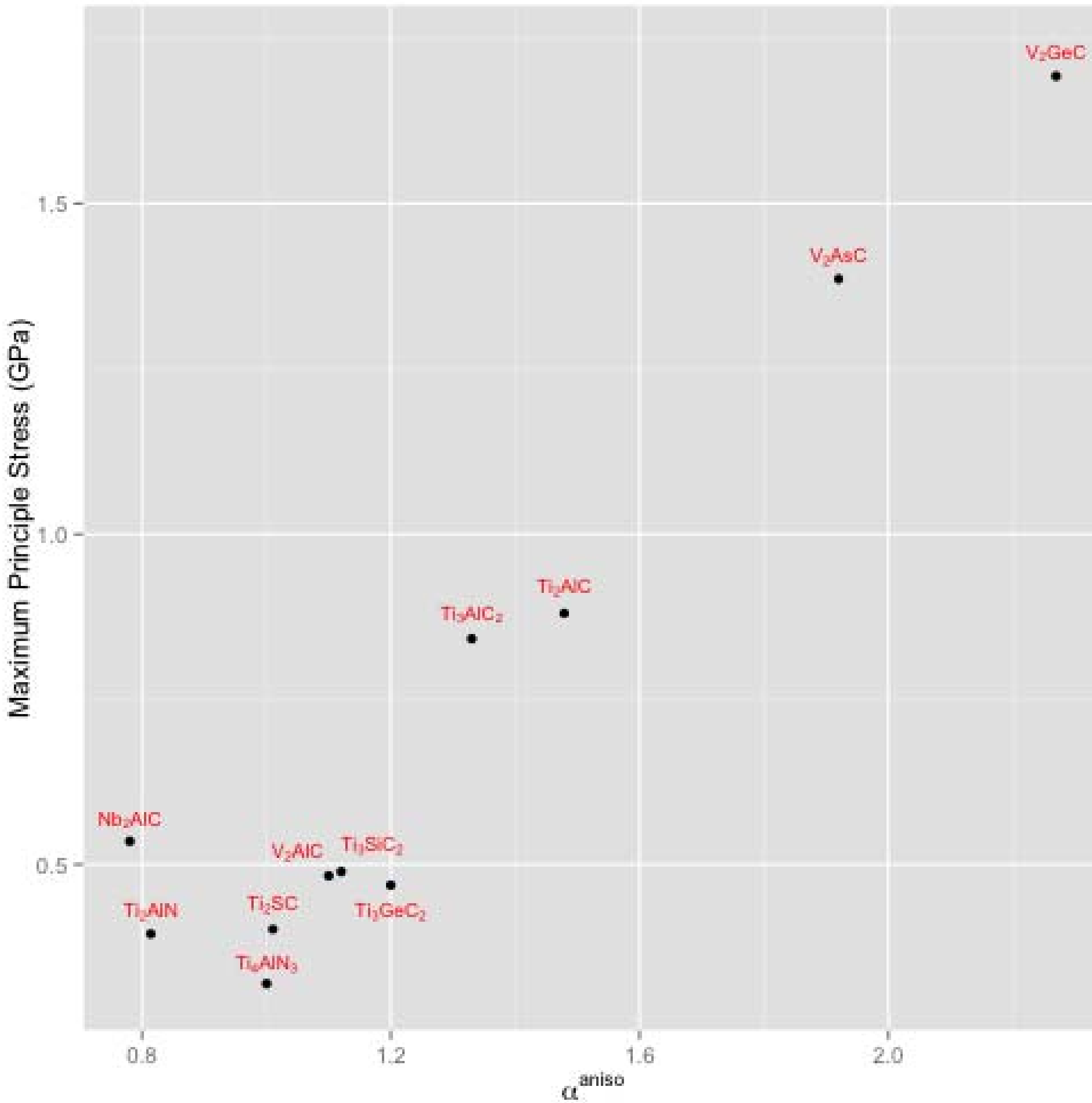

Industry Standard Systems: Stress

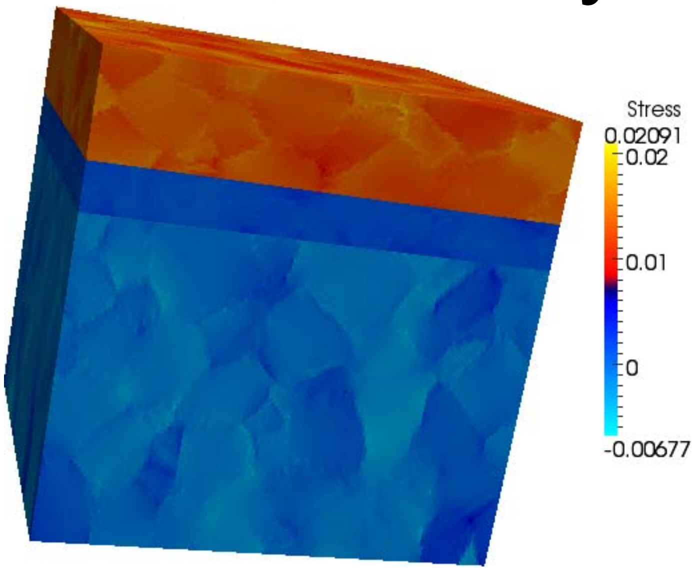

Periodic, flat

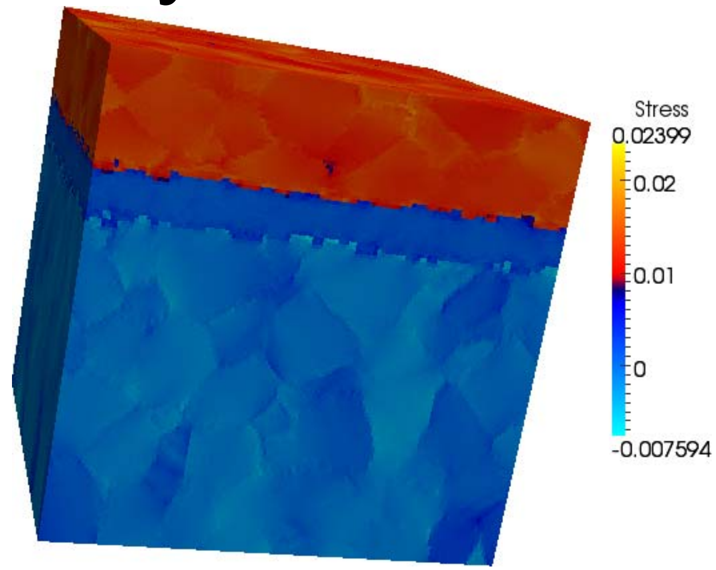

Periodic, rough

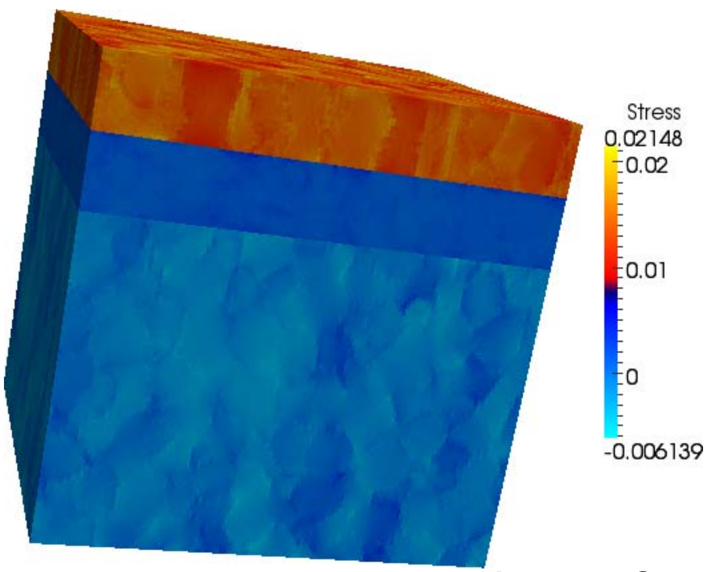

Industry, flat

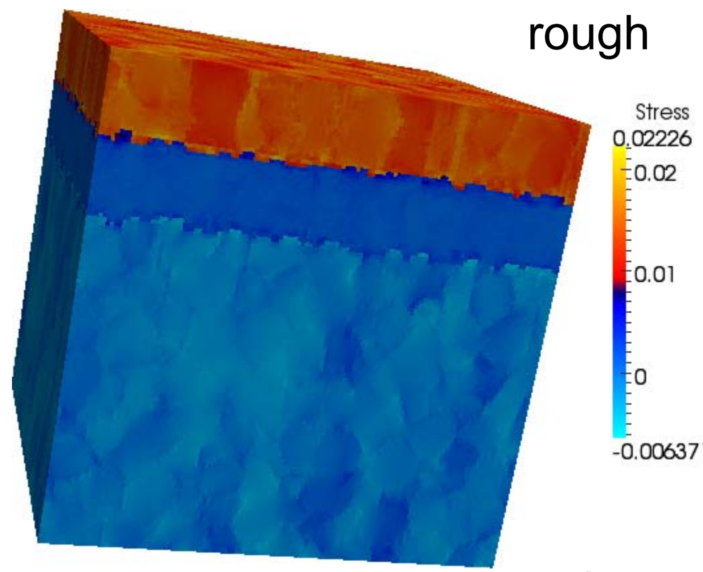

Industry,

DEPARTMENT OF MATERIALS SCIENCE AND ENGINEERING

Industry Standard Systems: Stress

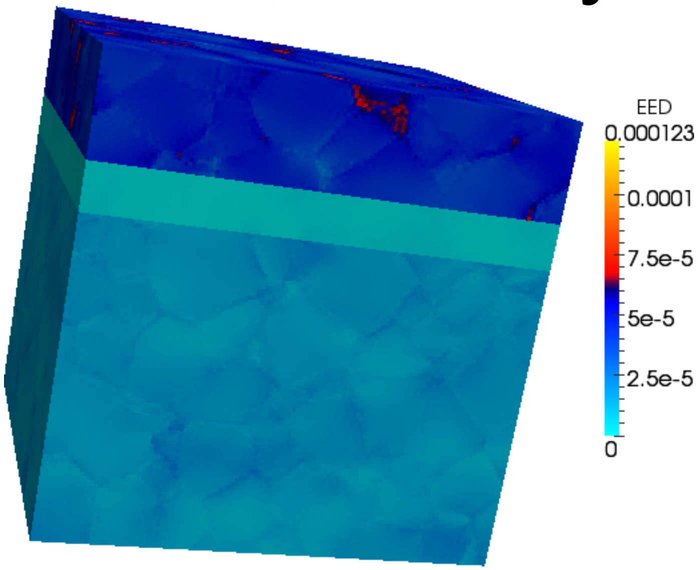

Periodic, flat

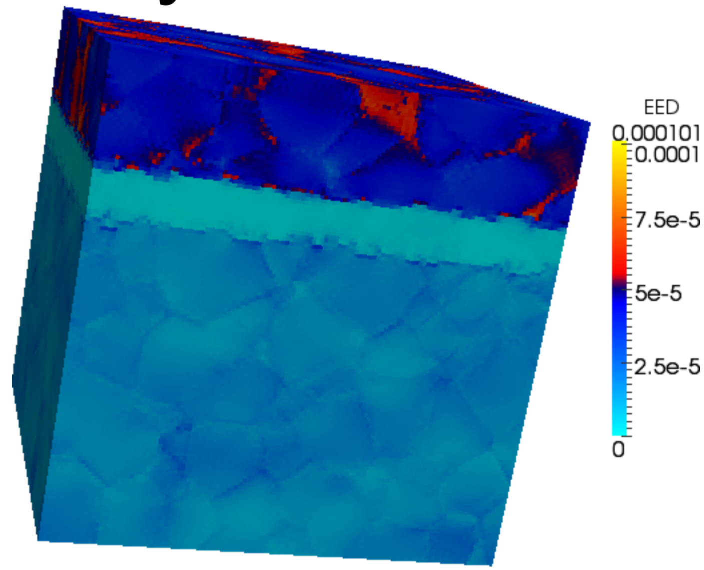

Periodic,

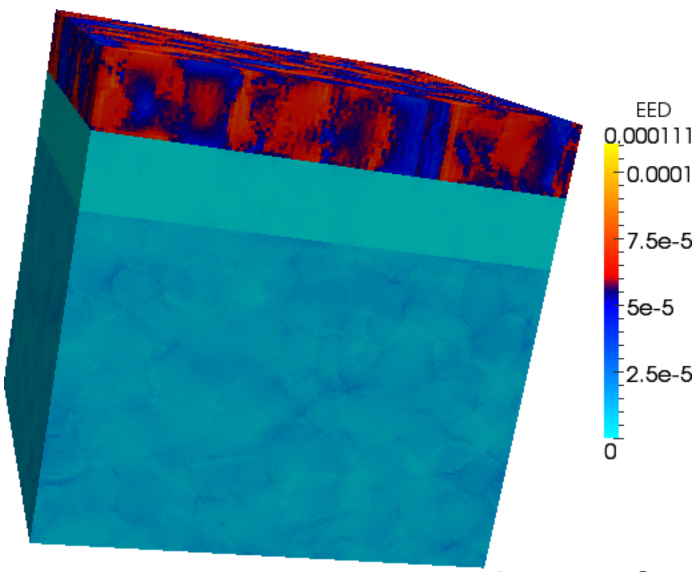

Industry, flat

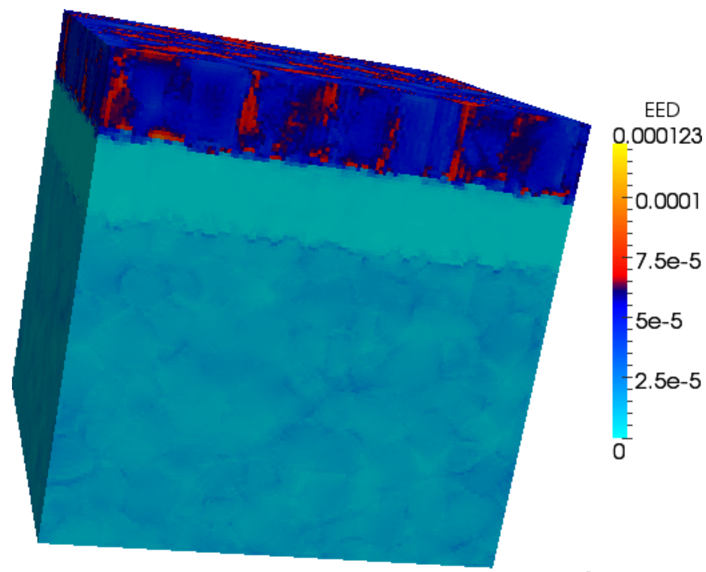

Industry,

Industry Standard Systems: POT Analysis

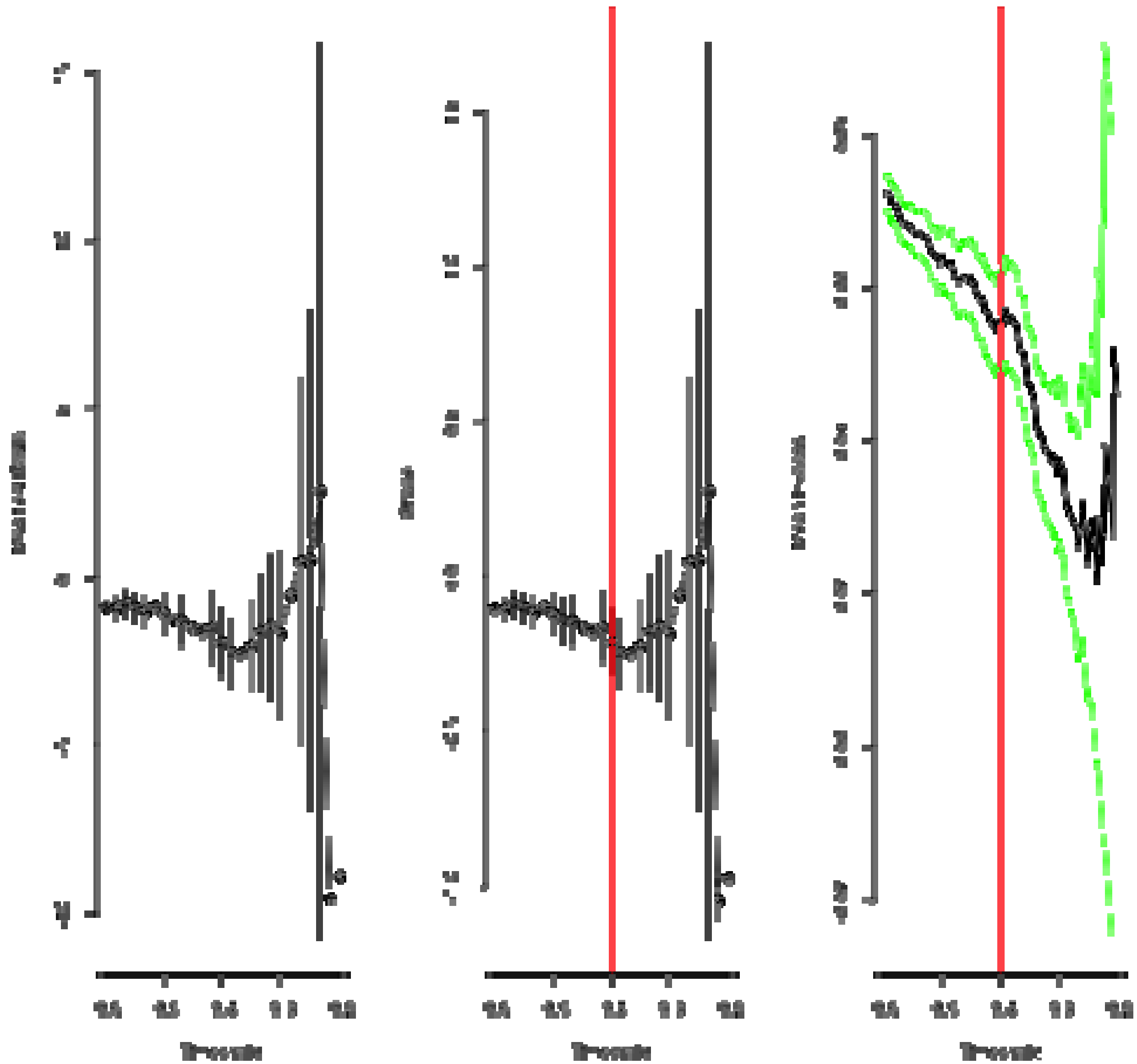

Industry, flat

Industry Standard Systems: POT Analysis

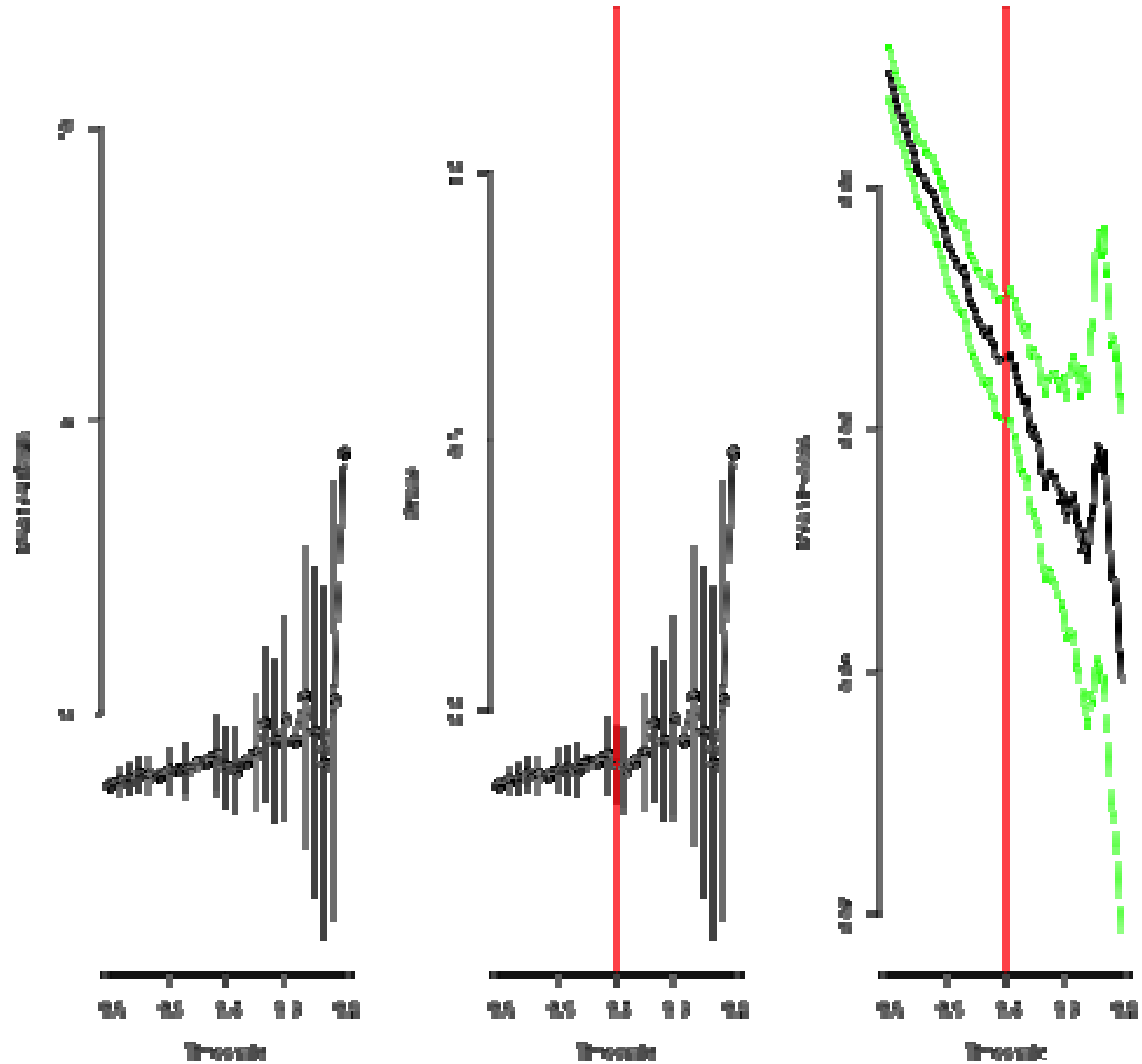

Industry,

Industry Standard Systems: POT Analysis

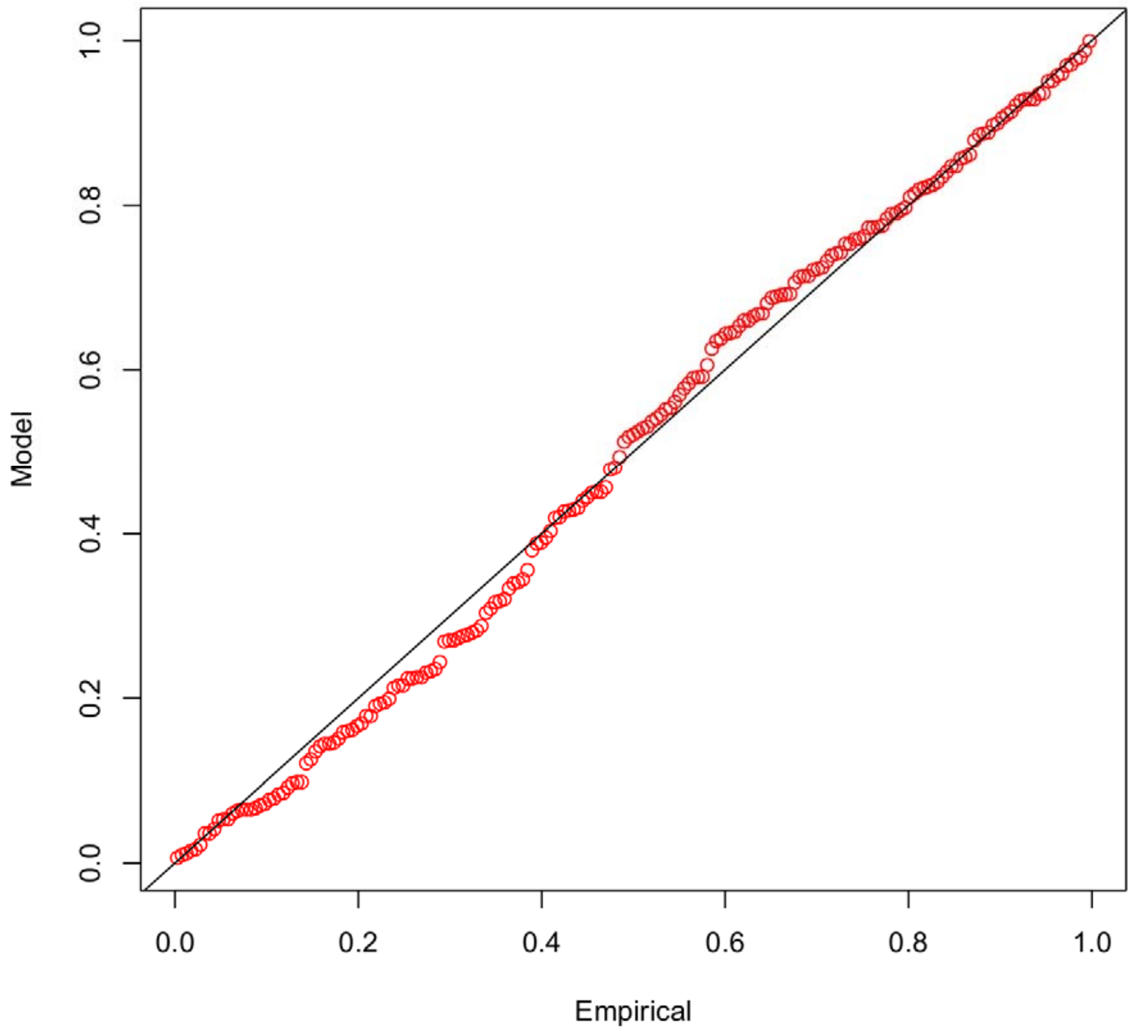

Industry, flat

Industry Standard Systems: POT Analysis

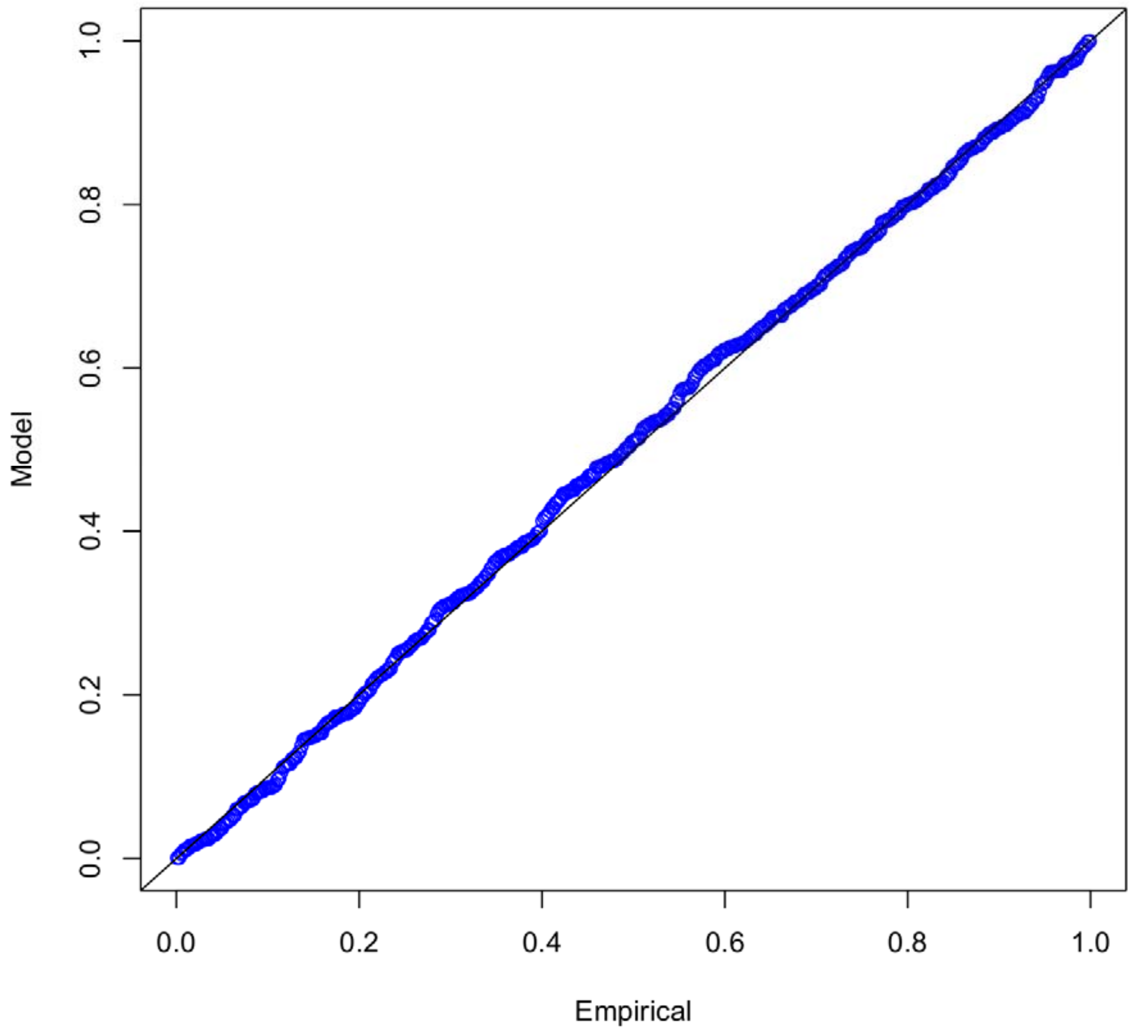

Industry,

DEPARTMENT OF
MATERIALS SCIENCE AND ENGINEERING

"Harpy's Eagle, world's most vicious raptor…"